CcpA-MEDIATED CARBON CATABOLITE REGULATION OF VIRULENCE

IN THE GROUP A STREPTOCOCCUS

APPROVED BY SUPERVISORY COMMITTEE

Kevin McIver _____

Eric Hansen _____

Larry Reitzer _____

Wade Winkler _____

DEDICATION

To my parents, who have always encouraged me to follow my dreams, even if they were a little off the beaten path. To my fiancée and best friend, Jonathan, for always being there for me, and making me smile even when my project was not working so well.

I would like to thank my mentor, Dr. Kevin McIver, for his patience and guidance in both science and life issues. I would like to thank my graduate committee Dr. Eric Hansen, Dr. Larry Reitzer, and Dr. Wade Winkler for their thoughtful insight on my project and their willingness to help from afar.

I would like to thank all the current and former members of the McIver lab, as they have not only provided generous assistance when needed, they are also great friends.

CcpA-MEDIATED CARBON CATABOLITE REGULATION OF VIRULENCE IN THE GROUP A STREPTOCOCCUS

by

TRACI L. KINKEL

DISSERTATION

Presented to the Faculty of the Graduate School of Biomedical Sciences

The University of Texas Southwestern Medical Center at Dallas

In Partial Fulfillment of the Requirements

For the Degree of

DOCTOR OF PHILOSOPHY

The University of Texas Southwestern Medical Center at Dallas

Dallas, Texas

August, 2008

CcpA-MEDIATED CARBON CATABOLITE REGULATION OF VIRULENCE IN THE GROUP A STREPTOCOCCUS

Traci L. Kinkel, Ph.D

The University of Texas Southwestern Medical Center at Dallas, 2008

Supervising Professor: Kevin S. McIver, Ph.D.

The group A streptococcus (GAS) is a strict human pathogen, which causes a broad spectrum of diseases ranging from the self-limiting diseases such as pharyngitis and impetigo to the more severe invasive disease such as necrotizing fasciitis. The coordinate expression of a wide array of virulence factors in response to the changing host environment represents a key step in the ability of the GAS to mediate disease in the human host. The present study investigates the role of the primary mediator of sugar metabolism regulation, carbon catabolite control protein (CcpA), in the regulation of virulence of the GAS. A putative CcpA-binding site or catabolite response element (*cre*) was identified upstream of

the promoter for the virulence gene regulator, Mga. CcpA was shown to specifically bind to this *cre*, and activate the transcription of *mga*. In addition, both transcription of *mga* and expression of Mga were reduced in a *ccpA* mutant strain; however, the expression of the Mga-regulated genes were not affected. Additional studies analyzing the role of CcpA in pathogenesis of the GAS, showed a "hypervirulent" phenotype in the absence of CcpA using two mouse infection models. Microarray analysis of the Δ*ccpA* strain determined that CcpA significantly represses the expression of *sagA*, the gene encoding the potent cytolysin, streptolysin S (SLS). Moreover, hemolytic activity due to SLS was increased in the Δ*ccpA* strain, and expression from P*sagA* demonstrated strong catabolite repression during growth in glucose compared to sucrose. Furthermore, purified GAS CcpA was shown to bind directly to the *cre* present in P*sag*A. The role of SLS in the increased pathogenesis of the Δ*ccpA* strain was investigated by the creation of a double mutant strain, which lacks the ability to secrete SLS. Importantly, systemic infection of mice with the Δ*ccpA sagB* double mutant resulted in complete attenuation of virulence and determined that the increased SLS expression is responsible for the "hypervirulent" phenotype in the absence of CcpA. Overall, these results have demonstrated a strong link between sugar metabolism regulation and virulence gene expression in the GAS.

TABLE OF CONTENTS

PRIOR PUBLICATIONS ..... **xiii**

List of Figures ..... **xv**

List of Tables ..... **xvii**

List of Appendices ..... **xviii**

List of Abreviations ..... **xix**

CHAPTER ONE: Introduction **1**

CHAPTER TWO: Literature Review **4**

HISTORICAL PERSPECTIVE **4**

CLASSIFICATION **4**

Hemolysis phenotype 4

Lancefield grouping 5

M and T antigen and opacity factor typing 5

Class determination 6

Microscopy and staining 7

Genetics 7

Growth requirements 8

CLINICAL DISEASE PRESENTATION **9**

Streptococcal throat infections 10

Streptococcal skin infections 12

Severe invasive streptococcal disease 14

Secondary sequelae 17

Vaccine strategies 19

VIRULENCE FACTORS **20**

Surface-associated factors 21

Secreted factors 27

Phage-encoded 30

REGULATION OF VIRULENCE **31**

Two-component systems 32

Stand-alone regulators 34

Other regulators 40

CARBON CATABOLITE REGULATION **41**

Phosphoenolpyruvate phosphotransferase system 42

Gram-negative CCR/ inducer exclusion 43

Gram-positive CCR 44

Evidence of CCR in the GAS 48

CHAPTER THREE: Materials and Methods **50**

BACTERIAL STRAINS **50**

Escherichia coli strains, media, and growth conditions 50

GAS strains, media, and growth conditions 50

DNA MANIPULATIONS **51**

Plasmid isolation 51

Chromosomal DNA isolation 52

Polymerase Chain Reaction 52

Enzymatic DNA modifications 55

BACTERIAL TRANSFORMATIONS **56**

E. coli competent cells 56

GAS competent cells 56

Electroporation 57
Temperature-sensitive allelic exchange 57
GENETIC CONSTRUCTIONS 58
Construction of insertional-inactivation mutation in *ccpA* 58
Construction of the P*mga* and promoterless luciferase transcriptional reporters 59
Construction of allelic exchange vector for *amrA* 60
Construction of recombinant GAS CcpA, HPr, and Hpr Kinase expression vectors 60
Construction of allelic exchange vector for creation of Δ*ccpA* strains 61
Construction of *ccpA* complementation vector 62
Construction of promoterless-Luciferase vector 62
Construction of P*mga*-Luciferase vectors 63
Construction of P*sagA*-Luciferase vectors 63
Construction of *sagB* insertional-inactivation vector 63
Construction of the P*mga* and promoterless luciferase reporter strains 64
DNA ANALYSES 64
Agarose gel analysis 64
Random prime labeling of probes 65
Southern blot analysis 65
RNA ANALYSES 66
RNA isolation 66
Northern blot 66
DNase I treatment. 67
Reverse transcriptase PCR 67
Microarray analysis 68
Real-time RT-PCR 70
PROTEIN ANALYSES 71

GAS protein extracts 71
SDS-PAGE gel analysis 71
Western blot analyses 71
Protein expression and purification 73
Streptolysin S hemolysis assay. 75
TRANSCRIPTIONAL REPORTER ASSAYS 75
GusA assay 75
Luciferase assay 76
MURINE INFECTION MODELS 78
Intraperitoneal route 78
Subcutaneous route 78
DNA-PROTEIN INTERACTIONS 79
PAGE oligonucleotide purification 79
Annealing double stranded oligonucleotides 79
Electrophoretic mobility shift assay 80
CHAPTER FOUR: CcpA-mediated carbon catabolite regulation and sugar metabolism influence the expression of *mga*. 82
INTRODUCTION 82
RESULTS 84
Identification of putative *cre* in the GAS genome 84
The catabolite control protein, CcpA, specifically binds to P*ccpA* and P*mga in vitro* 86
The *cre* is necessary for activation of P*mga* 89
Inactivation of *ccpA* affects *mga* expression 93
Inactivation of *ccpA* does not affect Mga-regulated genes 95
CCR and sugar metabolism affect *mga* expression and Mga-activity 96

Expression from P*mga* varies across growth 97

mga expression inversely correlates to glucose levels 99

Sugar source affects expression from *Pmga* 101

Deletion of AmrA reduces *mga* expression across growth 103

AmrA affects expression of *mga* and *emm* in a strain dependent fashion 104

DISCUSSION 106

The GAS *cre* 106

The role of CcpA and the *cre* in activation of *mga* expression 107

The influence of CCR on Mga-regulated genes 108

The influence of sugar metabolism on expression from P*mga* 110

AmrA-mediated activation of P*mga* is strain dependent 111

CHAPTER FIVE: CcpA-mediated repression of streptolysin S expression and virulence in the group A streptococcus 112

INTRODUCTION 112

RESULTS 114

A Δ*ccpA* mutant shows increased virulence in mice 114

Determining the CcpA regulon in GAS 119

Expression from P*mga* is reduced in the absence of CcpA 122

Expression of Streptolysin S (*sagA/pel*) is catabolite repressed by CcpA 124

CcpA binds directly to a *cre* in P*sagA* 128

Role of Streptolysin S in the CcpA-mediated repression of virulence 131

DISCUSSION 133

Defining the CcpA regulon of GAS 134

Determining a consensus GAS *cre* 137

CcpA represses virulence in mice 139

SLS is a CcpA-repressed virulence factor during GAS systemic infection 139

CHAPTER SIX: Conclusions and Recommendations 142

Direct link between regulation of sugar metabolism and expression of Mga 142

Identification of the CcpA regulon and its role in GAS pathogenesis 146

Global influence of metabolism on regulation in the GAS 151

Summary 155

APPENDIX I: Putative GAS *cre* from M1 SF370 156

APPENDIX II: MGAS5005 vs. isogenic Δ*ccpA* mutant microarray results 159

REFERENCES: 165

PRIOR PUBLICATIONS

Kinkel TL and McIver KS; *CcpA-mediated repression of streptolysin S and virulence in the Group A streptococcus*. Infect. Immun. 2008 Aug;76(8):3451-63

Kinkel TL*, Almengor AC*, Day SJ and McIver KS; *The catabolite control protein CcpA binds to Pmga and influences expression of the virulence regulator Mga in the Group A streptococcus*. J Bacteriology. 2007 Dec;189(23):8405-16 (*Co-first author)

Leday TV, Gold KM, Kinkel TL Roberts SA, Scott JR and McIver KS; *TrxR, a new CovR repressed response regulator that activates the Mga virulence regulon*. (Infect. and Immun. In Press)

THE UNIVERSITY OF TEXAS
SOUTHWESTERN MEDICAL CENTER
AT DALLAS

July 21, 2008

Journals Department
American Society for Microbiology
1752 N Street, N.W.
Washington, DC 20036-2904

To Whom It May Concern:

I am writing to request permission to reuse the information in the two papers listed below for my dissertation. This work, entitled "CcpA-mediated Carbon Catabolite Repression of Virulence in the Group A Streptococcus," will be used to fulfill the requirements set forth by the University of Texas Southwestern Medical Center for graduation from the Molecular Microbiology Program.

1) **Almengor, A. C., Kinkel, T. L., Day, S. J., and K. S. McIver.** 2007. The catabolite control protein CcpA binds to Pmga and influences expression of the virulence regulator Mga in the Group A streptococcus. Journal of Bacteriology **189:** 8405-16

2) **Kinkel, T. L., and K. S. McIver.** 2008. CcpA-mediated repression of Streptolysin S Expression and Virulence in the Group A Streptococcus. Infection and Immunity In Press

Thank you for attention to this matter,

Traci Kinkel

LIST OF FIGURES

Fig. 1: Depiction of the GAS virulence factors. 21

Fig. 2: PTS-dependent glucose transport and CCR 45

Fig. 3: Coomassie-stained SDS PAGE gel of purified proteins 74

Fig. 4: HPr phosphorylation reaction 74

Fig. 5: Comparison between Luciferase transcriptional reporters 77

Fig. 7: EMSA of *Pmga cre* using His-CcpA 88

Fig. 8: Real-time RT-PCR analysis of native P*mga* P1 and *mga* transcripts 90

Fig. 9: Deletion analysis of the P*mga* P1 promoter region 92

Fig. 10: Effect of a CcpA^{-} mutant on *mga* expression 94

Fig. 11: Real-time RT-PCR analysis of Mga-regulated genes in the *ccpA* mutant 95

Fig. 12: P*mga* and P*emm* GusA Assays with variable sugar source 97

Fig. 13: P*mga* luciferase assay for M6 GAS grown in THY broth or CDM 98

Fig. 14: Glucose variation P*mga* luciferase assay 100

Fig. 15: Luciferase transcriptional reporter assay for P*mga* grown in various sugars 102

Fig. 16: P*mga* luciferase assay in AmrA^{-} strain 104

Fig. 17: Real-time RT-PCR analysis of *mga* and *emm* transcripts in AmrA^{-} strains 105

Fig. 18: Model of transcriptional activation from P*mga* 109

Fig. 19: MGAS5005 Δ*ccpA* mutant and complementation 115

Fig. 20: A Δ*ccpA* mutant shows increased virulence in mice 118

Fig. 21: Validation of microarray studies 119

Fig. 22: P*mga* luciferase assay in Δ*ccpA* strain 123

Fig. 23: Streptolysin-S hemolytic activity is repressed by CcpA 125

Fig. 24: P*sagA* luciferase assay with varied sugar source 127

Fig. 25: EMSA with the P*sagA cre* 130

Fig. 26: Role of SLS in GAS systemic infection in mice..... 132

Fig. 27: Functions of CcpA-regulated genes 135

Fig. 28: GAS *cre*. 138

Fig. 29: Global regulatory interactions in the GAS 152

Fig. 30: Expression of the Mga regulon and SLS during the phases of GAS infection. 154

LIST OF TABLES

Table 1. Bacterial strains 51

Table 2. PCR primers 54

Table 3. Plasmids 59

Table 4. Real-time RT-PCR primers 69

Table 5. SDS-PAGE buffers 72

Table 6. Oligonucleotide probes 80

Table 7. Δ*ccpA* vs. MGAS5005 Microarray and Real-time RT-PCR validation 120

LIST OF APPENDICES

APPENDIX I: 156

Putative GAS *cre* from M1 SF370 156

APPENDIX II: 159

MGAS5005 vs. isogenic Δ*ccpA* mutant microarray results 159

LIST OF ABREVIATIONS

ackA	acetate kinase
ASPGN	acute post-streptococcal glomerulonephritis
arcA	arginine deaminase
AmrA	Activator of Mga regulon A
ARF	acute rheumatic fever
ATP	adenosine triphosphate
bp	base pair
BSA	bovine serum albumin
B. subtilis	*Bacillus subtilis*
CcpA	catabolite control protein A
CCR	carbon catabolite regulation
CD-1	Charles Dawley mice
cDNA	complementary DNA
cfu	colony forming units
cpm	counts per minute
C. perfringens	*Clostridium perfringens*
CovRS	control of virulence two-component system
cre	catabolite response element
DEPC	diethyl pyrocarbonate
DNA	deoxyribonucleic acid
DNase	deoxyribonuclase
dNTPs	deoxyribonucleic acid triphosphate monomers
DTT	dithiothreitol
E. coli	*Escherichia coli*
ECM	extracellular matrix
EDTA	ethylenediaminetetracetic acid
EI	enzyme I
EII ABC	enzyme II ABC proteins
emm	gene encoding M protein
EMSA	electrophoretic mobility shift assay

Fcr	Fc receptor
g	gravity
GAS	the group A streptococcus
GC	guanine and cytosine
gDNA	genomic DNA
GusA	ß-glucuronidase
His	histidine
HK	histidine kinase
HPr	histidine containing phosphocarrier protein
HprK	HPr kinase
hr	hours
Ig	immunoglobulin
Ihk/Irr	*isp*-associated histidine kinase and response regulator
i.p	intraperitoneal
IPTG	isopropyl-ß-D-galactopyranoside
isp	immunogenic secreted protein
kb	one-thousand base pairs
kDa	kilo-Dalton
L	liters
LB	Luria-Bertani medium
LD_{50}	lethal dose for 50 percent of animals
L. lactis	*Lactococcus lactis*
L. monocytogenes	*Listeria monocytogenes*
LTA	lipotechoic acid
luc	firefly luciferase gene
M	molar
MBS	Mga-binding site
Mga	multiple gene regulator of the group A streptococcus
min	minutes
µ	micro
Mrp	M-related protein

MsmR	multiple sugar metabolism regulator
NEB	New England Biolabs
ng	nanograms
Nra	negative regulator of the group A streptococcus
nt	nucleotide
OD	optical density
ORF	open reading frame
P(*gene*)	promoter designation
PAGE	polyacrylamide gel electrophoresis
PBS	phosphate buffered saline
PCR	polymerase chain reaction
pel	pleiotropic effect locus
PEP	phosphoenol pyruvate
PMN	polymorphonuclear leukocyte
PRD	PTS regulatory domain
PrtF1/SfbI	protein F/streptococcal fibronectin-binding protein
PTS	phosphoenolpyruvate phosphotransferase system
RALPs	RofA-like proteins
RR	response regulator
RivR	RofA-like protein IV
RNA	ribonucleic acid
RofA	regulator of protein F
RT	reverse transcriptase
S. aureus	*Staphylococcal aureus*
S. pneumoniae	*Streptococcus pneumoniae*
S. pyogenes	*Streptococcus pyogenes*
sag	streptolysin S-associated gene
s.c	subcutaneous
SclA	streptococcal collagen-like protein
ScpA	streptococcal C5a peptidase
Sda	phage-encoded streptodornase

SDS	sodium dodecyl sulfate
Sec	seconds
Sic	streptococcal inhibitor of complement
Ska	streptokinase
Slo	streptolysin O
SLS	streptolysin S
Sof	serum opacity factor
Spd	chromosomal streptodornase
Spe	streptococcal pyogenic exotoxins
STSS	streptococcal toxic shock syndrome
TCS	two-component system
THY	Todd-Hewitt yeast extract medium
TrxRS	two-component regulatory system X
v	volume
VIT	vectors for integration in Tn916
w	weight
WT	wild type

CHAPTER ONE:

Introduction

The group A streptococcus (GAS) is a strict human pathogen, which is responsible for a wide array of diseases ranging from the self-limiting, pharyngitis, to the severe invasive, necrotizing fasciitis (51). The incidence of GAS infection ranges from over 10 million cases of non-invasive to approximately 10,000 cases of invasive streptococcal disease. Although, the annual USA healthcare costs for treatment of GAS disease is approaching 500 million dollars per year, they are mainly associated with self-limiting infections; while the worldwide mortality rate, approximately 500,000 deaths per year, is associated with invasive streptococcal disease (156). GAS infections are also linked to several secondary sequelae including acute rheumatic fever, and glomerulonephritis, which necessitate treatment. While a vaccine is not available for prevention of GAS infections, self-limiting GAS infections are still treatable with penicillin; however, treatment of invasive GAS infections is not always successful.

Global transcriptional regulation of its many virulence genes represents a key step in the ability of the GAS to proliferate in the human host and cause such a wide variety of diseases (116, 153). The GAS senses the surrounding environment and in response, coordinately regulates the expression of factors required for survival. One of the major changes in the host environment that the GAS senses, are the availability of nutrients such as sugars. The GAS preferentially metabolizes glucose and therefore has adapted a regulatory system to prevent the ineffective utilization of alternative sugar sources when glucose is present. This mechanism, called carbon catabolite repression (CCR), is mediated by the transcriptional regulator carbon catabolite control protein A

(CcpA). CcpA mainly represses genes involved in alternative metabolism, but has recently been shown to regulate the expression of virulence factors in several closely related Gram-positive organisms. In addition to CcpA, there are many other global transcriptional regulators in the GAS, including the multi-gene regulator of the group A streptococcus (Mga), which regulates the gene encoding the major surface component, M protein as well as those for several other factors associated with virulence and evasion of the host immune response. Although, *mga* expression is autoregulated and is known to be strongly growth phase dependent, a specific signal for initiation of regulation has yet to be identified.

This study begins with the identification of a putative catabolite response element (*cre)* upstream of the P*mga* promoter. CcpA was found to specifically bind to this *cre*, and activate expression of *mga*. The *cre* was required for full expression from P*mga*, and shown to be required for expression from the P1 promoter. In the absence of CcpA, *mga* transcription and Mga expression were significantly reduced; however, expression of the Mga regulon was not affected. Further studies investigated the influence of sugar metabolism on transcriptional activation of *mga*. The results of these experiments support a model for CcpA-mediated activation of P*mga* P1, which leads to the production of Mga and further autoamplification of expression.

The second focus of research within this study assessed the role of CcpA in the pathogenesis of the GAS. A deletion of *ccpA* was made in a virulent strain of GAS, and was analyzed *in vivo* using two different mouse models of infection. Interestingly, the *ccpA* mutant strain resulted in a hypervirulent phenotype in both infection models. A transcriptome analysis identified that expression of *sagA*, the gene encoding streptolysin

S (SLS), which is a potent cytolysin, was highly upregulated in the *ccpA* mutant strain. It was shown that CcpA directly represses expression of *sagA* by binding to a *cre* present in the promoter. Moreover, the increased expression of SLS was found to be responsible for the hypervirulent phenotype seen in the mouse models of infection. The results presented within this dissertation indicate that CcpA contributes to both regulation of virulence and pathogenesis of the GAS.

CHAPTER TWO:

Literature Review

HISTORICAL PERSPECTIVE

Many in the 19th century had observed the presence of spherical organisms in chains, including Louis Pasteur, who identified these organisms in abscesses (187). In 1795 Gordon, had suggested that these spherical organisms were the communicable agent for puerperal or childbed fever (60). However, it was not until 1874, when Billroth described them using the Greek words *streptos,* for twisted chain, and *kokhos,* for berry or seed, that the name streptococcus became widely used (60). The streptococci were beginning to become associated with many other diseases as well, including epidemic outbreaks of pharyngitis and scarlet fever; pneumonia, and the common skin infections erysipelas and impetigo. The early nomenclature for the streptococci consisted of naming the species after the type of disease caused. This nomenclature system led to some confusion as to the classification of the individual organisms.

CLASSIFICATION

Hemolysis phenotype

The early nomenclature system for the streptococci resulted in the identification of many different streptococcal species, making the classification of these organisms more complicated. For example, the organisms isolated from patients of pharyngitis outbreaks, puerperal fever, Scarlet fever, and erysipelas became known as *Streptococcus epidemicus, Streptococcus puerperalis*, *Streptococcus scarlatinae,* and *Streptococcus*

erysipelatis, respectively. The classification of the streptococci became more ordered in the early 1900's when Schotmüller and later Brown began to separate the various streptococci based on their hemolytic reactions on blood agar plates (60). Their observations led to the current definitions of hemolysis where a greenish or partial clearance of the blood cells is called alpha (α) hemolysis, a full zone of clearing surrounding the bacteria is beta (ß) hemolysis, and no clearance or lysis is gamma (γ) hemolysis.

Lancefield grouping

To classify the ß-hemolytic streptococci, which she called *Streptococcus haemolyticus*, Rebecca Lancefield used an antisera-precipitin test for the presence of differing undefined antigens, termed C-antigens, from the various streptococci isolated from both human and animal origins. From her results, she concluded that the group A antigen in the precipitin reaction correlated to the strains isolated from human infection, whether it be Scarlet fever, tonsillitis or pneumonia (122). Further, she was able to determine that the specific antigen for the group A was carbohydrate in nature, later this was shown to be true for the other group antigens (B-E) as well. From Lancefield's pioneering experiments, the classification of the streptococci began to take shape and the group specific nomenclature for the streptococci is still used today.

M and T antigen and opacity factor typing

In addition to classifying the streptococci by carbohydrate antigen, Lancefield also developed a method for determination of the M-antigen present in the group A streptococcus (GAS). This method mixed acid extracts of the GAS, containing the M-

antigen, with a library of streptococcal antisera to determine the specific M-type based on the presence or absence of precipitate formation (120). Later, she was able to adapt her M-antigen typing protocol to a capillary precipitin test making it more practical for laboratory diagnostics and classification (211).

Griffith, who was also interested in the GAS, began to characterize the human isolates of ß-hemolytic streptococci, which he, like others, was beginning to believe were all the same organism, *S. pyogenes*. Similar to Lancefield, Griffith was interested in associating the various streptococcal diseases to the presence of certain antigens. To further his studies, he developed a slide agglutination test to classify the type of T-antigen present in the streptococcal extracts isolated from many types of diseases (84). Griffith's test was much more simple than Lancefield's initial M-antigen precipitin test, and thus was more readily used.

Another method for classification of the GAS is the characterization of an individual strain's ability to opacify serum. Developed in 1938 by Ward *et al.*, this method mixed the same streptococcal acid-extraction as Lancefield described with horse serum and then observing the opacity of the serum. Serum opacity was found to correlate specifically with M-type and was initially thought to be a property of the M protein (139). Since, all strains are not positive for opacity factor (OF), and due to its association with specific M-type, OF testing became useful in classification of the GAS.

Class determination

Although there were some factors that caused cross-reaction with the M protein, not much was known about them until 1989 when Bessen *et al.* determined that these factors were variable regions of the M protein (19). It was shown that one class of the

GAS appeared to have an extended conserved surface region of the M protein, whereas the other class seemed to lack this region of M protein but were mostly positive for serum OF. This led to the distinction of two different classes of the GAS; class I, containing an extended M protein, and class II, which lacks this conserved region of M protein but contains the added ability to opacify serum. Sequencing of many different genes has provided a stronger correlation to class based on the differing alleles present for a variety of genes including *emm* (15)*, mga* (235), and the presence or absence of *sof*.

CLASSIC CHARACTERISTICS

Microscopy and staining

One of the hallmark features of the streptococci is the chained-cocci appearance under the microscope, which many used to implicate the streptococci in specific diseases. Gram's staining technique showed that the streptococci, like the staphylococci, stained Gram-positive, indicating the presence of only one cell membrane and a thick peptidoglycan layer. While the streptococci share many identifying features in common, the GAS has a few characteristics that separate it from the other streptococci.

Genetics

There have been 12 different strains of the GAS sequenced encompassing 9 different M-serotypes (95). The GAS genome ranges in size from 1.83 to 1.93 Mbp, with the difference related to the number of bacteriophage present. The number of prophage can vary between strains, and currently strains have been found with the number of phage

ranging from as little as 2 to as many as 8 different prophage. Additionally, the number of predicted coding sequences varies from 1,697 to 1,987.

The first sequenced strain of GAS was the M1 serotype SF370 (72). This sequence showed a 38.5% G+C content, similar to other low G+C organisms in the lactic acid bacteria family. Sequencing identified that the GAS contains a complete glycolytic pathway, 14 different PTS-sugar transport systems, but lacks the genes necessary for a tricarboxylic acid cycle. In addtion, it was found that the GAS only contains the genes for synthesis of a few amino acids, however, there is a dedicated polyamine ABC transporter.

The SF370 genome is predicted to contain more than 40 different virulence factors, some of which will be discussed in the following sections. There were 13 predicted surface proteins containing the LPXTG motif and 6 new superantigen-like proteins identified. The genome from another M1 strain of *S. pyogenes*, named MGAS5005, has also been sequenced (206). This strain was isolated from the cerebrospinal fluid of an infected patient and contained the superantigen *speA2* allele. MGAS5005 was later found to be more virulent in animal models of infection and has an invasive phenotype due to a mutation in CovS (130). The MGAS5005 strain was also found to contain 36 Kb of an M12-like region with the additional virulence determinates Streptolysin O and NAD^+-glycohydrolase (206).

Growth requirements

The GAS is a facultative anaerobe, and is grown at 37ºC in either ambient air or at 5-10% CO_2. Like all streptococci, the GAS is both catalase and oxidase-negative. The

GAS is a nutritionally fastidious organism and has strict requirements for growth. *S. pyogenes* does not contain the necessary enzymes for a functional tricarboxylic acid cycle nor do they contain oxidative-cytochromes for electron transport; therefore they rely fully on fermentation of glucose for growth and energy production. The GAS is a member of the lactic acid bacteria and is homofermentative for lactic acid production from glucose fermentation (113). The specific components of the growth media for the GAS include neopeptone extracts, dextrose or glucose as the carbon source, and a complex mixture of nutrients from beef-heart infusion as first described by Todd and Hewitt in 1932 (216). The addition of 2% yeast extract to the Todd-Hewitt media (THY) was shown to further improve growth (222). The GAS is considered a multiple amino acid-auxotroph requiring nearly all amino acids to be present in the growth media (135).

CLINICAL DISEASE PRESENTATION

The GAS although only a strict human pathogen, causes a broad spectrum of clinical diseases ranging from the self-limiting to the severe invasive. For example, acute pharyngitis and the common skin infections impetigo and erysipelas are typical self-limiting GAS infections. Whereas, streptococcal toxic shock syndrome, septicemia, and necrotizing fasciitis are representative of severe invasive GAS disease. In addition to acute disease presentations, *S. pyogenes*-mediated disease is associated with several nonsuppurative sequelae, including acute rheumatic fever (ARF) and acute poststreptococcal glomerulonephritis (PSGN). The individual characteristics of each will be discussed, as well as diagnostic tests, available treatment options, and potential vaccines.

Streptococcal throat infections

Pharyngitis

Pharyngeal infections or abscesses of the throat were recognized as important in children's health in 1472 by Bagellardo (194). Today, the GAS is the most common bacterial cause of pharyngeal infection in children. In fact, GAS-mediated pharyngitis, or strep throat, comprises 15-20% of acute pharyngitis within children aged 5-15 (23). The major identifying clinical symptoms of streptococcal pharyngitis include: rapid onset, fever, swollen cervical lymph nodes, presence of erythema and exudates found on the tonsils and pharynx, occurrence of petechiae on the soft palate, and the absence of cough, diarrhea, runny nose, and conjunctivitis (194).

The current gold standard for diagnosis of strep throat involves swabbing of the throat, including the pharynx and tonsilar area, and culturing onto blood agar plates with incubation at 37ºC in 5-10% CO_2 for 24-48 hours. The plate is then checked for the presence of ß-hemolytic streptococci. Initial diagnosis is further confirmed by various methods, including microscopy, resistance to bacitracin, or latex agglutination tests (102). In 1993, a new diagnostic system for GAS-mediated pharyngitis was developed, which consists of an optical immunoassay that detects the Lancefield group A carbohydrate (90). This diagnostic system, known as the rapid-strep test, has provided a means for rapid diagnosis of strep throat, allowing clinicians to begin antibiotic therapy immediately. However, the rapid strep-test lacks sensitivity, and can yield a false negative. Therefore, those found to be negative should also be cultured onto blood agar for accurate diagnosis (102).

Since primary streptococcal infections are often self-limiting, the treatment of a such a disease, seems to be unnecessary. However, the association of streptococcal disease with rheumatic heart disease makes the complete eradication of this organism from the human host necessary. The GAS was first found to be susceptible to sulfonamides in the early 1940's. Although sulfonamides were not completely effective in eradication of the bacterium, they were still used to treat outbreaks of pharyngitis in attempts to reduce the spread of disease and as a prophylaxis (194). From the discovery of the antibiotic penicillin in 1928, to now, at least 60 years since mass production of this drug began, the GAS is still sensitive to penicillin and it remains the drug of choice for treatment of GAS-mediated pharyngitis (52). Additionally, for treatment of those with allergies to penicillin, the macrolide erythromycin is commonly used, although there are recent reports indicating that resistance is developing to this drug (234).

Scarlet fever

Although scarlet fever was once a more prevalent illness with a mortality-rate approaching 25-35%, the occurrence of this disease today is very rare and much more mild in nature (201). Due to a clinical appearance that is similar to measles, scarlet fever wasn't recognized as an individual disease until Sydenham noted the differences between the two, in the late 1800's. The clinical symptoms of scarlet fever were classified by Weaver into 2 major categories: benign or malignant (202). The benign cases could range from mild to moderate and would usually present with pharyngitis, a rash across the chest, fever, erythema of the cheeks, and strawberry tongue (41). The malignant forms of scarlet fever include a toxic and a septic variety, which are more severe and often result in death. The clinical manifestations of the toxic form of scarlet fever

includes a more acute form of benign disease with exceptionally high fever ranging from 107º-108ºF, delirium, and painful swollen cervical lymph nodes. A more severe case of toxic scarlet fever might present an even higher fever, convulsions, and death within 24 hours of onset of disease (202). The toxins mediating this severe variety of scarlet fever are the streptococcal pyrogenic exotoxins A and C, which have historically been associated with more severe outbreaks (24). The septic form of scarlet fever is more invasive in nature and historically has been described by many as the anginose form. Again the common features are similar, although more severe than benign scarlet fever, with the added local soft-tissue invasion at the site of infection. This leads to further complications such as necrosis of the tonsils and surrounding area leading to airway blockage, severe otitis media with rupture of the eardrum, and death (202). Scarlet fever epidemics were frequent prior to the introduction of antibiotics, and either due to the increased use of antibiotics or an attenuation of *S. pyogenes,* has diminished the incidence of this often-fatal childhood disease.

Streptococcal skin infections

Impetigo

Another common disease manifestation caused by the GAS is the skin infection called streptococcal pyoderma or impetigo. This disease is an infection of the dermis not extending beyond the deeper layers of the epidermis (8). A small lesion on the skin of the extremities usually the legs, characterizes typical disease, which is most common in children aged 2-5. This lesion can have the release of a characteristically clear fluid, which can build up into a crust surrounding the lesion. Staphylococci are also frequently

recovered from pyodermic lesions, which has led to confusion as to the specific disease-causing agent. Treatment of known streptococcal-mediated impetigo is penicillin, just as for normal streptococcal pharyngeal infection. However if the identity of the infecting agent is unknown, the use of antistaphylococcal drugs like erythromycin should be used for treatment instead (8). Several serotypes of GAS have been associated specifically with skin infection, notably strains that were initially thought to lack M protein production and were found to have similar T-antigen patterns (13). Unlike streptococcal pharyngitis, which is linked to the secondary sequelae of rheumatic fever, impetigo is linked to acute glomerulonephritis, both of which will be discussed later in this chapter. The incidence of streptococcal pyoderma is usually limited to warmer, humid climates and occurs more frequently during the summer months (41).

Cellulitis and erysipelas

Cellulitis is a streptococcal infection of the sub-cutaneous layer of the skin. Cellulitis results from skin irritation such as a burn or a puncture wound that can push the bacteria deep into the epidermis layers. Additionally, cellulitis is frequently associated with individuals that have chronic poor circulation. The symptoms are swelling, redness and heat at the site of infection, and fever may be present. Cellulitis usually responds well to penicillin treatment, and is typically cleared within a week (201).

Erysipelas is a more acute localized form of cellulitis, affecting the superficial layers of the skin. Erysipelas was recognized by Fehleisen in 1882, as its own disease and was referred as *S. erysipelatis* (60). Erysipelas comes from the Greek words meaning red skin, which along with presence of fever, is the defining characteristic for this

infection. Often the reddened skin has a raised border, and as the lesion begins to spread the point of origin for infection is apparent (41). Although it was a common disease in the 19th century, it occurs rarely today and is mostly seen in young children and elderly patients, who can have frequent recurrences of infection (41). Usually this disease occurs on the face or extremities but the torso variety is more severe especially without treatment. As with other GAS infections, penicillin is the treatment of choice.

Severe invasive streptococcal disease

Puerperal fever

One of the most significant diseases of the 19th century was childbed or puerperal fever. This disease of women who had recently given birth had a very high associated mortality rate. This disease often would sweep through the maternity wards in epidemic proportions. Puerperal fever is essentially a systemic disease caused by infection of the genital tract of postpartum women, which can lead to infection of the endometrial lining of the uterus and spread to the bloodstream (201). Although this disease was known to be communicable since 1795, it wasn't until the mid 19th century when Thomas Watson and Oliver Wendell Holmes suggested that physicians were responsible for transmitting puerperal fever. Semmelweis, whose pivotal presentation in 1846 showed that puerperal fever was indeed caused by lack of hand washing by doctors, further cemented the need for better hygiene and sterile technique within the hospital setting to prevent disease outbreaks (60). This disease was once responsible for the deaths of many women bearing children. However, the incidence of puerperal fever today is infrequent and with early diagnosis and antibiotic treatment it is rarely fatal.

Streptococcal toxic shock syndrome and bacteremia

Although, disease caused by the GAS is normally localized to the throat and skin, in some occasions, infection can spread to the bloodstream. Bacteremia, caused by the GAS, is occasionally found in burn patients, those with varicella (chickenpox) infection, the immunocompromised, young children, and intravenous drug users. Cases of sepsis from GAS in children typically result from streptococcal pharyngeal infections, whereas in the elderly it more commonly emanates from skin infections (202). Streptococcal bacteremia is a severe infection that will usually end in death without prompt intravenous antibiotic treatment.

More recently, the GAS has been associated with streptococcal toxic shock syndrome (STSS). Toxic shock refers to the hyper-response of the immune system that can cause multiple organ failure and ultimately death. The main cause for the severe symptoms of toxic shock is related to the superantigens found in the GAS. Most of the GAS superantigens are streptococcal pyrogenic exotoxins (Spe), which have been acquired from phage. Superantigens have the capacity to directly bind the T-cell receptor to the class II MHC without the presence of a specific antigen, which over stimulates the immune system and leads to T-cell proliferation and extreme production of a variety of cytokines including TNFα leading to tissue damage (138) (24).

The clinical presentation of STSS consists of rapid onset of fever, high blood pressure, chills, nausea, confusion and pain. Unlike the staphylococcal form of toxic shock syndrome, the streptococcal form does not result from tampon use; rather it is often associated with other streptococcal disease presentations including bacteremia. The

progression of STSS is extremely fast and can lead to multiple organ failure and death within 24-48 hours of onset. Specific M-types 1 and 3 have been found to have a higher association with STSS and invasive disease than other M-types (51). Treatment for STSS varies, and usually includes i.v. antibiotics; however, penicillin is not very effective and approximately 50% of patients still die. Nevertheless, recent evidence suggests the use of the antibiotic clindamycin, an inhibitor of protein synthesis, has a better success rate (51).

Necrotizing fasciitis

Necrotizing fasciitis was identified as a disease associated with hemolytic streptococcal infection by Pfanner in 1918. However, it was Meleney, in 1924, that recognized that streptococcal gangrene was an entirely separate presentation of disease for the GAS (146, 200). Although the GAS is one of the main causes of necrotizing fasciitis, several other organisms such as *Clostridium perfringens, C. septicum, Staphylococcus aureus* as well as a mixture of both aerobic and anaerobic bacteria can contribute to a similar disease progression. Due to the massive tissue damage occurring during infection, this disease has been spotlighted in the media as the 'flesh-eating disease'. The infection can begin with direct inoculation during a surgical procedure or with a relatively minor wound, which becomes immediately painful, and swells with heat produced at the site of infection. Within 24 hours of the initial injury, the redness surrounding the infection site begins migrating outward. The disease continues to develop very rapidly as bullae filled with fluid begin to form at 24-96 hours. Destruction of the tissue is severe and gangrenish as the skin and subcutaneous fascia become necrotic. At this point in the disease progression, the patient is very weak with fever and delirium as the organism can enter the bloodstream and cause sepsis and toxic shock.

Historically, this disease was treated with severe debridement of the tissues surrounding the site of infection to prevent further spreading, and in severe cases amputation (146). Through the use of this treatment was associated with a mortality rate as low as 20%, in modern times the rate has increased to 30-60% despite the use of antibiotics. About half of the cases of necrotizing fasciitis lead to a more severe form called myositis, which involves the spread of infection to the muscle tissue and results in a much higher rate of death approaching 100% (202).

Secondary sequelae

Acute rheumatic fever

Acute rheumatic fever (ARF) is a major nonsuppurative sequel of GAS infections and necessitates the treatment of even the self-limiting variety. ARF or rheumatic heart disease was the leading cause of heart disease in children in the 19th and early 20th centuries. The symptoms of ARF were fully recognized and described by Cheadle in 1898, although it wasn't until 1931 that the connection between GAS infection and ARF was made separately by Coburn and Collis (60).

The link between ARF and streptococcal infections, of pharyngeal origin has been shown to be an autoimmune disorder, where the immune system is triggered by the GAS antigens and begins cross-reacting with self-epitopes. There is growing evidence supporting a role for cell-mediated immune response in the advancement of ARF. Regions of the M protein have been shown to be ligands for stimulation of T cell activation (87, 228). Further studies have shown specific GAS antigens including the

group A carbohydrate and M protein trigger the production of myosin cross-reactive antibodies (50, 56).

In 1944, Jones developed specific criteria that defined ARF to aid in diagnosis preventing both over and under identification of this disease (108). The specific Jones criteria require the identification of two major manifestations or one major manifestation with two minor manifestations. The major manifestations are as follows: evidence of carditis with associated heart murmurs, polyarthritis, Sydenham's chorea, subcutaneous nodules, and erythema marginatum rash. There are minor manifestations as well including both the clinically related aspects of previous incidence of ARF, arthralgia, and fever; and the laboratory aspects of increased presence of acute phase reactants, sedimentation rate of erythrocytes, presence of C-reactive protein, and prolonged P-R interval in an electrocardiograph. These characteristics have been periodically reviewed and subsequently modified to include prior history of GAS disease as a condition of diagnosis and treatment (53).

The full effects of ARF cannot be cleared by treatment, although the use of the anti-inflammatory salicylates and steroids have reduced the symptoms of carditis, arthritis, and fever. In addition, penicillin should be administered prophylactically to eliminate remaining GAS and prevent further recurrence of this disease (137). ARF can lead to the severe complication of congestive heart failure requiring immediate treatment and a lifetime of monitoring and care.

Acute poststreptococcal glomerulonephritis

Acute poststreptococcal glomerulonephritis (ASPGN) is associated with preceding GAS infection, which affects the kidneys and can lead to renal failure. This disease is most common in children aged 2-6, and usually presents as clinical disease more often in young boys. ASPGN results after both pharyngeal and GAS skin infections, although the latent period is longer from the skin infections at about 3 to 6 weeks compared to 1 to 3 from throat infections. Symptoms of ASPGN most often include high blood pressure, edema, particularly in the kidneys, and the presence of blood in the urine. Diagnosis of ASPGN requires urinalysis testing for the presence of blood and proteins, an analysis of the streptococcal antibody profile, and the levels of complement protein in the blood. The pathogenesis of ASPGN is thought to be due to the affinity of a streptococcal protein for the glomerulus triggering a localized complement-mediated response and the build up of antibody complexes (96). Like in ARF, the M protein also appears to play a significant role in ASPGN, specifically in the development of antibody complexes found in the glomeruli (109). In addition, certain M-types including 1, 4, 12, 49, 55, 57, and 60 have been associated with ASPGN and have been termed nephritogenic strains (230). Although ASPGN infections can spontaneously clear within a week, the treatment for ASPGN mainly targets lowering the hypertension and reducing edema, which can usually be accomplished with a diuretic (96).

Vaccine strategies

Several antigens have been suggested as targets for a preventative vaccine against the pharyngeal strains to protect against the secondary sequelae, and the life-threatening

diseases caused by invasive strains of the GAS. Most notably, Lancefield showed that protective antibodies against M protein were produced during GAS infection (121). Several groups initially identified specific regions of the M protein that produced protective antibodies against GAS and began tests in humans (14, 165). However, it was later shown that antibodies to M protein could sometimes be cross-reactive to cardiac myosin, which limited the release of these vaccines for human use due to their potential relationship to ARF (56). Moreover, the early vaccine candidates were M-type specific as attempts to make a vaccine to the conserved region of M protein failed, and would therefore only provide protection against one M-type. This has led to the recent attempts to construct multivalent GAS vaccines, originally containing 4 then 8 and now 26, of the most common M-types (54, 55, 57). In addition to M protein, several other GAS antigens have been candidates for vaccine targets, including the C5a peptidase (158) and the group A carbohydrate (184). With the new advances in developing GAS vaccines, the potential for a viable vaccine in the future seems optimistic.

VIRULENCE FACTORS

The GAS possesses many virulence factors that are necessary for pathogenesis in both animal models of infection and the human host. There are several different varieties of GAS virulence factors including those that are surface-associated, those that are secreted, and those that are phage-associated (Fig. 1). These factors play important roles in establishing infection in the human host like adhesion, immune evasion, spread, and nutrient acquisition.

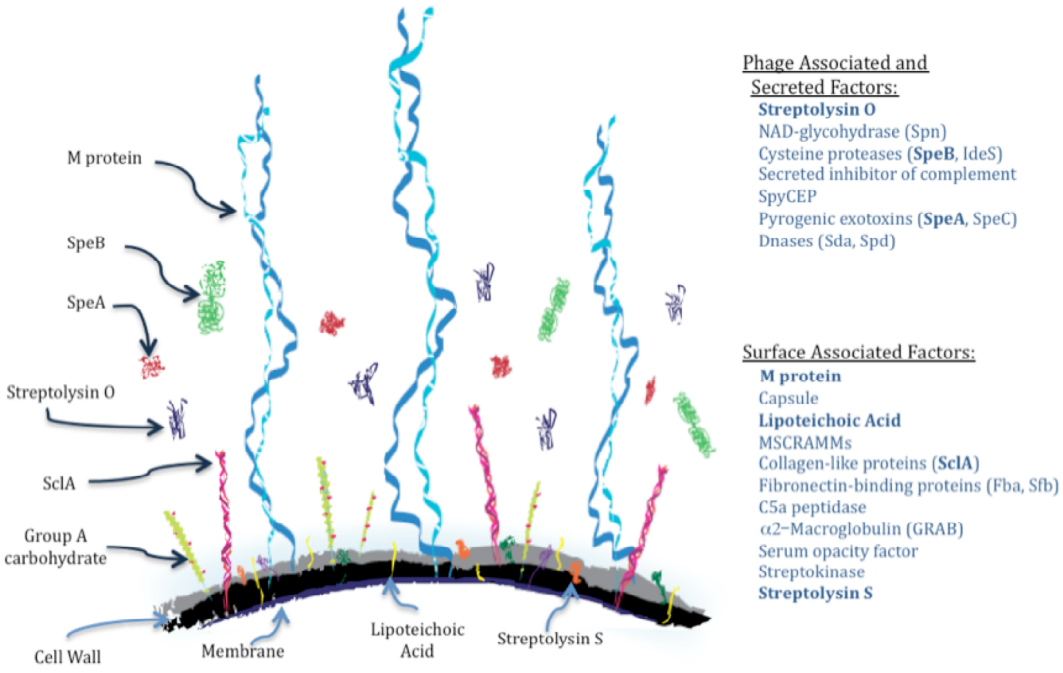

Fig. 1: Depiction of the GAS virulence factors.
Shown above are surface-associated, secreted, and phage-associated virulence factors of the GAS.

Surface-associated factors

Microbial Surface Component Recognizing Adhesive Matrix Molecules (MSCRAMMS)

The GAS contains several MSCRAMMs, which generally consist of proteins of similar structure that have a ligand-binding domain with between 3-6 repeat regions of 40-50 amino-acid-residue motifs (105). The main adhesion targets for the GAS MSCRAMMs tend to be components of the host extracellular matrix such as fibronectin. Several different types of GAS MSCRAMMs will be discussed below.

Lipoteichoic acid

One of the main characteristics of Gram-positive cell walls is the presence of lipoteichoic acid (LTA), which are the teichoic acid molecules attached by lipid anchors (Fig. 1). LTA is the main contributor to the hydrophobicity of the GAS cell wall (149). Although the precise function of LTA remains unknown, LTA does appear to play a role in adhesion to epithelial cells by binding to fibronectin (91). Additionally, it is known that LTA is a pathogen-associated molecular pattern (PAMP) recognized by toll-like receptors in the innate immune response (4).

Hyaluronic acid capsule

The hyaluronic acid capsule of the GAS, encoded by the *has* operon (*hasA-C*), is composed of repeating units of glucuronic acid and N-acetylgucosamine. The presence of capsule leads to the mucoidy or glossy colony phenotype observed by Todd in 1928 (119). The hyaluronic acid capsule mediates resistance to phagocytosis and has been established as a virulence factor in several different animal experiments showing the necessity for the presence of capsule in pathogenesis of the GAS (232, 233). The GAS hyaluronic acid found in the capsule is identical to human hyaluronic acid, thereby providing a mechanism to evade the host response. In addition, capsule is important in adherence and binds the hyaluronic acid receptor CD44 found on epithelial cells, the same receptor for human hyaluronic acid (185).

M protein

The major surface protein of the GAS is the M protein, which is encoded by the gene *emm* and is a coiled-coil protein with roles in adherence and immune evasion (Fig.1). M protein initially was important for classification of the GAS, but has since played a significant role in GAS research. The M protein is highly variable, and thus there have been over 80 different M-types of the GAS isolated since Lancefield's early studies.

As the major virulence factor of the GAS, the M protein is required for the pathogenesis of GAS. Studies in both mice and baboons showed that M protein mutants were completely attenuated for virulence (10, 46). One of the main functions of the M protein is adhesion, it is shown to play a role in binding to many different molecules for example: sialic acid in both pharyngeal epithelial cells and mucin (183), the complement regulatory components factor H (106) and C4 binding protein (214), human serum albumin and IgG (2), and fibronectin (31). In addition, the M protein functions in immune evasion, by both prohibiting phagocytosis via binding complement factor H, and preventing the deposition of the complement factor C3b on the surface of the GAS (98).

Most strains of the GAS typically produce 1-3 M or M-like proteins, which in some cases leads to correlation with disease type (21). The genes encoding the M-like proteins, including *mrp, arp, emmL, fcrA, sir, enn,* and *sph,* have been categorized by their structural organization (51). The M-like proteins are structurally related to M protein, containing similar domains for variable antibody (Ig) binding capabilities (26).

Streptococcal collagen-like protein

The streptococcal collagen-like protein (SclA) as its name implies is similar to collagen in structure, and has been shown to be important in adhesion (Fig. 1). It was found that SclA binds to lung epithelial cells (130) and fibroblasts (170), but not pharyngeal cells (172). Additionally, studies with mutant strains lacking SclA have shown the importance of this adhesin in GAS pathogenesis (130, 172). Recently, it has been shown that SclA binds a potent inhibitor of fibronolysis, and, via the recruitment of plasmin to the surface of the GAS, activates its anti-immune functions (157). Also, SclA binds to $\alpha_2\beta_1$ integrins leading to internalization and similar to M protein, it interacts with factor H to inhibit the alternative complement pathway (33, 34).

Fibronectin binding proteins

The GAS encodes a large number of fibronectin (Fn)-binding proteins, although not all are present in every strain (168). These Fn-binding proteins include Sof (49), protein F (SfbI) (89), protein F2 (SfbII) (101), SfbX (103), FbaA (212) and FbaB (213), Fbp54 (47), PFPB (181). The presence of multiple Fn-binding proteins strongly indicates the importance of this function in human host infection. Studies have shown a relationship between specific Fn-binding proteins with severity of disease (213). Fn-binding proteins are also important for internalization of the GAS, and therefore persistence after antibiotic treatment (155).

C5a peptidase

The C5a peptidase cleaves the complement chemotaxin C5a and prohibits recruitment of polymorphonuclear leukocytes (42). This surface-associated endopeptidase is important for virulence in the subcutaneous and intranasal colonization models of infection (104). In addition, the C5a peptidase as mentioned previously in the vaccine section, has become a candidate for a GAS vaccine to reduce nasal carriage (158).

Protein G-related α_2-macroglobulin-binding protein

The protein G-related α_2-macroglobulin-binding protein (GRAB) is an inhibitor of both human and GAS proteases (171). The gene encoding GRAB, *grab,* is found in all strains of GAS that have been tested (217). Several studies have identified a role for GRAB in virulence, with GRAB mutants being attenuated in two different mouse models of infection including a systemic infection and a localized subcutaneous skin infection model (171, 217).

Serum opacity factor

In addition to being useful in classification, the serum opacity factor (Sof) is an important adhesin for the GAS. Several studies have shown that Sof binds fibronectin (49) and fibrinogen (48) as further means for this organism to attach to host cells. Furthermore, inactivation of *sof* leads to attenuation in mouse models of infection (49). Recently, the mechanism of serum opacification was shown to be due to the binding of

high-density lipoproteins (45), which plays a role in reducing the antagonistic LTA induced-inflammation (86).

Streptokinase

Streptokinase (SK) is important in the spread of GAS infections, and is a potent activator of plasminogen. Surface-bound SK interacts with plasminogen that binds specifically to plasminogen-binding proteins on the surface of the GAS, to activate the conversion of plasminogen to plasmin. Interestingly, SK can only activate human plasminogen (178), and studies have shown increased virulence in mice that are transgenically expressing human plasminogen (209). In addition, the study has shown that a reduction in human plasminogen by treatment with snake venom reduced mortality of GAS infection, indicating that human plasminogen is a host susceptibility factor for pathogenesis of the GAS (209).

Streptolysin S

Streptolysin S (SLS) is an oxygen-stable cytolysin/hemolysin responsible for the ß-hemolytic phenotype seen on a blood agar plate. SLS is primarily cell surface-bound, which is thought to be due to its association with LTA (Fig. 1). This cytolysin lyses a variety of cell types including erythrocytes, lymphocytes (99), neutrophils, platelets, and even intracellular organelles such as mitochondria and lysozomes (110). The cytolytic capabilities of this toxin make it a potent virulence factor *in vivo* as studies in mice using the subcutaneous skin infection model show almost a complete reduction in pathogenesis

with SLS mutant strains (22, 59, 74). In addition to being able to lyse cells, SLS can also activate inflammation, and inhibit neutrophil phagocytosis (25, 81).

The structural toxin SLS is encoded by *sagA*, a streptolysin-associated gene (*sag*), and is the first of a 9-gene operon. It has since been shown that all genes within the *sag* operon are required for secretion of the mature toxin and production of the ß-hemolytic phenotype (59). A recent study has assigned functions to the other 8 genes in this operon, and determined that specific modifications made to the propeptide toxin are heterocycles (123). Initially, SLS proved difficult to characterize, purify, and develop antibodies against. However, it was later found that SLS is a propeptide that is stabilized in the presence of RNA, albumin, or a detergent agent such as Tween (80). Although, SLS is non-immunogenic in the human host, neutralizing antibodies were developed to the C-terminus of SLS peptides to inhibit hemolytic function of SLS (32). Furthermore, the mechanism of lytic activity by SLS was shown to be parallel to that of the complement pore forming activity (32).

Secreted factors

Streptolysin O

Another secreted cytolysin/hemolysin is the oxygen-labile streptolysin O (SLO) (Fig. 1). This protein is a cholesterol dependent cytolysin, which like SLS is a pore-forming toxin. However, due to its sensitivity to oxygen, SLO does not contribute to the ß-hemolytic phenotype. SLO is secreted as a monomer, which binds cholesterol to insert itself into the membrane, a pore as big as 30 nm can be formed when multiple monomers have inserted into the membrane (190). Recently, it was discovered by Caparon and

colleagues, that SLO is part of the cytolysin-mediated translocation (CMT) directed secretion apparatus of the GAS by forming the pore in eukaryotic cell membranes through which streptococcal proteins are secreted (133).

S. pyogenes NAD-dehydrogenase

The only identified effector protein secreted by the CMT system is *S. pyogenes* NAD-dehydrogenase (Spn), whichis encoded by the gene *nga*. Evidence from early experiments using SLO mutant strains of GAS, noted that there was a loss of additional effects on the host cell, which could not be fully attributed to the absence of SLO alone. It wasn't until the mechanism of the CMT system was determined that Spn was discovered to be the cause of the induced apoptosis and cytoskeleton rearrangement (182). In addition to producing nicotinamide, the GAS Spn also produces cyclic ADP-ribose, making it more similar to eukaryotic NAD^+ glycohydrases (27). Moreover, it was shown that Spn contributed to host-cell cytotoxicity, inhibited bacterial internalization into host cells by modulating actin rearrangement, and induced apoptosis likely through increased flux of calcium ions (27).

Streptococcal pyrogenic exotoxin B

Despite the name, the streptococcal pyrogenic exotoxin B (SpeB) is neither phage-encoded nor currently considered a superantigen, but performs many other immune-evading functions, including cleavage of streptococcal surface proteins, which are bound to opsonizing antibodies. SpeB, a cysteine protease, was first characterized in 1945, and was later shown to autocatalytically cleave its zymogen form into the active

form (68, 125). SpeB has also been shown to cleave streptococcal IgG binding proteins such that for the recruitment of complement to occurs away from the bacterial surface (224). Moreover, SpeB is involved in spread of the organism by cleavage of streptococcal surface proteins such as fibrinogen binding proteins like Protein F and Fba, which have tethered the organism to the host cells (169, 231). In addition to streptococcal proteins, SpeB can also cleave antibodies, specifically IgG, at the flexible hinge region (44). The link between SpeB and virulence remains unclear; some studies suggest an impact on pathogenesis (129) via the formation of necrotic lesions (69), whereas others studies show that reduction in SpeB has no effect on virulence systemically (9).

IgG degrading enzyme of S. pyogenes

The IgG degrading enzyme of *S. pyogenes* (IdeS) was identified following the unexpected cleavage of IgG in the absence of the known IgG-degrading SpeB (225). Identical to SpeB, IdeS cleaves IgG at the hinge region resulting in the production of 2 Fab fragments and the Fc portion. IdeS, however, is only able to cleave IgG, and does not exert any proteolytic affect on other antibody classes. IdeS also interferes with Fc-mediated phagocytosis by PMNs by degrading of the suface-bound IgG (225).

Secreted inhibitor of complement

The streptococcal secreted inhibitor of complement (Sic) was originally shown to prevent the deposition of the complement membrane attack complex (MAC) on the surface of *S. pyogenes* (3). However, due to the large peptidoglycan present in Gram-

positive organisms, the GAS is intrinsically resistant to complement-mediated lysis by the MAC. A recent study has identified additional functions of Sic, including the binding and inhibition of lysozyme, and secretory leukocyte proteinase inhibitor (71).

S. pyogenes cell envelope protease

The *S. pyogenes* cell envelope protease (SpyCEP) was found to be a protease capable of degrading human chemokines. SpyCEP was first shown to cleave the cytokine IL-8, which recruits and activates neutrophils to the site of tissue injury (65). Moreover, it was shown that SpyCEP additionally functions to cleave both the granulocyte chemotactic protein 2 and the growth-related onco-gene alpha (208). Furthermore, SpyCEP was shown to reduce localized lesion size, presumably by the decreased presence of inflammatory neutrophils at the site of infection (208).

Phage-encoded factors

Pyrogenic exotoxins

Although not all of the GAS pyrogenic exotoxins are phage-encoded, the two most notable, SpeA and C, are found on streptococcal-phage and are associated with STSS. In addition, there are many other exotoxins: SpeG, SpeH, SpeJ SpeI, SpeK, SpeL, SSA, SMEZ, and SMEZ-2. Not all exotoxins are present in all strains, and there are also different alleles of some, suggesting the potential for varied functions. In addition, not all exotoxins are phage-encoded, although most of those listed above are present in the various phage of the GAS. The structures for SpeA, SpeC and SMEZ-2 exotoxins have been determined, and were found to be similar to the superantigens of *S. aureus*. As

discussed in the STSS section, superantigens can simultaneously bind the T-cell receptor to the class II MHC directly, mediating extreme expression and release of cytokines (24, 138).

DNases

The GAS has many phage-encoded DNases associated with innate immune evasion and virulence. Not all DNases are present in every strain of GAS due to the variations in phage present, although every strain tested has DNase function (229). Several recent studies have implicated the various DNases in evasion of the innate immune response by degradation of the neutrophil extracellular traps, or NETs (28, 205). In addition, one of the DNases or streptodornases expressed by some strains of GAS, SdaD2, has been shown in two different animal models of infection to contribute significantly to virulence (205). Furthermore, the DNase Sda1 has been shown to be involved in the switch to invasive GAS infection (227).

REGULATION OF VIRULENCE

The GAS controls the expression of virulence factors through a variety of mechanisms. Unlike *E. coli* and *Bacillus* sp., the GAS does not appear to regulate virulence through alternative sigma factors. The GAS contains 13 two-component signal transduction systems (TCS), which sense the surrounding environment and coordinately regulate gene expression. In addition to TCS, GAS has growth-phase specific virulence regulators, termed stand-alone response regulators (SARR), including Mga, RALPs, and Rgg/RopB. The SARR coordinately control factors that are important for various phases

of the GAS host-pathogen life cycle (116). Furthermore, a direct link between sugar metabolism and regulation of virulence has begun to appear in many pathogenic Gram-positive organisms including the GAS.

Two-component systems (TCS)

The canonical TCS found most bacteria consists of a histidine kinase (HK) and a response regulator (RR). The HK usually resides in the membrane and receives a signal from the surrounding environment, which triggers an autophosphorylation event. This phosphate is then transferred to the receiver domain on the RR. The RR, a transcription factor, then mediates gene regulation by binding to DNA.

CovR/S

The most highly studied TCS in the GAS is the CovRS system named for control of virulence, which is also called CsrRS. The CovRS system has been shown to regulate approximately 10-15% of the GAS genome. CovR represses several important virulence factors including the genes encoding the hyaluronic acid capsule synthesis operon, SLS, Ska, SpeB, the DNase Sda (70, 82, 92), and the transcriptional regulator RivR (179). Interestingly, mutations in CovR and CovS have different effects on gene expression. CovR mutants show increased virulence in several animal models of infection and lead to a more severe invasive phenotype, whereas mutations in CovS do not alter gene expression of the virulence factors SLS and Sda (58). Additionally, CovRS plays an important role in responding to environmental stresses (58). Recent evidence suggests that the GAS incurs spontaneous mutations in CovS *in vivo* that allow further adaptation to the host environment and a more invasive disease progression (227).

Ihk/Irr

The TCS Ihk/Irr is named for immunogenic secreted protein (Isp)-associated histidine kinase and response regulator, respectively. Initially it was predicted that Irr would regulate Isp, located directly upstream from it, however this has never been shown (70). This TCS is highly expressed during acute pharyngitis and plays a direct role in the resistance of the GAS to PMN-mediated killing (226).

FasBCAX

The FasBCAX is an unusual TCS in that it contains 2 histidine kinases, a RR, and a small RNA that appears to be a regulatory component of this system (115). The Fas TCS regulates genes in a growth-phase dependent manner, and was initially thought to be a regulatory switch for transitioning from adherence to invasive gene expression (115). However, it was later shown the FasX regulatory RNA regulates genes important for adhesion and internalization, as well as cytotoxins, which may lead to induction of the host cell apoptosis response (112).

TrxRS

Recent work has characterized the tenth TCS or two component regulatory system X (TrxRS). TrxRS is repressed by CovR and is involved in virulence. A TrxR mutant was attenuated in the mouse subcutaneous skin infection model. Furthermore, microarray studies found that TrxRS positively influences the Mga regulon, which suggests the likely mechanism for the observed attenuation in the animal studies (T. Leday, and K. Gold unpublished data).

Other GAS TCS

Although the GAS contains 13 TCS, only the three discussed above have been researched in detail. However, 2 recent studies have begun to look at the remaining GAS TCS. One study assessed the contribution of 4 TCS *in vivo*, and found that mutations the MGAS5005 Spy0680/0681 TCS appeared to increase virulence in the soft-tissue mouse model of infection and up-regulation of several factors important in the host-pathogen interaction such as C5a peptidase, Sic, SilD, and PrtS (196). Additionally, this study identified several TCS that appear to be important in regulation of metabolic genes. For example, the MGAS5005 TCS Spy 0784/0785 appears to regulate the nearby mannose/fructose PTS operon, and the Spy 0830/0831 TCS is important in malate transport (196). Lastly, a study evaluating the growth of GAS in human saliva identified a TCS, SptRS, that enables the organism to persist in saliva (193).

Stand-alone response regulators

Mga

Another well-characterized system in the GAS is the multiple gene regulator of the group A streptococcus or Mga. Initially, Mga was identified because it was part of a locus found to regulate the major surface M protein and the loss of Mga resulted in an avirulent phenotype (197). Later it was shown that Mga had homology to DNA-binding proteins such as TCS RR (159). Because it lacks the typical sensor kinase, Mga was classified as a stand-alone response regulator (116).

Beyond regulating the M protein, it was found that Mga regulates several genes important for early stages of infection. Mga regulates genes important for colonization,

adherence, and immune evasion in a growth-phase dependent fashion including M protein, Fba, SclA, C5a peptidase, Sic and Sof (97, 143). Additionally, Mga autoregulates its own expression and is only transcribed during exponential phase, although Mga protein persists into stationary phase (145, 175). Furthermore, a recent study identified another core gene of the Mga regulon using comparative microarray analysis; this gene was named *grm* for gene regulated by Mga and currently has no known function (177). This study also showed that Mga influences the expression of several metabolic operons.

Mga binds to the Mga binding sites (MBS) present in three different classes of Mga-regulated promoters, which are determined based on the location of the binding site relative to the start of transcription. The first class of MBS are located directly upstream and proximal to the start of transcription and include the *emm* and *scpA* MBS (140). Another class of MBS are those that are distal to the start of transcription and they include both *sclA* and *sof* (6, 7). Binding of Mga to its own promoter represents a third class, which includes 2 separate MBS present between the 2 starts of transcription with activation leading to high expression from the proximal P2 promoter (145).

Mga responds to several different environmental signals including CO_2, the presence of sugars, iron concentration, temperature, and other growth signals (141). Additionally, a transposon screen identified AmrA, a putative sugar transporter located near the rhamnose cell wall operon, as a regulator of Mga activity (176). Mga was recently found to contain 2 putative phosphotransferase regulatory domains (PRD), suggesting that metabolism may play a role in regulation (97, 219). Moreover high expression of *mga* was observed in exponential phase during studies evaluating growth of

the GAS in human blood or saliva further suggesting that metabolism plays a role in influencing Mga activity (83, 191). In addition, recent studies investigating GAS disease *in vivo* using the pharyngeal model in cynomologus macaques have shown increased Mga regulon expression during the acute phase of infection along with several carbohydrate metabolism operons suggesting a link between carbohydrate metabolism and virulence expression (223).

RofA-like proteins (RALPs)

The major regulators of virulence at the transition from exponential growth phase to stationary phase consist of the RALP family of proteins. RofA was the first identified regulator of this family, and thus the other members of this group including Nra (Ralp2), Ralp3 and RivR (Ralp4) were designated as RofA-like proteins or RALPs. Not all of the RALPs are present in every strain, and they seem to have some overlap in function in the various strains studied, in addition to modulating the expression of the other RALPs. The RALPs most often function as negative regulators of gene expression, however they activate the expression of a limited number of genes as well.

RofA

RofA, initially, was found to positively regulate its own transcription and the expression of the divergently transcribed gene *prtF* (73). RofA was first shown to negatively influence the expression of genes important in virulence including, *mga, sagA*, and *speB* (16). However, it was later shown that there appeared to be strain-specific variation in RofA regulation (114). A consensus RofA binding sequence was identified in

the intergenic region between *rofA* and *prtF* (73), however no RofA binding sites were found near other RofA-regulated genes. This might imply indirect regulation by RofA, and suggest the need for analysis of the RofA transcriptome, which has not been completed.

Nra

Nra is a negative regulator of genes encoding adhesins including the collagen-binding pilus-associated surface protein Cpa (*cpa)*, and the second fibronectin binding protein SfbII (*prtF2)*. Similar to RofA, Nra negatively regulates the genes encoding the virulence factors SLS, SpeB, SpeA, and Mga (164). However, unlike RofA and Mga, there is no published evidence that Nra directly interacts with its regulated targets. Moreover, a further transcriptome analysis of a Nra mutant in the M49 strain NZ131 found that Nra mainly represses the expression of the genes encoding many virulence factors including, both the pilus and capsule synthesis operons, the genes involved in the CMT system, and the genes encoding the transcriptional regulators Rgg, RALP3, and RivR (117). A recent transcriptome analysis in the M53 skin strain identified Nra as an activator of the FCT pilus locus and does not affect transcription of *mga,* unlike the M49 strain (131). Interestingly, in the M53 strain the multiple sugar metabolism regulator, MsmR, represses *nra* and the Nra-activated gene *cpa*. However, in the M49 strain, MsmR activates the expression of *nra* while Nra represses *cpa* (131).

RALP3

RALP3 was recently shown to activate the expression of the newly described genomic region, termed ERES, containing the genes *eno, ralp3, epf/lsp,* and the *sagA* operon. In the M49 strain NZ131, RALP3 represses expression of *msmR* but activates expression of *nra*, both of which inversely influence expression of the FCT pilus locus (117). Interestingly, the presence of RALP3 is currently limited to only a few of the sequenced serotypes (M1, M4, M12, M28, and M49) and seems to have varied affects in different strains. Studies in the invasive M1T1 strain indicated that RALP3 represses *speB*, the capsule synthesis operon (*hasA-C)*, and the *epf/lsp* fibrinogen binding protein locus. Furthermore, a RALP3 mutant in this background was attenuated in mouse infection models and lacked the ability to grow in human blood due to increased sensitivity to antimicrobial peptides (118).

RivR

The fourth RALP named RivR, a recently characterized activator of virulence, is directly repressed by the CovRS TCS (179). Both RivR and the associated small RNA, RivX, can enhance the expression of the Mga regulon, although the mechanism for this interaction has yet to be identified. Also, both are able to individually complement the loss of the other for activation of the Mga regulon, suggesting the possibility of a feedback loop in their regulation. Moreover, a mutant of RivR was attenuated for virulence in the invasive subcutaneous mouse infection model (180).

Rgg/RopB

Rgg or RopB is a mediator of global gene expression affecting approximately 30% of the genome in the M49 strain NZ131. Rgg represses expression of genes during exponential phase and is the main activator of transcriptional regulation during stationary phase (63). The expression of *speB* is dependent on activation by Rgg, from which it is divergently transcribed (132). In addition to *speB*, Rgg regulates the expression of many other virulence factors and transcriptional regulators. During stationary-phase, Rgg represses expression of *mga*, but activates the expression of the *covRS, fasBCAX, ihk/irr*, and *lytRS* TCS, suggesting that Rgg may mediate some of its effects indirectly through alternative regulators (39, 63). The virulence factors influenced by Rgg includes repression of all the Mga-regulated genes, the genes involved in the CMT system, the DNases MF-1 and 3, and *ska*: and activation of the genes encoding the superantigen SpeG and the surface-localized GRAB protein (38, 40). *In vivo* studies with an Rgg mutant demonstrated an increase in virulence that may be attributed to the additional ability of Rgg to repress the expression of genes important in the oxidative stress response (36, 167). Furthermore, Rgg activates the expression of the amino acid catabolism operons for arginine, histidine, and serine and positively influences the utilization of the alternative sugar sources fructose, sucrose, and mannose. In tandem these function to make Rgg essential for growth in non-glucose environments (36, 38, 63).

Other regulators

Pleiotropic effect locus

A unique regulator in the GAS is the regulatory pleiotopic effect locus (*pel),* which represents an untranslated RNA located on the same coding strand within *sagA,* the gene encoding the structural toxin for SLS *(124),* (136). Both studies using either an M49 or M1 isolate of GAS, identified that mutations within this regulatory RNA had additional pleiotropic effects on both transcription and translation of a variety genes. Initially, a mutation resulting in loss of *pel* was found to reduce the transcripts of *emm* and *speB*, as well as decrease secretion of Ska, indicating *pel* positively affects transcription and translation (124). Additionally, a *pel* mutant also showed reduced transcription of *sic, emm*, and *nga*, in addition to a reduction in activity of the secreted cysteine protease, SpeB. Furthermore, this later study defined that *pel* was indeed a regulatory RNA and determined that its expression was under growth-phase control (136). The specific region containing the *pel* RNA has not been determined and some strains have not shown the pleiotropic effect by mutation of the *sagA* region (59).

Multiple sugar metabolism regulator

The multiple sugar metabolism regulator (MsmR), activator of the Nra-regulon, was initially identified in the closely related *Streptococcus mutans* and a homolog was subsequently identified in the GAS (154). MsmR is adjacent to the FCT pilus region, and is only found in strains containing this region (20, 168). Studies on this regulator have yielded contradictory results, originally it was shown to activate expression of the Nra-

regulon in an M49 skin strain (154), but the opposite was seen in the M53 skin strain (131).

CodY

The regulator CodY is involved in regulation of the amino-acid starvation response in the low G-C Gram-positive bacteria. Several studies have assessed the role of nutritional limitation and amino-acid starvation on virulence gene regulation (198, 199). CodY was found to up-regulate the virulence-associated TCS, CovRS, with subsequent repression of the CovRS-regulated gene *ska* (198). Further studies using a wild-type M49 strain and a CodY mutant, analyzed the expression of virulence of in human blood (135). This study determined that CodY positively influences several different regulators in addition to CovRS including, Mga, the FasBCAX TCS, and the SptRS TCS. These regulators may then modulate their own regulons, leading to global changes in virulence gene expression, mediated by CodY (135).

CARBON CATABOLITE REGULATION

Carbon catabolite repression (CCR) is a global regulatory mechanism of carbon source utilization that both Gram-negative and Gram-positive bacteria employ to conserve energy by preventing inefficient utilization of alternative carbon sources when the preferred substrate, usually glucose, is present (215). In a nutrient rich environment, such as some niches in the human host, bacteria would expend energy needlessly if they were to simultaneously metabolize all available carbon sources instead of just the preferred source. Thus, in the presence of glucose bacteria use CCR to inhibit the

expression of enzymes and transporters necessary for consumption of alternative carbon sources.

Phosphoenolpyruvate phosphotransferase system (PTS)

Overview

The PTS is a primary mechanism for modulating sugar intake into the bacterium and can act as a sensor for the metabolic state of the cell. The PTS system, utilized by both Gram-negative and Gram-positive, is generally composed of three main components: the enzyme II complex (EII ABC), enzyme I (EI), and the histidine containing protein (HPr). Each component of the PTS system plays an important role in sugar influx. The EII ABC complex consists of a membrane spanning protein, EIIC, which transports the sugar into the cell, and two phosphate transfer proteins, EIIA and B, which are sugar specific. EI is a general phosphotransfer protein that receives the phosphate from the conversion of phosphoenolpyruvate (PEP) to pyruvate in glycolysis of the incoming sugar. EI transfers this phosphate to a histidine residue of HPr, a metabolic sensor of the cell, which can then lead to the activation of the CCR systems of both Gram-negative and Gram-positive organisms (166, 203).

HPr and EI

HPr and EI are the two major phosphotransferase proteins of the PTS system. Each protein is a part of the general phosphotransfer reaction for the intake of all sugars through the PTS system. The phosphotransfer reaction, consistent in both Gram-negative and Gram-positive organisms, results in HPr becoming phosphorylated on the His 15

residue from the conversion of PEP to pyruvate in glycolysis. Furthermore, each protein has been characterized and purified from both types of bacteria. Both proteins were found to be soluble, with the molecular weight of HPr being roughly 7-16 kDa, and EI much larger at 44-85 kDa.

Interestingly, mutations made in *ptsH* and *ptsI*, the genes encoding HPr and EI respectively, resulted in the inability to yield productive fermentation during growth on several different carbohydrate sources. However, this growth defect had different phenotypes in Gram-negative and Gram-positive bacteria, leading to the speculation that the mechanism for carbon regulation is different. Later, it was found that cyclic AMP (cAMP) was able to complement this growth deficiency only for Gram-negative organisms.

Gram-negative CCR/ inducer exclusion

CCR in Gram-negative bacteria was first recognized with the classic paradigm, inducer exclusion of the Lac operon (166). Inducer exclusion involves the phosphorylation state of the glucose specific EIIA ($EIIA^{Glc}$) from the PTS system. When glucose, the preferred carbon source, is present, the $EIIA^{Glc}$ remains unphosphorylated and inhibits the permeases of alternative carbon sources. However, in the absence of glucose, $EIIA^{Glc}$ becomes phosphorylated and activates the conversion of ATP to cAMP via the adenylate cyclase (111). The cAMP can then bind the cAMP receptor protein (Crp), which activates the expression of alternative catabolic operons. Furthermore, sequences present in the promoters of several metabolic operator genes led to the identification of a consensus Crp binding site consisting of a symmetrical 22 base pair region with the core-binding region being TGTGA (29, 203).

Gram-positive CCR

General mechanism

In Gram-positive bacteria such as *Bacillus subtilis*, CCR involves the central protein of the PTS, HPr (61). HPr, a sensor for the metabolic state of the cell, is phosphorylated on a serine residue (S46) by HPr kinase during growth in glucose. Phosphorylated HPr can complex with the carbon catabolite control protein A (CcpA), a primary regulator of CCR in Gram-positive organisms. The HPr-CcpA complex mediates CCR by binding to catabolite response elements (*cre)* present within the promoters or coding regions of regulated genes. A 14 base-pair consensus *cre* has been determined in *B. subtilis*: TGWAARCGYTWNCW (204), however, slight variations have been observed in other Gram-positive bacteria (236). Upon binding to these *cre,* CcpA either represses expression of genes that might be involved in alternative sugar source utilization or activates transcription of genes that may function in glucose metabolism (215) (85) (75).

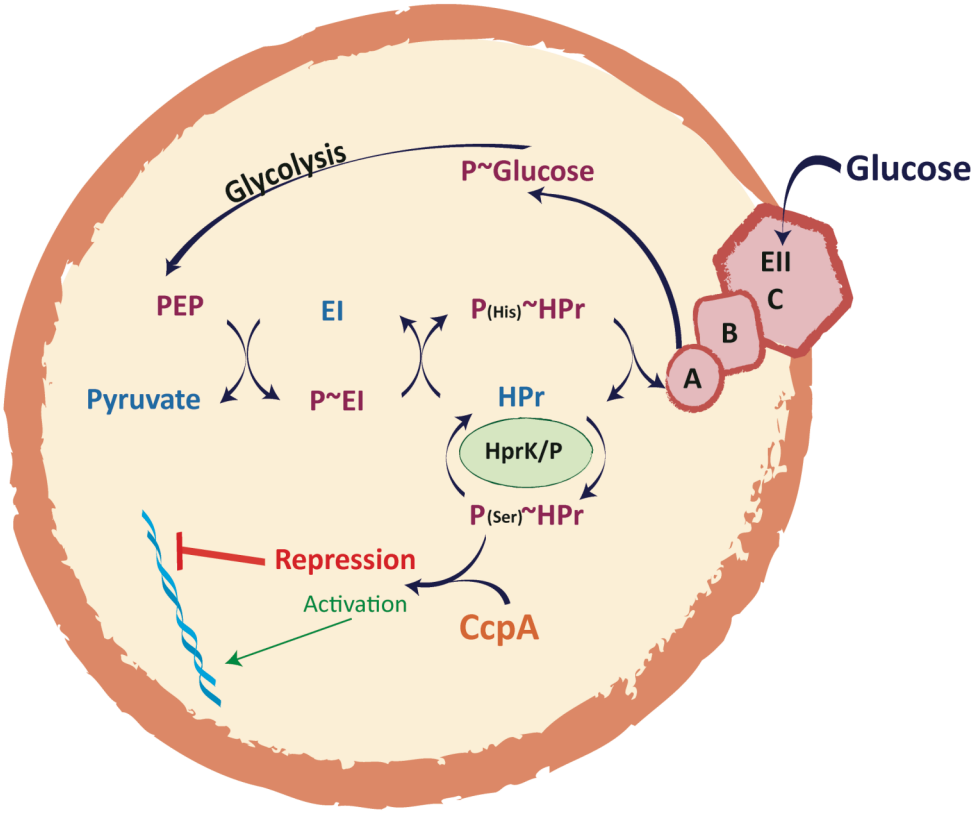

Fig. 2: PTS-dependent glucose transport and CCR
Glucose is brought into the cell via the PTS EIIABC transporter, and enters directly into glycolysis. The resulting PEP transfers the phosphate to EI, which in turn transfers the phosphate to the His15 residue of HPr. Alternatively, Hpr kinase recognizes intermediates of glycolysis and phosphorylates HPr on the Ser46 residue. HPr-P-Ser46 then complexes with CcpA and mediates CCR.

HPr kinase

HPr kinase (HPrK) catalyzes the ATP-dependent phosphorylation of HPr on the serine 46 residue upon recognition of glycolytic intermediates to stimulate CCR in Gram-positive bacteria. Although the specific gene for HPrK (*hprK*/*ptsK*) wasn't identified until 1998 (76, 174), it was known that in an ATP-dependent reaction a serine-threonine kinase was responsible for HPr Ser 46 phosphorylation (62). Furthermore, this phosphorylation of HPr could be demonstrated utilizing crude extracts from *S. pyogenes in vitro*, a process still in use today.

Carbon catabolite control protein A

CcpA, a 76 kDa homodimeric protein, is a member of the LacI/GalR transcriptional regulator family and controls the expression of a wide variety of genes important for metabolism in Gram-positive bacteria. CcpA can both activate and repress gene expression when in complex with Ser-phosphorylated HPr (107). The type of regulation mediated by CcpA typically depends on the location of the *cre* site relative to the start of transcription. Gene expression is usually repressed if the *cre* is located in the promoter between the canonical -35 sequence and the start of transcription, or if it is present in the coding region for the protein. Alternatively, activation by CcpA occurs when the *cre* lies upstream of the -35 sequence, typically in multiples of 10 bp or nucleotides, to position the binding site on the correct side of the DNA helix (236). Recently, the crystal structure of CcpA from both *Bacillus megaterium* and *Lactococcus lactis* has been determined (126, 195).

CCR of virulence in Gram-positive bacteria

Listeria monocytogenes

The major activator of virulence in *L. monocytogenes,* PfrA, was shown to be under CCR (148). However, the mechanism for CCR-mediated repression of PfrA was not a result of direct regulation by CcpA (17). Recently, the mechanism for CcpA-independent CCR of PfrA was found to involve the co-repressor of CCR in Gram-positive organisms, Ser 46 phosphorylated HPr (94). Inactivation of HPr-K resulted in reduced PrfA-regulated gene expression. Furthermore, interruption of the PTS phosphorylation cascade through EI and HPr also lowered expression of the PfrA regulon (94).

Clostridium perfringens,

In the anaerobic pathogen *C. perfringens,* expression of enterotoxin (*cpe*) was shown to be CcpA-mediated, and that mutations in CcpA prevented efficient sporulation (221). In addition, CcpA was necessary for the production of the collagenase, and repressed synthesis of the polysaccharide capsule (79). Recently, CcpA was also shown to repress expression of the Type IV pilus, which generates the gliding motility for this organism (147).

Streptococcus pneumoniae

Importantly, in the human pathogen *S. pneumoniae,* a mutation in the CcpA homologue RegM attenuates this organism for nasopharygeal colonization and virulence in the mouse pneumonia model of infection (100). In addition, the CcpA mutant strain

also showed reduced ability to colonize and infect the lungs of mice in the pneumonia model. An additional study suggests a role for RegM/CcpA in activation of capsule synthesis, providing a possible mechanism for attenuation in the animal models (79).

Staphylococcus aureus

Studies on CcpA and CCR in the pathogen *S. aureus* identified that CcpA-mediates expression of factors important for antibiotic resistance and other virulence determinants. A CcpA mutation in a strain of *S. aureus* that was highly methicillin resistant showed reduced resistance to the antibiotic oxacillin. In addition, this study identified that CcpA negatively-influences the expression of the staphylococcal α-hemolysin, capsule, and protein A. Furthermore, this study showed CcpA-mediated activation of the virulence regulator RNAIII, an effector molecule for the *agr* locus involved in global regulation (189).

Evidence of CCR in the GAS

M protein

Prior to the knowledge of the Mga regulon, the M protein was an intensely studied factor of the GAS. Many physiological studies assessed the growth of *S. pyogenes* in various conditions and evaluated the production of M protein as an end-point. Interestingly, reducing the amount of glucose from 1% to 0.25% in a semi-synthetic medium resulted in a significant increase in the production of M protein. This was attributed to the absence of lactic acid production resulting in a pH above 6.7, which did not induce expression of the extracellular proteases (43). Further studies by Pine and

Reeves in the early 1970's investigated the role of metabolism and sugar source on the production of M protein (161, 162). Their studies showed that expression of M protein was highest during exponential growth phase, although they also observed a burst of M protein production in stationary phase as all growth substrates were being depleted. Additionally, they showed that the highest levels of M protein were produced when GAS was grown in medium with glucose as the sole carbon source as compared to sucrose and trehalose (162). Interestingly, while growth in multiple sugars did not yield the classic diauxic growth curve, the production of M protein followed this pattern. The conclusions from these elegant physiological studies began to suggest a link between sugar metabolism and production of the main virulence factor of the GAS.

SpeB

The influence of metabolism and varied environmental conditions on the production of SpeB has also been the focus of several studies. Initially, the production of extracellular proteinases was only evaluated in reference to the level of degradation of M protein; however this early work identified several conditions that favor production of GAS proteases. Interestingly, the authors found that normal laboratory growth conditions for the GAS most often inhibited the production of the proteinases (43). More recent studies directly assessing the production of SpeB identified that SpeB is only produced in stationary phase, and that glucose appears to inhibit production (37). Furthermore, additional studies concluded that SpeB production was dependent on presence of peptides in the media, and that glucose only inhibited SpeB expression in complex media (163).

CHAPTER THREE:

Materials and Methods

BACTERIAL STRAINS

Escherichia coli strains, media, and growth conditions

E. coli strains used in this study are listed in Table 1. *E. coli* strain DH5α was used as the host strain for plasmid constructions and was cultured in Luria-Bertani (LB) medium (EM Science). *E. coli* was grown at 37ºC with shaking under normal aerobic conditions. Growth was measured by a spectrophotometer (Ultraspec 10, Amersham Biosciences) at OD_{600}. Antibiotics were used at the following concentrations: ampicillin at 100 μg/ml; spectinomycin at 100 μg/ml; kanamycin at 50 μg/ml; and erythromycin at 500 μg/ml.

GAS strains, media, and growth conditions

GAS strains constructed and used in this study are listed in Table 1. GAS was cultured in Todd-Hewitt medium supplemented with 0.2% yeast extract (THY; Difco) and growth was assayed by absorbance using a Klett-Summerson photoelectric colorimeter with the A filter. Chemically defined media (CDM) was prepared according to the manufacturers instructions (JRH Biosciences) at a 2x concentration, followed by filter sterilization. Prior to use, freshly prepared sodium bicarbonate (44 mM) and L-cysteine (6.2 mM) were added in addition to a sugar source at a final concentration ranging from 0.25-2% (v/v). Antibiotics were used at the following concentrations: spectinomycin at 100 μg/ml; kanamycin at 300 μg/ml; and erythromycin 1 μg/ml.

Table 1. Bacterial strains

Strains	Description	Reference
BL21(DE3)	*E. coli,* F– *ompT hsdSB*(rB– mB–) *gal dcm* (DE3)	Novagen
DH5α	*E. coli, hsdR17 recA1 gyrA endA1 relA1*	(88)
GA19681	M6 GAS, clinical invasive isolate, Mga^+	(177)
GA19681.586	M6 GAS, clinical invasive isolate, Mga^-	(177)
GA19681.710	M6 GAS, clinical invasive isolate, Mga^+, $AmrA^-$	This study
JRS4	M6 GAS, streptomycin-resistant derivative of D471	(188)
KSM148	M6 GAS, P*emm-gusA* in VIT locus, Mga^+	(176)
KSM148.586	M6 GAS, P*emm-gusA* in VIT locus, Mga^-	(176)
KSM148 Adel	M6 GAS, P*emm-gusA* in VIT locus, Mga^+, $AmrA^-$	(176)
KSM310	M6 GAS, P*mga* (full)-*gusA* in VIT locus, Mga^+	(5)
KSM310.150Lg	M6 GAS, P*mga* (full)-*gusA* in VIT locus, Mga^-	(5)
KSM310.700	M6 GAS, P*mga* (full)-*gusA* in VIT locus, Mga^+, $CcpA^-$	This study
KSM438	M6 GAS, P*mga* (Δ*cre*) in native locus	(5)
KSM440	M6 GAS, P*mga* (full length) in native locus	(5)
KSM444	M6 GAS, P*mga* (Δ*cre*)-*gusA* in VIT locus, Mga^+	(5)
KSM444.150Lg	M6 GAS, P*mga* (P1 only)-*gusA* in VIT locus, Mga^-	(5)
KSM445	M6 GAS, P*mga* (P1 Δ*cre*)-*gusA* in VIT locus, Mga^+	(5)
KSM445.150Lg	M6 GAS, P*mga* (P1 Δ*cre*)-*gusA* in VIT locus, Mga^-	(5)
KSM777	M6 GAS, P*mga-luc* in VIT locus, Mga^+	This study
KSM778	M6 GAS, Promoterless-*luc* in VIT locus, Mga^+	This study
KSM779	M6 GAS, P*mga-luc* in VIT locus, Mga^-	This study
MGAS315	M3 GAS, clinical invasive isolate, Mga^+	(18)
MGAS315.519	M3 GAS, clinical invasive isolate, Mga^-	(177)
MGAS315 233-*rmeA*	M3 GAS, clinical invasive isolate, Mga^+, $AmrA^-$	(176)
MGAS5005	M1 GAS, clinical invasive isolate, Mga^+, *CovS*	(206)
MGAS5005.718	M1 GAS Mga^+, $CcpA^-$ (Δ*ccpA* strain)	This study
MGAS5005.718 (pKSM719)	Δ*ccpA* strain with pCcpA complementation vector	This study
MGAS5005.718.732	Δ*ccpA* strain with insertional inactivation of *sagB*	This study
MGAS5005.732	M1 GAS, clinical invasive isolate, Mga^+, *sagB*	This study
RTG229	M6 GAS containing VIT locus for exchange	(78)
RTG231	M6 GAS containing VIT locus for exchange, Mga^-	(220)
SF370	M1 GAS	(72)
VIT-GusA	M6 GAS, Promoterless gusA in VIT locus, Mga^+	(5)
VIT-GusA-586	M6 GAS, Promoterless gusA in VIT locus, Mga^-	(5)

DNA MANIPULATIONS

Plasmid isolation

Plasmid DNA was isolated from *E. coli* by alkaline lysis using either the Wizard Miniprep (Promega) or Midi/Maxi prep purification systems (Qiagen) according to the

protocols provided. DNA fragments were isolated from agarose gels using the QIAquick gel extraction kit (Qiagen).

Chromosomal DNA isolation

GAS chromosomal DNA was isolated using previously described methods (12, 35). Briefly, cells were grown overnight at 37ºC with 20 mM glycine and pelleted in the morning. Cells were washed in 10 mM Tris, resuspended in Solution I (1 M Tris pH 8, 0.25 M EDTA pH 8, and 50% Sucrose) supplemented with fresh lysozyme (130 mg/ml), and incubated for 1.5 hrs with rotation. Cells were pelleted and resuspended in Solution II (1 M Tris pH 8, 0.25 M EDTA pH 8, 20% SDS) and incubated for 15 min at 37ºC. RNaseA (10 mg/ml) and Proteinase K (20 mg/ml) were added and the cells are incubated at 55ºC for 30 min with frequent inversion. The cell lysate is then phenol-chloroform extracted, beginning with a phenol extraction (TE-saturated phenol pH 6.6) followed by several extractions with a 1:1 phenol chloroform-isoamyl alcohol (IAA, 1:24) mix, with the final extraction in chloroform-IAA alone. The DNA is ethanol (EtOH) precipitated by adding 1:10 volume of 3 M sodium acetate and 2 volumes of cold 100% EtOH incubated overnight at -20ºC or 30 min at -80ºC followed by centrifugation at 13,000 x g for 15 min at 4ºC. The DNA concentration is measured by the A_{260} absorbance on a spectrophotometer (Ultraspec 2100 pro, Amersham Biosciences).

Polymerase Chain Reaction

PCR for cloning was performed using Phusion high-fidelity polymerase (New England Biolabs, NEB). Briefly, annealing temperatures for primers were determined

using the Finnzymes Tm calculator for PCR (www.finnzymes.fi/tm_determination.html). Between 30-35 cycles of the following: a denaturation step at 98ºC for 10 sec, followed by a 30 sec annealing step at a pre-determined temperature, an extension step at 72ºC for approximately 15-30 sec per kb of DNA, and with a final extension step of 4 min and the completion of the reaction. PCR reactions were purified using the QIAquick PCR purification system (Qiagen). PCR for diagnostic assays was performed using Taq DNA polymerase (NEB), with a few modifications to the PCR protocol including: only 29 cycles, denaturation at 95ºC, and longer extension times at about 1kb per min. Primer pairs listed in Table 2 were designed using Vector NTI software package (version 7.0) and optimum annealing temperatures for Taq reactions were also determined. DNA sequencing was performed by either the automated sequencing core at the McDermott Center, UT Southwestern Medical Center, or by GeneWiz, Inc.

Table 2. PCR primers

Target	Primer	Sequence (5'-3')	Reference
aad9	*aad9* R1	CCCGTGTCCATAGTTAA	This study
	aad9 L2-bglII	gcgcagatctGGGTGACTAAATAGTGAGGAG	This study
	aad9 R2-bglII	gcgcagatctGGCATGTGATTTTCC	This study
amrA			
	*rmeA*L1	AAGAAGTGGCCCTTATGAAA	(176)
	*rmeA*R1	TTTAGTCATAGATTGTTGCA	(176)
ccpA			
	*ccpA*L	TTCAATGGCAACCGTTAG	This study
	ccpA-L2	AAAGTGCGCTTAGCAGGT	This study
	ccpA-L3	ACACTCGTCCCCAATTTGA	This study
	ccpA-L5	TATTTGGTGATGAATGGT	This study
	ccpA-PCRS#1	CTACTTGAGCAGCTGTTACACCTGGTTT	This study
	ccpA-PCRS#2	*ATGCTAACAagatct*ATTCATTTTTTATCTTCC	This study
	ccpA-PCRS#3	*agatctTGTTAGCAT*GCGGATGTT	This study
	ccpA-PCRS#4	CAGAGCTTCTATAAAACCTGGTATATCGG	This study
	*ccpA*R	TCCTGACACAAAAGCGAT	This study
	*ccpA*R1	CCCTAAGGCTGATTTTAGTATT	This study
	ccpA-R2	GTCAACATCCGCATGCTA	This study
	ccpA-M6-R3	ATCGCTCGACCAATTCCT	This study
	M6*ccpA*_NcoI-L	catccatggCTAATACAGATGATACCAT	This study
	M6*ccpA*_XhoI-R	gcgctcgagTTACTTAGTTGTCCC	This study
	PccpA-L1	GCCAATTCAGCTCCCTTT	This study
	PccpA-R1	CTTCACGGGCAACATCAT	This study
emm			
	OM6-35	AACAGCAAATTAGCTGCTC	(142)
	OM6-16	GTTTCCTTCATTGGTGCT	(142)
gusA			
	gusA-PE	GTTGGGGTTTCTACAGGACG	(6)
	Steph-*gusA*-PE	TTGTTTAAACAAATAGACGA	(5)
ptsH			
	ptsH-L2	ggctcgagGTCTTATGCCAATCC	This study
	ptsH-R2	gggccatggCTTCAAAAGACTTTC	This study
ptsK			
	HprK-NcoI-L	ggccatggCAACCGTTACTGTAAAGA	This study
	HprK-XhoI-R	gcctcgagTCATTGACTCACCTCA	This study
luc			
	*luc*L	gcaggagagTTCAGATGGGAGCTCGAATTCCAGCTTGGCA	This study
	*luc*R	acgcgtcgacTTACAATTTGGACTTTCCGC	This study
	*luc*R1	CGCACTTTGAATTTTGTA	This study
M13			
	1201 M13 Rev	AACAGCTATGACCATGATTACG	Clonetech
	1211 M13 For	GTTGTAAAACGACAACCAGT	Clonetech
Pmga			
	Δ*cre*-L	TTTTTGTGAACTGGTTAA	(5)
	Δ*cre*-R_Bam	cgggatccAATATTGGAGTAAATTGAC	(5)
	OYL-14-X	ggctcgagGTCACTAACTTAATTAGAT	This study
	OYR-14-B	ggggatccAATTTGCGAGATTAGAGTAAT	This study
	OYR3	TCTTGATATAGGTCTTAC	(145)
	Pmga-X	ggctcgagACCTTGTATACCCTTCTTTT	(145)

PsagA			
	M1_*sagA-cre* L	GACATTTCTACTTGATTG	This study
	M1_*sagA-cre* R	AAGTAACTGATAAGAACG	This study
	PsagA-L1-B	gcggatccGACATTTCTACTTGATTG	This study
	PsagA Left-L	GAGGCTACTAAAGTATTA	This study
	PsagA Left-R	CTTTTTAATATTATCAAA	This study
	PsagA-R1-X	gcctcgagAAGTAACTGATTAAGAACG	This study
	PsagA Right-L	TATTAATCATTTTTTACTATAA	This study
	PsagA Right-R	AATTACCACTTCCAGTAG	This study
rpsL			
	GAS-*rps*L6	GTGCGCCACGAACGATATG	(144)
	Spn-*rps*L1	GAATGTAGATGCCTACAATTAACCA	(144)
sagB			
	sagB-L	ATACAAACCACTTGTCCTT	This study
	sagB-R	ATGCCGATAACACCTTA	This study
spy0515			
	Spy0515-L	GCATGGGCATTCTACAGA	This study
	Spy0515-R	CATCAATTCCTTTCCTCA	This study

Table 2. Lowercase letters indicate additional sequence added, and underlined text denotes added restriction enzyme site. Italicized and underlined lowercase text indicates region of overlap for PCR sewing.

Enzymatic DNA modifications

Enzymatic DNA modifications were performed using enzymes with the conditions suggested by the manufacturer. Restriction enzyme digests were performed in the buffers supplied by the manufacturer (NEB) for 2 hrs to overnight. Ligation reactions using T4 ligase (NEB) were set up using a 1:3 vector to insert ratio as determined by agarose gel analysis, with overnight incubations at 16ºC. Fill-in reactions were performed using T4 polymerase (NEB) to create blunt ends with incubation at 12ºC for 20 min followed by 20 min at 70ºC. T4 polynucleotide kinase (PNK, NEB) was used for radioactive end labeling of probes and to phosphorylate ends of PCR products for ligation reactions by incubation at 37ºC for 30 min. Antarctic alkaline phosphatase (NEB) was used to dephosphorylate the vector ends for cloning with incubation at 37ºC for 1 hr.

BACTERIAL TRANSFORMATIONS

E. coli competent cells

To prepare DH5α competent cells, 500 ml of LB broth was inoculated with 5 ml of an overnight starter culture and grown to an OD_{600} of 0.6. Cells were then placed on ice for 30 min to cool cells and stop growth prior to centrifugation at 7,000 x g for 30 min at 4ºC. After pelleting, cells were washed and resuspended in ice-cold sterile 10% glycerol (EP solution) and washed twice more. After the final wash, cells were resuspended in 800 µl of EP solution and split into 50 µl aliquots, which were stored at -80ºC for 6 months to one year.

GAS competent cells

To prepare competent GAS cells for transformation, 150 ml of THY broth with 20 mM glycine was inoculated with 7.5 ml of an overnight starter culture and incubated static at 37ºC until OD_{600} was between 0.2 and 0.4. Cells were kept on ice prior to centrifugation at 7,000 x g for 30 min at 4ºC. The pelleted cells were washed and resuspended in 20 ml of EP solution, and centrifuged again twice more. Upon completion of the washes, the pelleted cells were resuspended in 1 ml EP solution and split into 200 µl aliquots, which were stored at -80ºC for 6-8 months.

Electroporation

To remove excess salts prior to electroporation of DNA into either *E. coli* or GAS, the DNA was drop dialyzed against H_2O using 0.025 μm membrane filters (Millipore) for 30 min.

Electroporation of both *E. coli* and GAS was performed using a GenePulser Xcell (Bio-Rad). The 50 μl *E. coli* competent cell aliquot was mixed with drop dialyzed DNA in a pre-chilled 2 mm cuvette and transformed using the electroporator settings as follows: 2.5 kV, 200 Ω, and 25 μF. Cells were then added to 1 ml LB broth and outgrown for 1 hr at 37ºC with shaking, prior to centrifugation at 13,000 x g. Pelleted cells were resuspended in 300 μl saline and 100 μl were plated with the appropriate antibiotic for selection. Transformations into GAS were carried out using the electroporator settings as follows: 1.75 kV, 400 Ω, and 25 μF. After electroporation, GAS cells were added to 10 ml THY broth and outgrown for 2-4 hrs, at 37ºC without shaking, prior to centrifugation at 7,000 x g. After pelleting, cells were resuspended in 500 μl and plated with the appropriate antibiotic for selection.

Temperature-sensitive allelic exchange

Transformation of GAS with the temperature-sensitive plasmid pJRS233 (Table 3) containing plasmid based erythromycin (Erm) selection for allelic exchange follows a previously described protocol (160). Briefly, after electroporation, cells are outgrown at 30ºC prior to plating with Erm selection at 30ºC overnight to allow for plasmid replication. Isolated colonies are then inoculated into liquid cultures with Erm and other applicable antibiotics for selection and passaged overnight at 30ºC. Cells are passaged

one more time in fresh media, without Erm selection to allow for possible integration. Cells are further passaged to fresh media and grown at 37ºC without Erm selection but with other applicable antibiotics still for a total of two times. After passaging is complete, cells are serially diluted onto THY agar with applicable selecting antibiotics but not Erm and incubated at 37ºC. Isolated colonies are then back screened for sensitivity to Erm to verify complete loss of the plasmid.

The temperature-sensitive vector pJRS233 was also used to construct insertional-inactivation mutants using a very similar strategy and was described by Ribardo *et. al* (176). Briefly, transformation and passages followed the same protocol as above, however Erm is continuously used as the selecting antibiotic to allow selection of the complete integration of the vector into the chromosome at the permissive temperature.

GENETIC CONSTRUCTIONS

Construction of insertional-inactivation mutation in *ccpA* in the P*mga-gusA* reporter strain KSM 310

To produce the *ccpA* mutant strain KSM310.700 (Table 1) and the plasmid pKSM700 (Table 3), a 511-bp internal region of *ccpA* was amplified by PCR (described in detail earlier) from the serotype M6 strain JRS4 genomic DNA (gDNA) using the primer pair *ccpA*L/*ccpA*R (Table 2). The resulting fragment was blunt-ligated into EcoRV-digested pJRS233 to form pKSM700 and verified by PCR using the primer pair *ccpA*L/*ccpA*R (Table 2). The temperature-sensitive plasmid, pKSM700, was transformed into the JRS4-derived P*mga-gusA* reporter strain KSM310 (Table 1) using an insertional-

inactivation strategy. Erythromycin-resistant integrants were isolated at 37°C following serial dilution plating and verified by PCR using the primer pair 1201/*ccpA*R1 and 1211/P*ccpA*-L1 (Table 2).

Table 3. Plasmids

Plasmids	Description	Reference
pBluescript II KS-	ColE1 ori Amp^r *lacZ*α	Stratagene
pJRS233	Temperature sensitive shuttle vector	(160)
pJRS525	GAS replicating plasmid with Spec resistance	(143)
pJRS9160-Adel	AmrA delection construct	(176)
pKSM201	Replicating vector for GAS with Kan resistance	This study
pKSM700	Internal fragment of M6 *ccpA* in pJRS233	(5)
pKSM701	P*mga-luc* in pBluescript II KS-	This study
pKSM702	Initial P*mga-luc* vector	This study
pKSM703	Initial promoterless-luc vector	This study
pKSM710	AmrA deletion plasmid with Km Ω cassette	This study
pKSM711	M6 *his-ccpA* in pProEX-HTb	This study
pKSM712	Expression vector containing M1 GAS His-HPr	This study
pKSM713	Expression vector containing M1 GAS His-HPr Kinase	This study
pKSM715	*ccpA* complementing vector with Spec resistance	This study
pKSM716	pBluescript II KS- with PCR-sewn region of *ccpA*	This study
pKSM717	pKSM716 with PCR sewn *ccpA* region containing *aad9*	This study
pKSM718	Δ*ccpA* Mutagenic plasmid with non-polar *aad9*	This study
pKSM719	*ccpA* complementing vector with Kan resistance	This study
pKSM720	GAS replicating plasmid with firefly luciferase and RBS	This study
pKSM721	P*mga-luc*	This study
pKSM727	GAS replicating plasmid with P*sagA* running luciferase	This study
pKSM728	Km^R Pmga-luc	This study
pKSM732	*sagB* Insertional inactivation vector	This study
pKSM777	Vector for exchanging P*mga-luc* into VIT locus	This study
pKSM778	Vector for exchanging Promoterless-*luc* into VIT locus	This study
pLucMCS	Firefly luciferase vector with multiple cloning site	Stratagene
pP*mga*-blue	pBluescript II KS- containing P*mga* for cloning	(220)
pProEX-HTb	Expression vector N-terminal 6x His	Invitrogen
pSL60-1	Vector containing non-polar *aad9* gene	(128)
pUC4Km2	pMB1 ori, ΩKm2	(159)
pVIT164	Plasmid vector for integration into Tn*916*	(30)

Construction of the P*mga* and promoterless luciferase plasmid-based transcriptional reporters, pKSM702 and pKSM703

The firefly luciferase gene (*luc)* was amplified with Platinum *pfx* (Invitrogen) from pLuc-MCS (Table 3) using the primers *Luc*-L and *Luc*-R (Table 2). The *Luc*-L

primer added a SalI restriction site for cloning and a RBS binding site. The *luc* PCR product was digested with SalI and ligated into SalI/EcoRV digested pP*mga* blue (Table 3) to yield the plasmid pKSM701 (Table 3). P*mga-luc* was amplified from pKSM701 with Platinum *pfx* using the primer pair 1211/1201 (Table 2) and blunt-ligated into pJRS525 (Table 3) to yield the P*mga-luc* reporter plasmid pKSM702 (Table 3). P*mga* was removed by digestion with PstI and the re-ligated vector resulted in creation of the promoterless luciferase reporter pKSM703 (Table 3).

Construction of allelic exchange vector for *amrA*, pKSM710

As previously described by Ribardo *et al.* (176), an *amrA* deletion construct, pJRS9160-Adel (Table 3), contained homology from both upstream and downstream of *amrA* and lacked ~500 bp internal to *amrA*. pUC4ΩKm2 was digested with BamHI to yield the KmΩ cassette, which was ligated into BamHI digested pJRS9160-Adel resulting in the creation of pKSM710 (Table 3).

A Km-marked *amrA* deletion was made in the M6 strain GA19681 (Table 1) by transformation with XmnI-linearized pKSM710, followed by outgrowth and plating at 37ºC. The *amrA* mutation was verified by PCR using the primer pair *rmeA*L1/R1 (Table 2).

Construction of recombinant GAS CcpA, HPr, and Hpr Kinase expression vectors, pKSM711, pKSM712, and pKSM713

Amino-terminal fusions of 6x His to CcpA from M6 GAS and HPr and Hpr Kinase from M1 GAS were constructed as described below. For CcpA a 1,019 bp region

containing the entire *ccpA* gene was PCR amplified from serotype M6 GA19681 (Table 1) gDNA using the primer pair M6*ccpA*_NcoI-L and M6*ccpA*_XhoI-R (Table 2). For both HPr and Hpr Kinase, a 261 bp region containing *ptsH* (HPr) and a 930 bp region containing *ptsK* (HPr Kinase) were amplified from serotype M1 SF370 (Table 1) gDNA using the primer pairs *ptsH*L2 /*ptsH*R2 and HprK-NcoI L/HprK-XhoI R (Table 2). For all three constructs the resulting products were digested with NcoI/XhoI and ligated into NcoI/XhoI-digested pProEX-HTb to produce pKSM711 (CcpA), pKSM712 (HPr), and pKSM713 (Hpr Kinase) (Table 3). Following verification by PCR and DNA sequence analysis, recombinant expression vectors were transformed into BL21 [DE3] Gold (Table 1) for protein expression.

Construction of allelic exchange vector pKSM718 for creation of Δ*ccpA* strains

PCR sewing was used to delete the *ccpA* gene. The primers *ccpA*-PCRS#1 and *ccpA*-PCRS#2 (Table 2) were used to amplify a 1005 bp upstream region containing the first 6 nucleotides of *ccpA*, a BglII site and a 9-bp overlap with the second fragment at the 3' end. The primers *ccpA*-PCRS#3 and *ccpA*-PCRS#4 (Table 2) were used to amplify an 1115 bp downstream region containing the last 100 nucleotides of *ccpA*, with a BglII site at the 5' end. These fragments were then combined as template DNA with the *ccpA*-PCRS#1 and *ccpA*-PCRS#4 primers (Table 2) to generate the deletion. The resulting product was blunt-ligated into EcoRV-digested pBluescript II KS- to yield pKSM716 (Table 3). The non-polar spectinomycin gene was amplified from pSL60-1 (Table 3) using the primers *aad9*-L2-bglII and *aad9*-R2-bglII (Table 2), digested with BglII, and ligated into BglII-digested pKSM716 to create pKSM717 (Table 3). The BamHI/XhoI

digested-fragment containing the PCR-sewn Δ*ccpA* region and the *aad9* cassette from pKSM717 was ligated with BamHI/XhoI-digested pJRS233 to yield pKSM718 (Table 3).

A Δ*ccpA* mutant was created using a temperature-sensitive allelic exchange as previously described above (160). Mutants were screened for sensitivity to erythromycin and verified by PCR using the primers *ccpA*-L5 and *aad9*-R1 (Table 2) and by Southern blot.

Construction of *ccpA* complementation vector, pKSM719

ccpA with its native promoter was amplified from the serotype M1 strain MGAS5005 (Table 1) using the PCR primers P*ccpA*-L1 and *ccpA*R1 (Table 2) and blunt-ligated into EcoRV digested pJRS525 (Table 3) to create the Sp^R CcpA complementing vector pKSM715 (Table 3). To produce a kanamycin-resistant complementing plasmid, the *aad9* spectinomycin gene from pJRS525 was removed by digestion with AflIII, the ends filled in, and further digested with SwaI. The *aphA3* kanamycin resistance gene from puc4Ωkm2 was digested with SmaI and blunt-ligated into pJRS525 to yield pKSM201 (Table 3). The P*ccpA*-*ccpA* fragment from pKSM715 was cloned into pKSM201 using PvuII/NcoI to create the Km^R CcpA complementing vector pKSM719 (Table 3).

Construction of promoterless-Luciferase vector, pKSM720

The firefly luciferase gene (*luc)* was amplified from pLuc-MCS (Table 3) using the primers *Luc*-L and *Luc*-R (Table 2). The resulting fragment was blunt-ligated into EcoRV-digested pJRS525 (Spectinomycin-resistant) to create pKSM720 (Table 3).

Transformants were screened for orientation using the primers 1211 and *Luc*-R1 (Table 2).

Construction of P*mga*-Luciferase vectors, pKSM721 and pKSM728

P*mga* was amplified from MGAS5005 (Table 1) with Phusion high-fidelity polymerase (NEB) using the primers OYR-14-B and P*mga*-X (Table 2). The promoter PCR fragment was BamHI/XhoI digested and ligated into BglII/XhoI digested Spectinomycin-resistant luciferase plasmid pKSM720 to form pKSM721 (Table 3). To construct a Kanamycin-resistant version, P*mga-luc* was digested with PvuII/NcoI from pKSM721, gel extracted, and ligated with PvuII/NcoI digested pKSM201 to yield pKSM728 (Table 3).

Construction of P*sagA*-Luciferase vectors pKSM727

The P*sagA* promoter fragment was amplified from the M1 strain MGAS5005 (Table 1) using the primers P*sagA*-L1-B and P*sagA*-R1-X (Table 2), digested with BamHI/XhoI and ligated into BglII/XhoI-digested pKSM720 to create the Spectinomycin-resistant pKSM727 (P*sagA-luc*) (Table 3).

Construction of *sagB* insertional-inactivation vector pKSM732

To create non-SLS producing strains, a polar mutation was made in *sagB*, the second gene in the *sag* operon. Briefly, a 500 bp fragment internal to *sagB* was amplified from MGAS5005 using the primers SagB-L and SagB-R (Table 2) and blunt ligated into an EcoRV-digested pJRS233 to yield pKSM732 (Table 3). The resulting plasmid was

electroporated into both WT and Δ*ccpA* mutant strain using a temperature-sensitive inactivation strategy as described previously. Strains were verified by loss of hemolysis on blood agar plates and PCR using the primers 1211 and SagB-L or SagB-R (Table 2).

Construction of the P*mga* and promoterless luciferase reporter strains KSM777, KSM778 and KSM779

P*mga-luc* was excised from SalI/BamHI-digested pKSM701 and religated with SalI/BamHI-digested pVit164 (Table 3) to yield the plasmid pKSM777 (Table 3), which was verified by sequencing with the primers *Luc*R, OYR3, and 1211 (Table 2). pKSM777 was linearized with XmnI and transformed into the strain RTG229 (Table 1) as previously described (78, 176) yielding the P*mga-luc* reporter strain KSM777. Additionally, the Mga$^-$ strain RTG231 (Table 1) was transformed with linearized pKSM777 to yield the strain KSM779 (Table 1).

To create a promoterless-*luc* reporter strain, P*mga* was removed from pKSM777 by a sequential digestion with PstI and BamHI, the ends were then filled-in and religated to form the plasmid pKSM778 (Table 3). pKSM778 was linearized with XmnI and transformed into RTG229 resulting in the strain KSM778 (Table 1).

DNA ANALYSES

Agarose gel analysis

DNA from PCR and restriction digests were run on a 1% agarose gel composed of 0.5 g of agarose added to 50 ml of 1x TBE (90 mM Tris-base, 90 mM boric acid, and 2 mM EDTA) with 5 µl of ethidium bromide (10 mg/ml). Samples are mixed with 5x load

dye (50% glycerol, 50% 10x TBE, 0.001% SDS, with bromophenol blue and xylene cyanol for color), and run with 1 kb molecular weight ladder (Promega). Gels were run at a range from 60V to 100V for about 20-40 min depending on the size of the fragment.

Random prime labeling of probes

Radioactive labeling of probes for Southern and northern blotting was completed using the RadPrime label kit (Invitrogen). Briefly, 500 ng of probe DNA was mixed with random primers, Klenow fragment, dNTPs, and 20 μCi of [α^{32}P]-dATP (Perkin Elmer) and incubated at 37ºC for 30 min. The probe was then purified over a G-25 sephadex Quickspin column (Roche), and counted using either a Geiger counter or through an LS 6500 scintillation counter (Beckman-Coulter).

Southern blot analysis

Chromosomal DNA (7.5 μg) was digested with HindIII and separated on a 0.7% agarose gel. The DNA was denatured in the gel by soaking in 0.4 M hydrochloric acid for 40 min followed by neutralization with 0.4 M NaOH. The DNA was transferred downward to a positively charged nylon membrane overnight under alkaline conditions followed by UV crosslinking in a crosslinker (Strategene). The blot was hybridized for 2 hrs with 5 x 10^6 cpm of the radiolabeled probe at 42ºC in a rotating hybridization oven (HB1000 UVP laboratory products). Following hybridization the blot was washed twice in low stringency buffer (0.3 M sodium chloride, 30 mM sodium citrate, and 0.1% (w/v) SDS) followed by 2 more washes in high stringency buffer (30 mM sodium chloride, 3 mM sodium citrate, and 0.1% (w/v) SDS) each for 20 min at 42ºC. Blots were exposed

to a phosphorimager cassette for 30 min to overnight and scanned using a Storm 860 (GE Healthcare).

RNA ANALYSES

RNA isolation

RNA was isolated using a Triton X-100 method as previously described (210). Briefly, 10 ml THY broth was inoculated 1:20 from an overnight starter culture and grown to the appropriate optical density or Klett unit. Cells were then pelleted by centrifugation at 7,000 x g for 20 min at 4ºC. Cells were resuspended in 1 ml of TE buffer (10 mM Tris pH 7.4 and 1 mM EDTA) with 0.2% (v/v) Triton X-100 added and boiled for 10 min. The lysate was chloroform-IAA extracted twice and EtOH precipitated overnight at -20ºC. The precipitation reaction was pelleted at 13,000 x g for 15 min at 4ºC and the RNA was resuspended in DEPC treated H_2O. To quantify the RNA, the 260/280 absorbance was determined using a spectrophotometer. The RNA was assessed for quality on a formaldehyde gel (18% (v/v) formaldehyde, 1% (w/v) agarose, 72% (v/v) DEPC treated H_2O, and 10% (v/v) 10x MOPS buffer (0.4 M 3-[N-Morpholino] propanesulfonic acid pH 7.0, 0.1 M sodium acetate, 0.01 M EDTA).

Northern blot

Northern blots of total RNA were performed using a NorthernMax Protocol (Ambion) as previously described (175). Briefly, 1-10 µg of total RNA was separated on a formaldehyde-agarose gel and downward transferred with 20x SSC (3 M sodium chloride, 0.3 M sodium citrate) to a positively charged nylon membrane and UV

crosslinked (Stratagene). Hybridization and scanning for the northern blots were done as detailed for Southern blots above.

DNase I treatment.

RNA for microarray and real-time RT-PCR analysis was treated with DNase I (Ambion) to remove genomic DNA from the sample. Briefly, approximately 20 µg of total RNA was incubated with DNase I (Ambion) at 37ºC for 30 min according to the manufacturers instructions. A test PCR reaction was completed on 2 µl of the DNase I reaction, to verify complete degradation of the gDNA.

Reverse transcriptase PCR (RT-PCR)

RNA for RT-PCR was treated with DNase I to remove residual gDNA. cDNA was generated using the SuperScript First-strand synthesis kit for RT-PCR (Invitrogen) according to the protocol provided. Briefly, DNA-free RNA was denatured at 65ºC for 5 min, snap cooled on ice, and incubated with dNTP's and the random hexamer primers for 10 min at 25ºC. Reactions with and without reverse transcriptase were then incubated at 50ºC for 50 min to allow for cDNA synthesis. Heating to 85ºC for 5 min terminated the reaction, and the original RNA was degraded by treatment with RNase H for 20 min at 37ºC. PCR reactions using Taq polymerase (NEB) were then completed on the cDNA from RT^+ and RT- cDNA samples, along with a gDNA control using the primer sets as follows: *ccpA*L2/R2, *ccpA*L3/*ccpA*-M6-R3, and Spy0515L/R (Table 2).

Microarray Analysis

Microarray experiments were performed as previously described (177). Briefly, 10 μg RNA from 3 biological replicates was isolated from MGAS5005 and the isogenic Δ*ccpA* strain MGAS5005.718 using a Triton X-100 isolation protocol (210). RNA was DNase I treated and analyzed for quality on formaldehyde-agarose gel. RNA samples were converted to cDNA with an amino-allyl UTP and were labeled with both Cy3 and Cy5 dye using the Cyscribe Post-Labeling Kit (GE Healthcare) to allow for dye-swap experiments. Yield and incorporation of dye was determined using a Nanodrop ND-1000 (Nanodrop Technologies). 25 μl of labeled Cy3 cDNA and Cy5 cDNA, were dried under vacuum, resuspended in 23.8 μl of dH_2O and boiled for 5 min followed by cooling on ice for 1 min. 17 μl of 5x Hyb Buffer (GE Healthcare) and 27.2 μl formamide was added to the cDNA and applied to array slides under raised cover slip (Lifterslip, Inc). Microarray slides were hybridized at 50 $^{\circ}$C overnight in slide chambers (Array It). Slides were washed twice for 10 min each in the following buffer concentrations and temperatures: 6x SSPE (diluted 20x stock solution: 3 M NaCl, 0.2 M NaH_2PO_4, 0.2 M EDTA at pH 7.4) with 0.01% Tween-20 at 50 $^{\circ}$C, 0.8x SSPE with 0.001% Tween-20 at 50 $^{\circ}$C, and 0.8x SSPE at room temperature. Slides were scanned using a Genepix 4100A personal array scanner and GenePixPro 6.0 software (Axon Instruments).

Data from the output GenePix results file (gpr) was analyzed using Acuity 4.0 software (Axon Instruments). Microarray data was normalized using the ratio of the means. Datasets were then generated by analyzing data points whose mean of the ratio (635/532) was ≥ 2.0 or ≤ 0.50, followed by removal of samples where 4 out of the 6 microarray hybridization experiments (67%) did not show significance. Array data has

been submitted to the NCBI GEO database and is accessible through series number GSE11328. Array validation was carried out on 12 differentially regulated genes with real-time RT-PCR (see below) using real-time primer pairs (Table 4). Correlation coefficients for the arrays were determined by plotting the log value of the array (X) to the log value of the real-time RT-PCR (Y). An equation describing the line of best fit was determined with the resulting R^2 value representing the fitness of the data, with higher correlations approaching $R^2=1$.

Table 4. Real-time RT-PCR primers

Target	Primer	Sequence (5'-3')[a]	Reference
amyA			
	amyA M1 RT L	GTTTGGGTACTTGGCAATGG	This study
	amyA M1 RT R	TGGGTGATGTTTTTGAGATGG	This study
arcA			
	arcA M1 RT L	GAAAATGGTGGTCAGCACGTTA	This study
	arcA M1 RT R	CGTCTTCGCCGTTCATGAT	This study
atpB			
	atpB M1 RT L	AATCTGGCTTTTGACCTTGC	This study
	atpB M1 RT R	TAGCCAAACGTTTCAAATGG	This study
bglP			
	bglP M1 RT L	ACTGCGACGATTGTGTTAGC	This study
	bglP M1 RT R	GCAACACTCACTTGCTTTGG	This study
ccpA			
	ccpA M1 RT L	GTGAATCGTTGCTGGTGATGAT	(177)
	ccpA M1 RT R	TGGTCGTCATCAAGTGATCC	(177)
celC			
	celC M1 RT L	TGGTCGTCATCAAGTGATCC	This study
	celC M1 RT R	CTTGCCCAAGAAGCTAGTGG	This study
covS			
	covS M1 RT L	CATCTCCTGGCTTGCATGGT	This study
	covS M1 RT R	GGAAAACCCACGATACTGATCTTC	This study
emm			
	emm1 RT L	ACTCCAGCTGTTGCCATAACAG	(177)
	emm1 RT R	GAGACAGTTACCATCAACAGGTGAA	(177)
gyrA			
	gyrA M1 RT L	CGACTTGTCTGAACGCCAAAGT	(177)
	gyrA M1 RT R	ATCACGTTCCAAACCAGTCAAAC	(177)
hasA			
	hasA M1 RT L	CGACTTGTCTGAACGCCAAAGT	(177)
	hasA M1 RT R	ATCACGTTCCAAACCAGTCAAAC	(177)
malX			
	malX M1 RT L	CCATAACCGGCAATTAAACC	This study

	malX M1 RT R	TTTGCTTTTGCCTCTGAACC	This study
mga			
	mga M1 RT L	CGCTGAGTTGAGCCTGATTTC	(177)
	mga M1 RT R	AGACTCACCAACGGGCTGTC	(177)
	mga M6 RT L	AGATGAATCCAGTTGGTCACTTTTC	(5)
	mga M6 RT R	AAATCGGTTATGCGTTTGATAGC	(5)
	*mgaP1*_L2	TAAATAATGAACAAAAAGGAATAATTGCG	(5)
	*mgaP1*_R2	AATACCTTTCAAATTCTTTCATTAAAATCC	(5)
ptsA			
	ptsA M1 RT L	TTTTTTAAAACCAGGCGAAGC	This study
	ptsA M1 RT R	TTGTCTCAGGGACCAAATCC	This study
pyk			
	pyk M1 RT L	GGAAGGCAGATGAATCTAAACG	This study
	pyk M1 RT R	TACCCGGTTGAATCTGTTCG	This study
rivR			
	rivR M1 RT L	GACGGCCTGTGTCATAAAGC	This study
	rivR M1 RT R	GATCAATATCAAGGCAACATGC	This study
rofA			
	rofA M1 RT L	CGAAGAGTGGATGGCCAAAC	(177)
	rofA M1 RT R	CTCGACATAGTGGCAAAAAAGATG	(177)
sagA			
	sagA M1 RT L	GCTACTAGTGTAGCTGAAACAACTCAA	This study
	sagA M1 RT R	AGCAACAAGTAGTACAGCAGCAA	This study
scpA			
	scpA M1 RT L	TTTCGACACGCATCAAAAGC	This study
	scpA M1 RT R	TGCTCCATCTGAAACGAAAGAAC	This study
slo			
	slo M1 RT L	TTGTTGAGGATAATGTAAGAATGTTTAG	This study
	slo M1 RT R	TCCTGGCTTGCAACTGATTG	This study
spy1680			
	Spy1680 M1 RT L	GGCAAGCCCTACTAAAAGAGG	This study
	Spy1680 M1 RT R	GGAAACGGATTTCAGTCAGC	This study

Real-time RT-PCR

Briefly, 25 ng of DNaseI-treated total RNA was added to SYBR Green Master mix (Applied Biosystems) containing 5 µg of each specific real-time primer (Table 4) for the 1-step protocol. The real-time RT-PCR experiments were completed using a Lightcycler 480 (Roche) and levels presented represent ratios of WT/experimental relative to the level of *gyrA* transcript. The real-time primers were designed using Primer 3: WWW Primer tool (biotools.umassmed.edu/bioapps/primer3_www.cgi).

PROTEIN ANALYSES

GAS protein extracts

Whole cell GAS protein extractions were performed as previously described (142). Briefly, GAS cells were inoculated 1:20 into 10 ml THY broth, grown to the appropriate optical density or Klett unit, and pelleted by centrifugation at 7,000 x g for 20 min at 4ºC. Cells were washed in saline, and resuspended in 500 µl of saline. The cells were lysed by mixing with the FastPROTEIN blue matrix and by bead-beating in a Fast-prep cell disruptor (Bio101, Inc.) for 45 sec at speed 6. Lysates were rested on ice for 15 min, followed by centrifugation at 13,000 x g for 10 min and the supernatant was recentrifuged once more to remove all of the lysing matrix. Protein concentration was assayed using the Bio-Rad protein assay kit and reading the absorbance at 595 nm on the spectrophotometer.

SDS-PAGE gel analysis

SDS-polyacrylamide gels (SDS-PAGE) were made as follows: a 10-15% resolving gel was mixed and poured using the components listed in the Table 5 followed by a 6% stacking gel (Table 5). Upon the gel setting, it was either used immediately or stored at 4ºC for later use. Protein samples were mixed with 5x cracking buffer (Table 5) and loaded into the wells. SDS-PAGE gels were run at 150 V for about 1 hr.

Western blot analyses

SDS-PAGE gels were transferred to nitrocellulose membranes using the Mini-Protean apparatus (Bio-Rad) in 1x transfer buffer (Table 5). Blots were blocked

overnight in blocking solution (5% (w/v) dried milk in PBS-tween). Western blots were incubated with a 1:1,000 dilution α-Mga-pep2 antiserum (142) followed by three 15 min washes in PBS-tween (Table 5). Blots were then incubated with a 1:25,000 dilution of α-rat (Santa Cruz Biotechnologies) HRP-conjugated secondary antibody and visualized using the Western Lightning chemiluminescence system (Perkin Elmer) followed by exposure to X-ray film.

Table 5. SDS-PAGE buffers

10- 15% Resolving gel	**6% Stacking gel**
26% (v/v) Lower gel stock 25-37.5% (v/v) 40% Acrylamide/ bis sol. 0.5% (v/v) 10% ammonium persulfate 0.1% (v/v) tetramehylethylene diamine Brought up with H_2O	25% (v/v) Upper gel stock 15% (v/v) 40% Acrylamide/ bis sol. 0.5% (v/v) 10% ammonium persulfate 0.1% (v/v) tetramehylethylene diamine Brought up with H_2O

Lower gel stock	**Upper gel stock**
1.5 M Tris HCl pH 8.8 0.4% (w/v) SDS Brought up with H_2O	0.5 M Tris-HCl pH 8.8 0.4% (w/v) SDS Brought up with H_2O

SDS running buffer	**Coomassie blue stain**
25 mM Tris 190 mM Glycine 0.1% (w/v) SDS Brought up with H_2O	0.25% (w/v) coomassie blue 45.4% (v/v) methanol 9.2% (v/v) glacial acetic acid Brought up with H_2O

Destain solution	**Gel drying solution**
5% (v/v) methanol 7.5% (v/v) glacial acetic acid Brought up with H_2O	3% (v/v) glycerol 20% (v/v) EtOH Brought up with H_2O

5x Cracking buffer	**Transfer buffer**
0.3 M Tris pH 6.8 25% (v/v) 2-mercaptoethanol 51% (v/v) glycerol 10% (w/v) SDS 0.01% (w/v) bromophenol blue Brought up with H_2O Heated at 55ºC	25 mM Tris base 0.2 M glycine Brought up with 20% methanol
	PBS-Tween
	0.01 M PBS pH 7.4 0.5% Tween-20 Brought up with H_2O

Protein expression and purification

GAS His-CcpA, HPr, and Hpr Kinase were purified via Ni-NTA resin (Qiagen) based on the manufacturer's protocol. Briefly, expression of proteins was induced at an OD_{600} of 0.6 for 4 hrs with 1 mM IPTG and resulting cell pellets stored at -80 ˚C. The frozen pellets were lysed in the presence of 1 mg/ml lysozyme and 1x Complete Protease inhibitors (Roche) using a Branson sonicator (5 cycles of 30 sec pulses at 50% duty cycle, output of 7.5). His-tagged proteins were purified from the resulting lysate over Ni-NTA resin under native conditions and protein concentration was determined for each fraction using Protein assay reagent (Bio-Rad) using an Ultrospec 2100 spectrophotometer (GE Healthcare). Samples from the protein purification were run on SDS PAGE gel for analysis (Fig. 3). Chosen fractions were dialyzed with two buffer changes in 4 L of TKED buffer (100 mM Tris-HCl, 150 mM potassium chloride, 1 mM EDTA, 0.1 mM DTT) and glycerol was added to 10% prior to storage of protein aliquots at -20˚C.

HPr phosphorylation reaction

To produce phosphorylated HPr (HPr-P), 20 µg of GAS His-HPr Kinase and His-HPr were incubated in a reaction mixture containing 10 mM ATP, 20 mM Tris, 7.5 mM fructose 1-6 bisphosphate, 5 mM $MgCl_2$, and 1 mM DTT at 37ºC for 15 min. Initial reaction was completed using [γ^{32}P]-ATP to verify specific phosphorylation of HPr (Fig. 4).

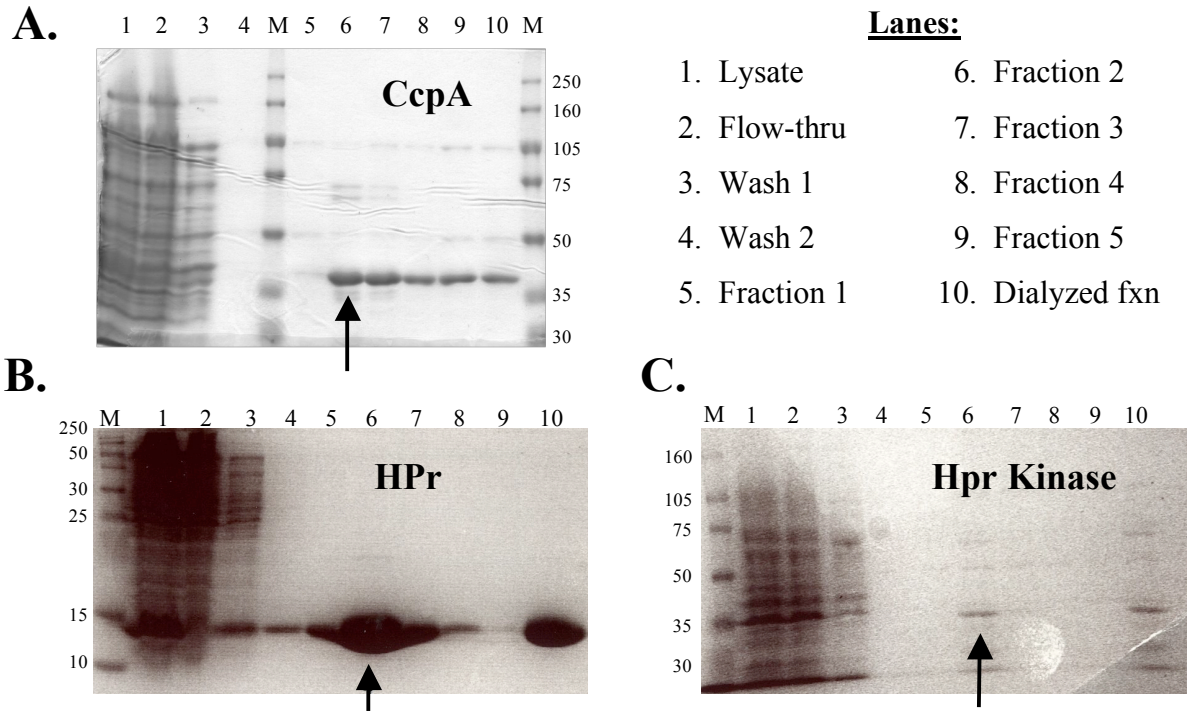

Fig. 3: Coomassie-stained SDS PAGE gel of purified proteins
(A) CcpA **(B)** HPr and **(C)** Hpr Kinase Ni-NTA column fractions (lanes are indicated in the list above). Arrow indicates fraction chosen for dialysis and used in further studies.

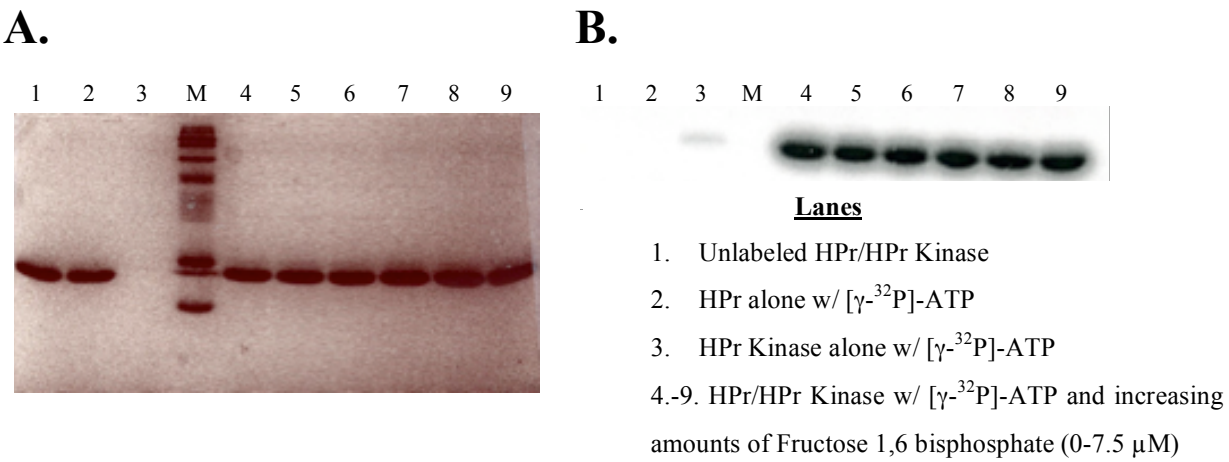

Fig. 4: HPr phosphorylation reaction
(A) Coomassie-stained SDS-PAGE gel **(B)** Phosphorimage scan of HPr phosphorylation reaction.

Streptolysin S (SLS) hemolysis assay

Hemolysis assays were performed as previously described (173). Briefly, strains were grown in THY broth supplemented with 10% heat-inactivated horse serum. Samples were taken every hour for a total of eight hours, and immediately frozen at -80ºC. Bacterial cells were pelleted and a 1:10 dilution was made of the supernatant. 500 µl of this dilution was added to an equal volume of 2.5% (v/v) difibrinated sheep red blood cells (RBC), which were washed three times with sterile PBS pH 7.4. This mixture was incubated at 37ºC for 1 hr and cleared by centrifugation at 3000 x g. Supernatants were measured at an absorbance of 541 nm using a plate reading spectrophotometer (Molecular Dynamics) to determine release of hemoglobin by lysed RBC. Percent hemolysis was defined as ((Sample Abs - Blank)/ (100% lysis Abs.)) x (100). To assay for SLO-mediated hemolytic activity, the SLS inhibitor Trypan blue (13 µg/µl) was added to samples prior to incubation.

TRANSCRIPTIONAL REPORTER ASSAYS

GusA Assay

GusA assays were performed as previously described (67). Briefly, cells were grown to late logarithmic phase, and protein lysates were collected using a FastPrep cell disruptor (Bio101, Inc.) as described above. The lysates were incubated with p-nitrophenyl ß-D glucuronide for 3 hrs at 37ºC until a yellow color developed indicating GusA activity. Results are reported in GusA units, which are equivalent to the A_{420} of the lysate divided by the concentration of total lysate protein (µg/µL).

Luciferase Assay

Luciferase assays were performed by inoculating 13 ml of liquid THY broth or CDM with 1:20 dilution of the overnight starter culture. Upon reaching Klett 30, 500 µl samples were taken every 15 Klett units. Samples were pelleted, and the supernatant was discarded and samples were placed at -20ºC overnight. The luciferase assay was performed using the Luciferase Assay system (Promega). Pellets were resuspended in various amounts of 1x Lysis buffer to normalize for cell unit according to the equation 4.5 = (x ml)((Klett 65)/2). The luciferase assay was read using a Centro XS^3 LB 960 luminometer (Berthold Technologies) where 50 µl of Luciferin-D reagent was directly injected. A comparison between the chromosomal-based and the plasmid-based luciferase system can be seen below (Fig. 4).

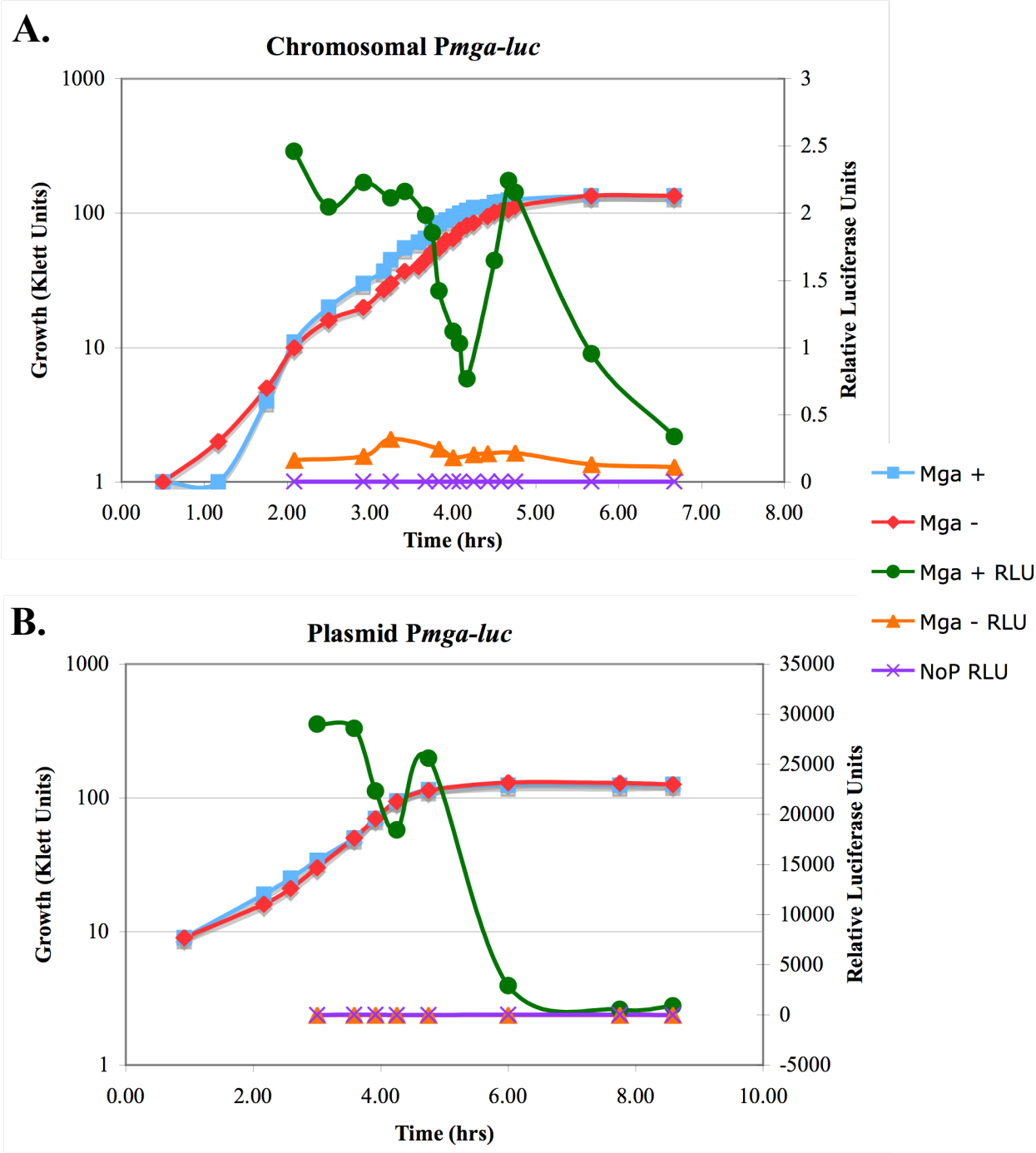

Fig. 5: Comparison between Luciferase transcriptional reporters
(A) Chromosomal-based or **(B)** plasmid-based P*mga*-luciferase transcriptional reporters. Shown for each is the growth in Klett units for the wild-type (Mga^+) and negative control (Mga^-) strains. The relative luciferase units (RLU) or luciferase profile for Mga^+, Mga^- and a promoterless control (NoP RLU) is shown and graphed on the right Y-axis. Samples for the luciferase experiment were collected every 15 Klett, beginning at Klett 30, with multiple points taken in stationary phase.

MURINE INFECTION MODELS

Intraperitoneal (i.p) route

An overnight culture (5 ml) was used to inoculate 75 ml of THY and incubated static with appropriate antibiotics at 37 °C until late-logarithmic phase. Approximately 2 x 10^7 colony forming units (CFU)/ml, as determined by microscope counts and verified by plating for viable colonies, was used to infect 6 to 7-week old female CD-1 mice (Charles River Laboratories). Mice were injected with 100 µl (2 x 10^8 CFU) of the cell suspension by the i.p route and were monitored as necessary for 72 hrs post infection. Mice were euthanized by CO_2 asphyxiation upon signs of systemic morbidity (hunching, lethargy, hind leg paralysis). Survival data was assessed by Kaplan-Meier survival analysis and tested for significance by logrank test using GraphPad Prism (GraphPad Software).

Subcutaneous (s.c) route

The invasive skin model of infection was performed as described previously (186). Briefly, 6 to 7-week old female CD-1 mice (Charles River Laboratories) were anesthetized and depilated for an ~2 cm^2 area of their haunch with Nair (Carter Products, New York, NY) and 100 µl of a cell suspension (2 x10^8 CFU/mouse) was injected subcutaneously. Mice were monitored twice daily and were euthanized by CO_2 asphyxiation upon signs of morbidity. Lesion sizes (L x W) were measured at 72 hrs post infection with length (L) determined at the longest point of the lesion. Lesion size data was analyzed using GraphPad Prism (GraphPad Software) and tested for significance using an unpaired two-tailed t-test.

DNA-PROTEIN INTERACTIONS

PAGE oligonucleotide purification

The oligonucleotides for electrophoretic mobility shift assays (EMSA) were PAGE purified prior to annealing. Briefly, the lyophilized oligonucleotides pellet (Integrated DNA Technologies) was resuspended in 100 µl dH_2O with 20 µl formamide stop solution (SequiTherm Excel II kit, Epicentre). To pour the gel, 60 ml of the 10% sequencing gel solution (42% (w/v) urea, 20% (v/v) 5x TBE, 25% (v/v) 40% acrylamide bis sol.) was added to the polymerizing agents (175 µl 10% ammonium persulfate and 75 µl of tetramehylethylene diamine). The oligonucleotides were loaded and the gel was run for 1 to 1.5 hrs at 400 V. After the gel was run, the front glass plate was removed, the gel was placed on an intensifying cassette and a short-wave UV light was flashed to locate the DNA bands. The bands were excised and extracted by soaking in 10 mM Tris pH 7.4 overnight, followed by a phenol-chloroform extraction the next day to remove acrylamide.

Annealing double stranded oligonucleotides

Double stranded DNA (dsDNA) probes were generated by annealing 30 bp sense and antisense oligonucleotide pairs listed in Table 6. Briefly, gel-purified oligonucleotide pairs were annealed by heating to 85˚C for 5 min in 12.5 µg of each pair in 10 mM Tris-HCl pH 8.0, 5 mM $MgCl_2$ and slowly cooling to room temperature for 30 min. Annealed oligonucleotides were end-labeled with [γ^{32}P]-ATP using T4 PNK (NEB) and the resulting radiolabeled probes were purified across a G-25 sephadex quick spin column (Roche).

Table 6. Oligonucleotide probes

Target	Primer	Sequence (Strand is designated)[a]
P*ccpA*		
	5'P*ccpA*CRE	5'TTAATTTTTGAAAACTTTTTCAAAAATTAA
	3'P*ccpA*CRE	3'AATTAAAAACTTTTGAAAAAGTTTTTAATT
P*ccpA* Scr		
	P*ccpA* Scr Sense	5'ATAAATTATTTTAGAATTCTATTAACTTAA
	P*ccpA* Scr Antisense	3'TATTTAATAAAATCTTAAGATAATTGAATT
P*mga*		
	5'P*mga*CRE	5'TTAGCTCTTGAAAACGTTTCTACGATGTTT
	3'P*mga*CRE	3'AATCGAGAACTTTTGCAAAGATGCTACAAA
P*mga* Mut		
	5'mutated*Pmga*CRE	5'TTAGCTCTTACGAAAGTTTCTACGATGTTT
	3'mutated*Pmga*CRE	3'AATCGAGAATGCTTTCAAAGATGCTACAAA
P*mga* Scr		
	5'scrambled*Pmga*CRE	5'CATGTATGTCTCAGTCGTTATGTATATTCA
	3'scrambled*Pmga*CRE	3'GTACATACAGAGTCAGCAATACATATAAGT
P*sagA*		
	P*sagA*CRESense	5'TATTAAAAAGAAAGGGTTTACATATTAATC
	P*sagA*CREAntisense	3'ATAATTTTTCTTTCCCAAATGTATAATTAG
rivR		
	*ralp4*CRESense	5'CCAATCTTTGATAACGGTTTCAAGCTTATC
	*ralp4*CREAntisense	3'GGTTAGAAACTATTGCCAAAGTTCGAATAG

[a] -*cre* shown in shaded regions

Electrophoretic mobility shift assay (EMSA)

EMSA was performed as described previously (140). For ds oligo EMSA, a constant amount of labeled ds oligo probe (ca. 1-5 ng) and increasing amounts of purified GAS His-CcpA (5-20 μM) were used in each reaction. Competition assays were performed by addition of 700 ng unlabeled double-stranded oligonucleotide probes to binding reactions. For the PCR probe EMSA, probes were end-labeled as previously described, extracted by crush and soak elution, and run over a PCR purification column (Qiagen). 20 μM HPr-P was added to a constant amount (10-25 ng) of end-labeled probe, and increasing amounts of GAS His-CcpA (1-4 μM) was added. After incubating

for 30 min at 30 °C, reactions were mixed in 1% (v/v) ficoll, 0.02% (w/v) bromophenol blue and separated on a 5% polyacrylamide, 10% (v/v) glycerol gel at room temperature. Gels were dried under vacuum at 80 °C for 1 hr and exposed overnight to a phosphor imaging screen. Screens were scanned using a Storm860 (Amersham Biosciences) and resulting data was analyzed with the ImageQuant analysis software (version 5.0).

CHAPTER FOUR:

CcpA-mediated carbon catabolite regulation and sugar metabolism influence the expression of *mga*

INTRODUCTION

CCR and sugar metabolism regulation are important factors in virulence regulation for several Gram-positive pathogens. Several recent studies have highlighted the significance of CcpA, a major mediator of CCR in Gram-positive organisms, as also being important for regulation of virulence. For example, in *C. perfringens* the expression of the *cpe* enterotoxin is under CcpA-mediated CCR (221). Furthermore, a study in the closely related Gram-positive pathogen *S. pneumoniae* showed that deletion of *ccpA* attenuated the organism for pathogenesis and the ability to colonize the nasopharynx of a mouse model of infection (100).

Although *B. subtilis* is not a human pathogen, much of the work to define CcpA-mediated CCR has been completed in this model organism. The studies in *B. subtilis* has helped to construct a model for CcpA-mediated CCR in Gram-positive organisms, a diagram of which can be found in the Review of the Literature section (Fig. 2). Another major contribution from the *B. subtilis* studies was the development of a consensus CcpA-binding site or *cre* (204). In addition, many CcpA-regulated genes have been identified such as *ackA* encoding for acetate kinase and *arcA* encoding for an arginine-deaminase, which are positively and negatively regulated by CcpA, respectively (64, 218).

Several studies completed in *S. pyogenes* have identified a role for sugar metabolism and virulence, specifically in the expression of the major surface virulence factor M protein. Early physiological studies showed that M protein expression was higher during growth in glucose compared to growth in sucrose (162). The gene encoding M protein, *emm,* has since been found to be directly regulated by the virulence regulator Mga (140). In the absence of Mga, there are almost no detectable levels of *emm* transcription (159), indicating that Mga is required for M protein expression. These data might suggest that this influence of sugar metabolism on M protein could be mediated through Mga via regulation at the level of transcription.

The structure of the *mga* promoter is complex; it contains two transcriptional start sites separated by two Mga-binding sites from which it can positively autoregulate expression (145). The proximal P*mga* promoter, or P*mga* P2, mediates auto-regulation of *mga* expression, whereas the distal promoter, P*mga* P1 is predicted to be involved in basal levels of transcription. Several factors have been shown to influence *mga* expression including growth phase, CO_2 levels, and iron concentration, and the recently identified putative sugar transporter AmrA (141, 176).

A transposon screen looking for regulators of Mga was completed using a GusA transcriptional reporter strain fused to the Mga-regulated promoter, P*emm*. This study identified the putative sugar transporter AmrA, as a regulator of Mga (176). AmrA (activation of Mga regulon expression locus A) is located near the rhamnose cell-wall operon, and is closely related to transporters for several surface localized components such as teichoic acid. Further experiments with a deletion of *amrA* showed that AmrA alone was responsible for the reduction in both *emm* and *mga* expression.

Given the information from other important Gram-positive pathogens as well as from the GAS, it was hypothesized that CCR influences virulence expression through regulation of *mga*. In the present study, an in silico search for *cre* sites was completed on the M1 SF370 GAS genome and a putative *cre* was identified in the P*mga* promoter upstream of the P1 transcriptional start site. This result along with previous data is beginning to reveal a link between CCR, sugar metabolism, and virulence gene regulation in the GAS.

RESULTS

Identification of putative *cre* in the GAS genome

As an initial step to find GAS genes under CcpA-mediated CCR, the genome of the serotype M1 strain SF370 was scanned for putative *cre* based on similarity to the published *B. subtilis* consensus sequence TGWAARCGYTWNCW (204). Allowing for a single mismatch from the consensus, 60 *cre* were identified on the direct strand, and 58 were identified on the complementary strand, resulting in 98 unique sites scattered throughout the genome (Appendix I). Many of the putative *cre* in the M1 genome were located upstream or within annotated ORFs similar to genes regulated by CcpA in *B. subtilis* (150, 152), including *ndk*, *ackA, arcA, lctE* and numerous sugar transport operons (Fig. 6B and Appendix I). The promoter of *ccpA*, which can be autoregulated (66), was also found to have a *cre* similar to the *B. subtilis* consensus with a single mismatch (Fig. 6B). Thus, the location of *cre* identified in the GAS genome corresponds to known CcpA-regulated genes.

A.

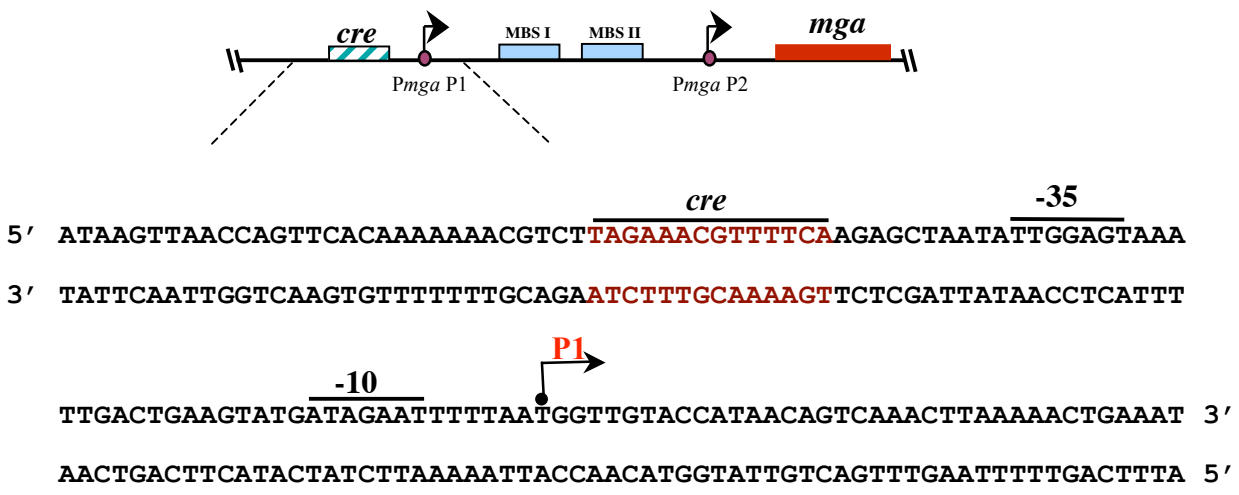

B.

cre	TGWAARCGYTWNCW
P*ccpA*	TGAAAACTTTTTCA
P*ackA*	TGAAATCGTTTTCT
P*arcA*	TGTAAGCGATTACT
P*mga* *	TGAAAACGTTTCTA
P*mga* M18	TGAAAATGTTTCTA

Fig. 6: Location of P*mga cre* and alignment of identified *cre* in GAS genomes
(A) Location of the putative P*mga cre* (striped box) relative to the P1 start of transcription in the M1 SF370 GAS genome. The P1 start of transcription (arrow), -10 and -35 hexamers (overlines). **(B)** The putative *cre* from the P*mga* region of the M1 serotype of the GAS is shown (* also the same for serotypes: M3, M4, M5, M6, M12, M23, M28, M49, and M50), whereas the M18 serotype has an additional varied nucleotide at position 7. Also shown are the putative *cre* identified in the promoters of known CcpA-regulated genes P*ccpA*, P*ackA*, and P*arcA*. The *B. subtilis* consensus *cre* (shown in red text with degenerate nucleotides) was used to identify the GAS *cre* sites with one mismatch allowed.

One such *cre* was identified within the *mga* promoter (P*mga*) upstream of the distal P1 start of transcription (Fig. 6A). The site was found to be highly conserved among all serotypes of the GAS for which genome sequence is available (Fig. 6B). Based on CcpA studies in *L. lactis*, the position of the P*mga* P1 *cre* centered at -54.5 bp from the start of transcription strongly suggests that it might play a role in activating P*mga* activity (236).

The catabolite control protein, CcpA, specifically binds to P*ccpA* and P*mga in vitro*

To determine if CcpA interacts with *cre* identified in the bioinformatic screen of the GAS M1 genome, electrophoretic mobility shift assays (EMSAs) were performed on P*ccpA* and P*mga*. Double stranded oligonucleotide probes (30 bp) were generated that contained either the P*ccpA* (positive control) or the P*mga cre* (14 bp each) centered within the sequence (Table 6). To address specificity of CcpA binding, probes consisting of a random rearrangement of the respective nucleotides (Scrambled P*ccpA* and P*mga*) or a probe containing four specific mutations in the P*mga cre* (Mutated P*mga*) were generated (Table 6). Since CcpA is capable of binding DNA in the absence of phosphorylated HPr-Ser *in vitro* (11), assays were performed using purified GAS N-terminal 6xHis-tagged CcpA alone (see Materials and Methods).

Studies in other Gram-positive bacteria predict that CcpA will bind to a *cre* located within its own promoter (134, 236); therefore, the ability of purified His-CcpA to bind to the identified GAS P*ccpA cre* probe was tested initially. Increasing amounts of His-CcpA (5.0 to 7.5 μM) resulted in a mobility shift of labeled P*ccpA*, indicating DNA

binding (Fig. 7A, lanes 1-3). The ddition of 700 ng of cold P*ccpA* to the reaction was able to compete for His-CcpA interaction, whereas the addition of the same amount of a cold scrambled P*ccpA* probe had no effect (Fig. 7A, lanes 4 and 5). Thus, GAS His-CcpA is able to bind specifically to the P*ccpA cre in vitro*.

The *Pmga cre* probe also demonstrated slower migration upon addition of increasing amounts of purified His-CcpA (7.5 to 12.5 μM), indicating protein/DNA interaction (Fig. 7B). The addition of 700 ng of either cold P*mga* or P*ccpA cre* probes to the reaction was able to compete for binding of His-CcpA to the labeled P*mga* probe to varying degrees (Fig. 7B, lanes 6 and 8). In contrast, a scrambled P*mga cre* probe (9/14 mismatches) was not able to compete for His-CcpA (Fig. 7B, lane 9), suggesting that the interaction with P*mga cre* is specific. In support of this conclusion, mutation of only 4/14 nucleotides in the predicted P*mga cre* exhibited an intermediate level of competition (Fig. 7B, lane 7). Thus, GAS His-CcpA is capable of binding directly to the predicted *cre* sequences located upstream of the P*ccpA* and P*mga* P1 promoters *in vitro*.

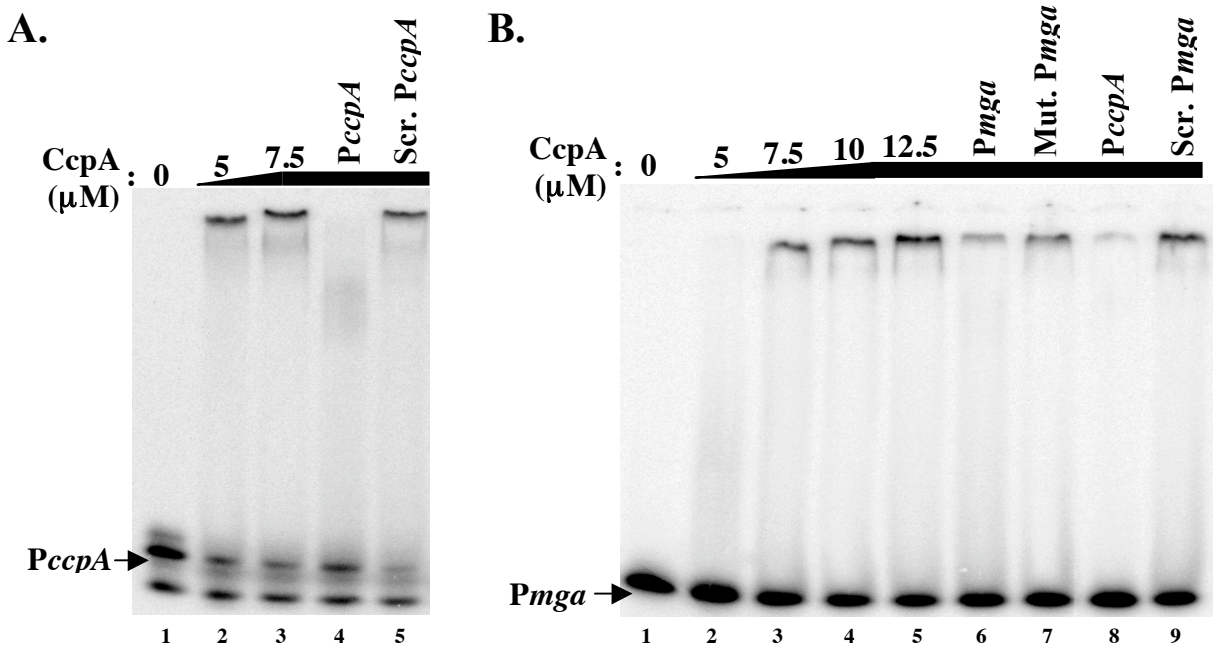

Fig. 7: EMSA of *Pmga cre* using His-CcpA
(A) EMSA was performed on radiolabeled *PccpA*-annealed or **(B)** P*mga*-annealed oligonucleotide probes. A constant amount (1 to 2 ng) of [γ-^{32}P]ATP-labeled probe was incubated with increasing amounts (5 to 12.5 μM) of purified GAS His-CcpA for 30 min at 30°C prior to separation on a 5% polyacrylamide, 10% glycerol gel. The specificity of His-CcpA binding to P*ccpA* and P*mga* was assayed by addition of 700 ng of unlabeled competitor annealed oligonucleotide probes corresponding to P*mga* (B. lane 6), mutated (Mut.) P*mga* (B. lane 7), P*ccpA* (A. lane 4 and B. lane 8), scrambled (Scr.) *PccpA* (A. lane 5) and Scr. P*mga* (B. lane 9) using the oligonucleotide pairs listed in Table 6.

The *cre* is necessary for activation of P*mga*

To assess the role that the *cre* upstream of P1 P*mga* plays in activation of *mga* expression, quantitative real-time RT-PCR was utilized to assess the effects of deleting the *cre* region on the expression of *mga.* Deletion of the *cre* upstream of P*mga* was created by allelic exchange with a kanamycin cassette (Δ*cre*), and an additional strain was created with the cassette inserted directly upstream of the *cre* as a control for the presence of the cassette (full P*mga*). Real-time RT-PCR was completed using total RNA isolated from the wild type M6 JRS4 strain (Parent), full P*mga*, and Δ*cre* strains grown to late logarithmic phase. Given that transcript levels from P*mga* P1 are often quite low (145), both P*mga* P1 alone (Fig 8AB) and total P*mga* (Fig. 8AC) transcripts were detected using the *mga* P1 RT and *mga* RT primer pairs (Table 4), respectively, and results were normalized to transcript levels of the housekeeping gene *gyrA*.

As expected, relative levels of *mga* transcribed from P*mga* P1 alone and total P*mga* were similar between the parent strain, JRS4, and the full P*mga* control strain (Fig. 8B and C), indicating that the ΩKm2 cassette inserted upstream of P*mga* had little effect on the transcription of *mga* (Fig. 8B and C). Importantly, deletion of the *cre* in P*mga* caused an approximately two-fold reduction in the levels of both P*mga* P1 and total P*mga*, suggesting that the *cre* is important in the activation of *mga* transcription.

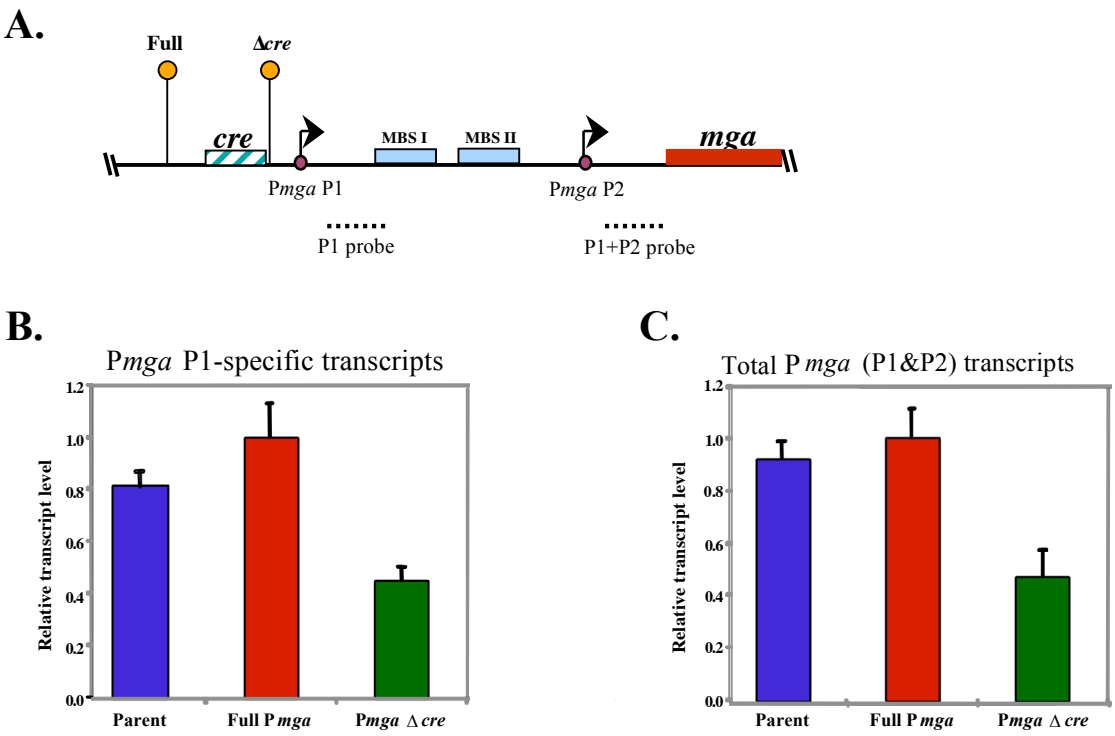

Fig. 8: Real-time RT-PCR analysis of native P*mga* P1 and *mga* transcripts
(A) Real-time RT-PCR was performed on total RNA isolated from the JRS4-derived strains containing either the Full P*mga* promoter, or the P1 P*mga* Δ*cre*, as shown in the schematic (lollipops) along with all relevant P*mga* elements. The location of the P1 and the P1 & P2 probes are indicated (dotted lines). **(B)** Levels of *mga* transcribed from the P*mga* P1 start site only were assessed using the P1 probe. **(C)** Total P*mga* transcript levels were assessed using the P1 & P2 probe. Transcript levels are shown as the fold transcript level above that of the full-length P*mga* promoter that had been normalized to levels of the *gyrA* control. Reactions were performed in triplicate for three independent experiments. Error bars represent standard errors for the samples.

The *cre* is required for transcriptional activation of P*mga* P1

In order to further assess the effect of the *cre* on the activity of P*mga* P1 alone, a *gusA* transcriptional fusion was made to P*mga* P1 with and without the *cre* into an ectopic locus of wild type and Mga$^-$ M6 GAS to form full length and P1Δ*cre* strains, respectively. Since GusA activity from the reporter strains was too low to detect, transcript levels were assessed directly using semi-quantitative primer extension. Total RNA was extracted from late logarithmic phase from cells containing the full length P*mga* P1, the P1 Δ*cre*, and the promoterless control *gusA* reporter strains either in the presence or absence of a functional *mga*. Primer extensions were performed simultaneously for both *gusA* and the constitutive *rpsL* for each of the strains.

Promoter-specific products were not observed in either the absence of RNA (Fig. 9, lane 1) or in the no promoter control strains (Fig. 9, lanes 6 and 7), with the exception of two light background bands (Fig. 9, *). However, a product of the predicted size for P*mga* P1 was detected in the strains contain the *cre* (Fig. 9, lanes 2 and 3), while it was reduced approximately 4.2-fold in the strains without the *cre* as determined by densitometry (Fig. 9, lanes 4 and 5). This correlates with the Δ*cre* results from the real-time RT-PCR analysis of P*mga* P1 at its native locus (Fig. 8B). As expected from the absence of Mga-binding sites in P1, Mga had no detectable effect on transcription from P*mga* P1 (Fig. 9, lanes 2-5) when its transcript levels were normalized to *rpsL*. Thus, the *cre* is necessary for transcriptional activation from the P*mga* P1 start site.

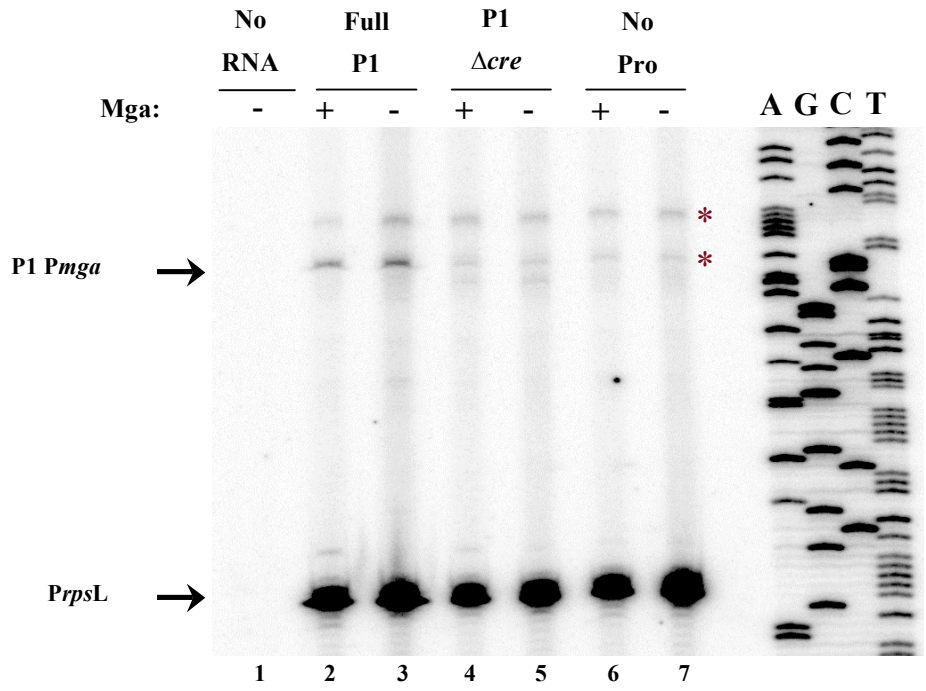

Fig. 9: Deletion analysis of the P*mga* P1 promoter region
Semiquantitative primer extension analysis was performed on total RNA from the full-length P1, P1 Δ*cre*, and no-promoter reporter strains using the radiolabeled antisense primers Steph_*gusA*-PE for *gusA* and GAS-*rpsL*5 for *rpsL* (Table 2) in the same reaction. The starts of transcription for *gusA* (P1 P*mga*) and *rpsL* (P*rpsL*) are shown at the left, and a P*mga* P1 sequence ladder is provided at the right. Nonspecific background bands are indicated with an asterisk. Results presented in this figure were completed by Dr. Audry Almengor.

Inactivation of *ccpA* affects *mga* expression

The role of CcpA-mediated activation of P*mga* on *mga* expression was assessed using an insertional-inactivation mutant of *ccpA* in an M6 serotype reporter strain containing a fusion of the full P*mga* promoter to *gusA*. Although the *ccpA*-defective strain had a longer lag phase, it did not exhibit any significant growth defects upon entry into log phase when grown in rich THY media compared to the wild type Mga^+ strain (Fig 10A). Inactivation of *ccpA* resulted in a greater than 3-fold reduction in P*mga*-specific GusA activity compared to the parental Mga^+ strain in samples grown to late-logarithmic phase in THY broth (Fig. 10B). The resulting GusA activity was slightly higher than background levels observed in the Mga^- control strain (Fig. 10B). In addition, western analysis of whole cell extracts found that steady state levels of Mga were also reduced in the $CcpA^-$ mutant at the same point in growth (Fig. 10C). These data indicate that CcpA is important for production of Mga during logarithmic phase, a point in growth when the Mga virulence regulon shows maximal expression (143).

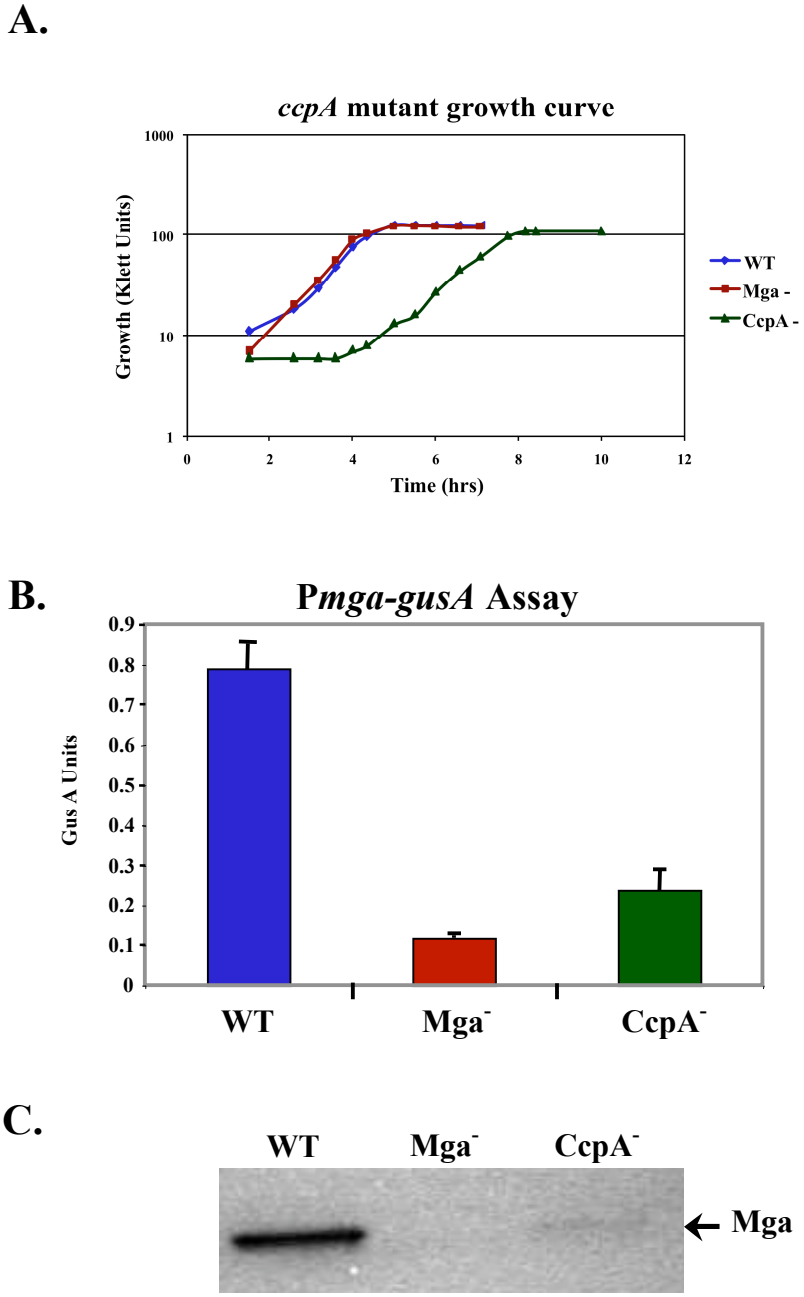

Fig. 10: Effect of a CcpA⁻ mutant on *mga* expression
(A) Growth curve **(B)** GusA reporter assay and **(C)** Western blot analysis for the M6 GAS P*mga-gusA* reporter strain (WT), the *mga*-inactivated derivative (Mga⁻), and the *ccpA*-inactivated derivative strain (CcpA⁻). **(A)** Strains were grown in THY broth. **(B)** Samples for GusA assay were taken at mid-log phase. GusA data is reported in GusA units (OD_{420}/ (Total protein concentration [µg/µl])) and represents the mean from four independent experiments with error bars showing standard error. **(C)** Mga protein production was assessed using Western analysis on whole-cell protein extracts probed with an anti-M6 Mga antibody.

Inactivation of *ccpA* does not affect Mga-regulated genes

To determine if CcpA influences the expression of other genes in the Mga regulon, real-time RT-PCR was performed on total RNA isolated from Mga$^+$, Mga$^-$, and CcpA- strains using the real-time RT-PCR primers for the Mga-regulated genes *emm* and *scpA* (Table 4). Unexpectedly, CcpA does not appear to be required for normal levels of *emm* and *scpA* expression, as transcript levels were within the 2-fold range of normal gene expression (Fig. 11). The *ccpA* real-time RT-PCR primers (Table 4) were used as a control to verify the loss of *ccpA* in the CcpA$^-$ strain, but not the Mga$^+$ or Mga$^-$ strains. In addition, the Mga$^-$ strain showed approximately a 9 and 4-fold reduction in *emm* and *scpA,* respectively but not in *ccpA* (Fig. 11). Although CcpA activates both the transcriptional activation of P*mga* as well as Mga expression, these results indicate that CcpA does not directly activate expression of the Mga-regulated genes *emm* and *scpA*.

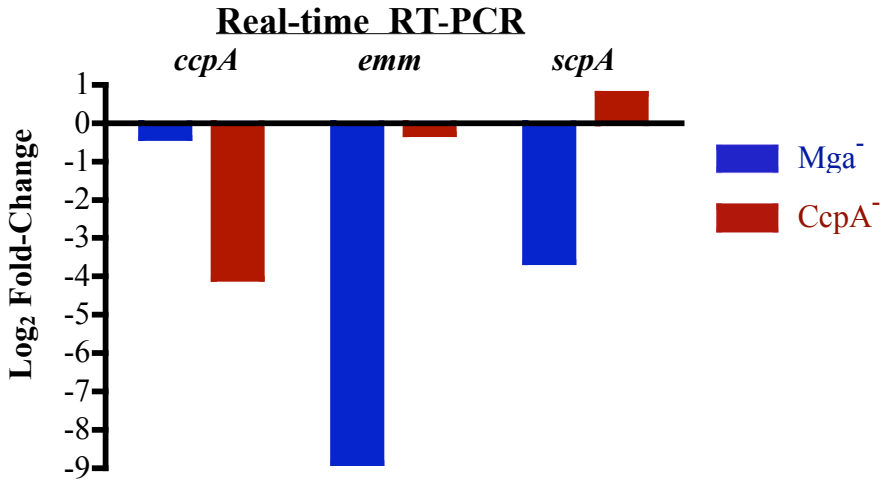

Fig. 11: Real-time RT-PCR analysis of Mga-regulated genes in the *ccpA* mutant
Real-time RT-PCR was performed on total RNA isolated from the M6 GAS P*mga-gusA* reporter strain (WT), the *mga*-inactivated derivative (Mga$^-$), and the *ccpA*-inactivated derivative (CcpA$^-$). Results are presented as the Log_2-fold change of relative transcript levels for the sample compared to the *gyrA* transcript, normalized such that WT = 0. The *ccpA, emm,* and *scpA* real-time RT-PCR primers used in this analysis are listed in Table 4.

CCR and sugar metabolism affect *mga* expression and Mga-activity

The GusA reporter strains with P*mga* and the Mga-regulated promoter, P*emm*, were used to analyze the affect of various sugar sources on both the activation of *mga* expression and Mga activity. Chemically defined media (CDM) containing a sugar source of either glucose, sucrose, or a mixture of both sugars was prepared. The P*mga-gusA* reporter strain showed a significant reduction of GusA expression levels when grown in the non-CCR inducing sugar, sucrose, compared to glucose ($P < 0.0367$) (Fig. 12A). This reduction in expression from P*mga* was also seen in cells grown in the mixture of both sugars indicating that the presence of sucrose might inhibit P*mga* transcriptional activation and thereby CCR-mediated activation of *mga* expression. When analyzing transcriptional activation from the Mga-regulated promoter P*emm*, expression was once again highest when grown in glucose (Fig. 12B). Expression from P*emm* was reduced almost by half when grown in sucrose compared to growth in glucose ($P < 0.0026$), indicating that sucrose does not induce CCR activation of *emm* expression, likely direct through effects on *mga* expression. Interestingly, cells grown in the glucose/sucrose mixture had GusA expression similar to cells grown in glucose alone demonstrating CCR-mediated activation of P*emm* when glucose is present.

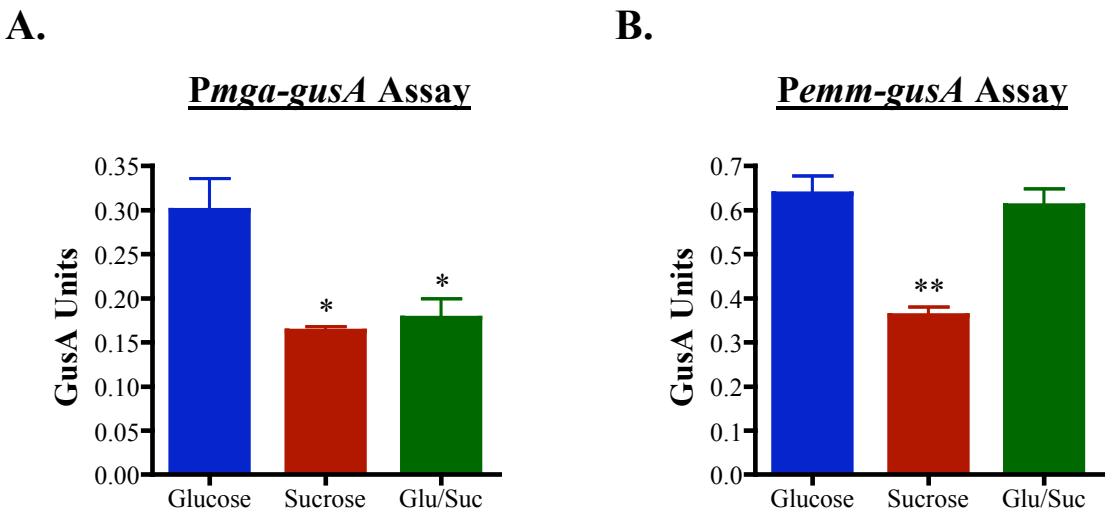

Fig. 12: P*mga* and P*emm* GusA Assays with variable sugar source
(A) P*mga* **(B)** P*emm* GusA reporter assays with samples from mid-log phase of cells grown in CDM containing 2% of one of the following: glucose, sucrose, or a mixture of both sugars. Data is reported in GusA units (OD_{420}/total protein concentration [µg/µl]), and is the mean from 4 independent experiments with standard error shown.

Expression from P*mga* varies across growth

In order to assess transcriptional activation across growth, a firefly luciferase system was implemented. Luciferase, unlike GusA, has a shorter half-life allowing for monitoring of promoter activity at multiple time points across growth. As indicated in the Materials and Methods (Fig. 5A and B), the plasmid-based luciferase system showed similar expression trends in *mga* expression, and was therefore used throughout these studies due to the ease of transfer between different strains. To begin characterizing P*mga* expression across growth, the clinical M6 strain GA19681 (Table 1), containing either the P*mga-luc* plasmid or a promoterless-*luc* control plasmid, were grown in rich media (THY broth) or CDM containing glucose. While the promoterless-*luc* plasmid did

not show any detectable expression of Luciferase at any time points in either media, cells grown in CDM had almost 2-fold higher levels expression from P*mga* at all time points, compared to cells grown in THY broth (Fig. 13). One possible explanation for this might be the increased levels of glucose present in CDM (2%) compared to THY broth (0.25%).

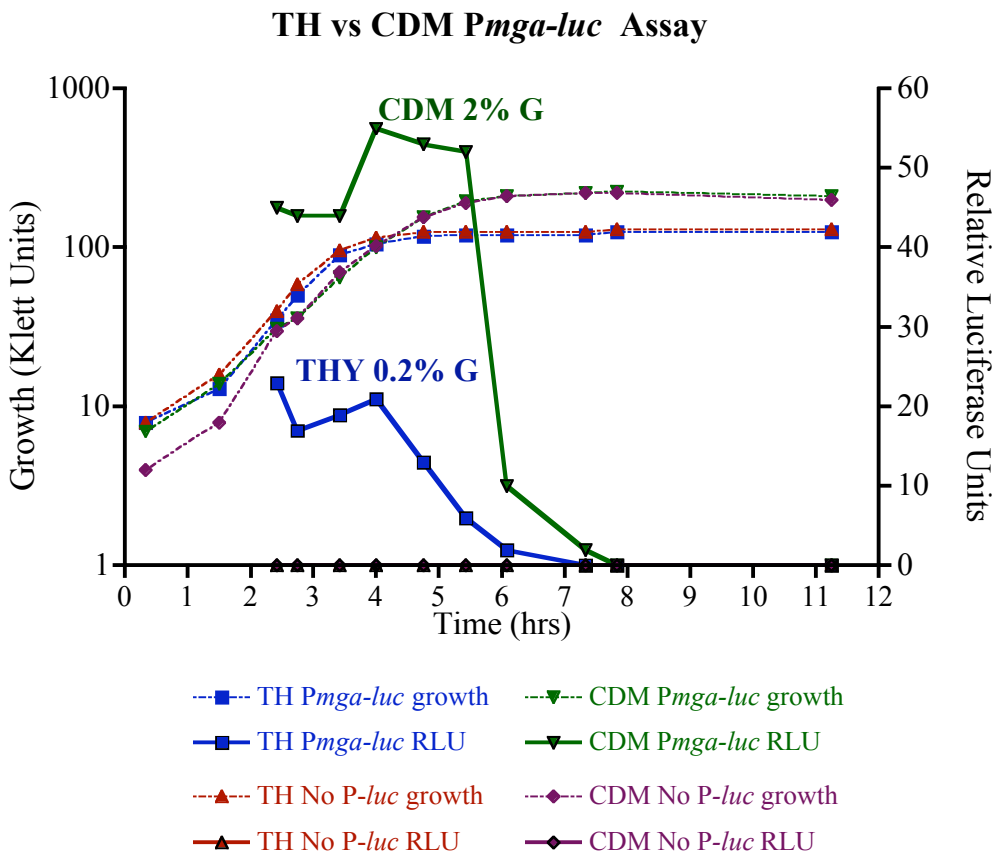

Fig. 13: P*mga* luciferase assay for M6 GAS grown in THY broth or CDM
The growth curve for the P*mga-luc* and No promoter-*luc* strains are shown in Klett Units with dashed lines, while the relative luciferase unit profiles for each are shown in solid bold lines. Samples for the luciferase assay were taken every 15 Klett units beginning at Klett 30 and continuing through late stationary-phase. Data is representative of 3 independent experiments.

***mga* expression inversely correlates to glucose levels**

To address the possibility that sugar levels affect expression from P*mga*, the P*mga-luc* strain was grown in CDM with varied levels of glucose ranging from THY broth levels of 0.25% to normal CDM levels of 2% (w/v). Unexpectedly, expression from P*mga* was highest when cells were grown in lower amounts of glucose, with higher expression in mid-log phase and then peaking at 3-fold higher levels in late stationary phase (Fig 14). In contrast, cells grown in higher amounts of sugar had much lower levels of P*mga* activation at all time points, and lacked the peak in late stationary phase. These data show that transcriptional activation of P*mga* inversely correlates to glucose levels. Furthermore, the amount of sugar present along with the composition of the media begins to suggest a link between sugar utilization and expression from P*mga*.

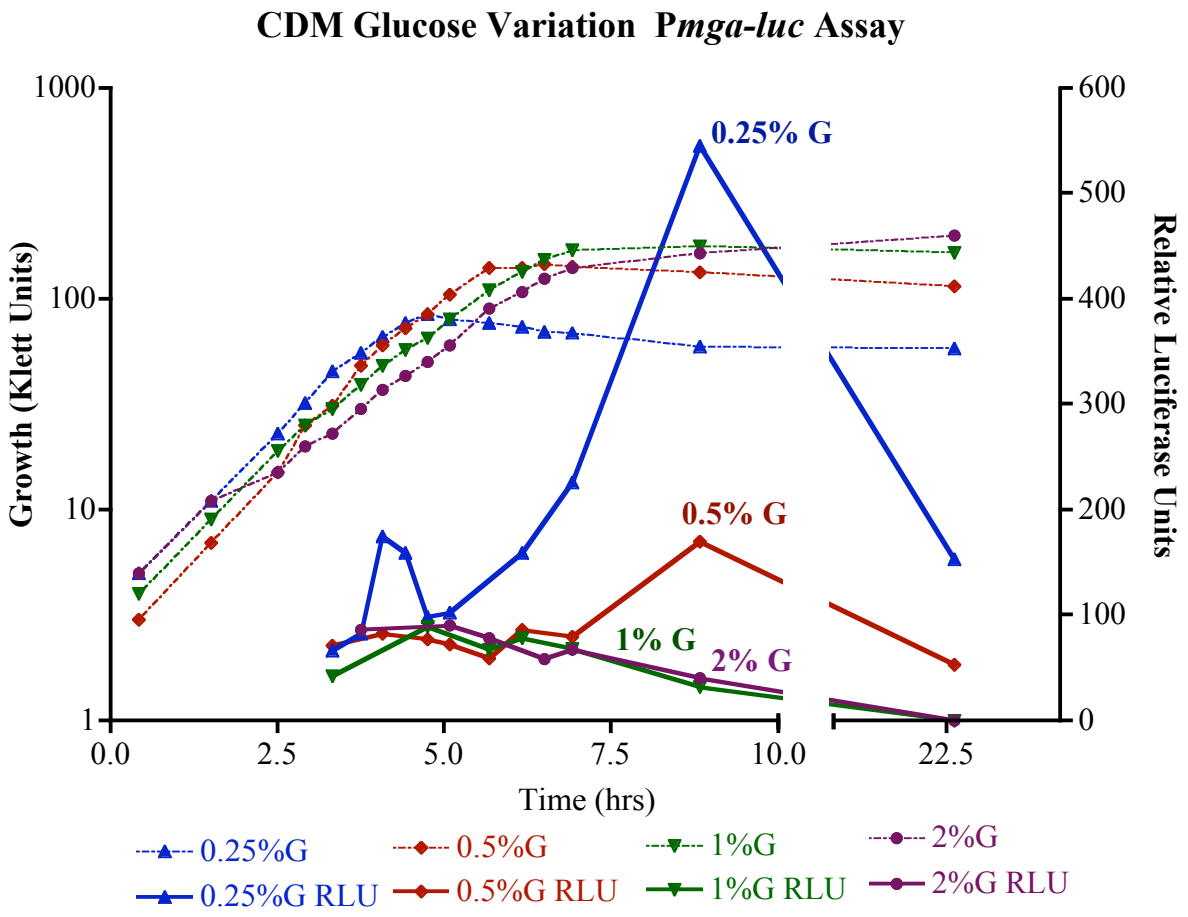

Fig. 14: Glucose variation P*mga* luciferase assay
The clinical M6 strain GA19681 bearing the P*mga-luc* reporter plasmid was grown in CDM containing varied amounts of glucose ranging from 0.25% to 2% (w/v). Growth in each amount of glucose is shown in the dashed lines, while the relative luciferase profile is shown in solid bold lines. Samples for the luciferase assay were taken every 15 Klett Unit beginning at Klett 30 through late stationary phase and at an overnight time point. Data is the representative of three independent experiments.

Sugar source affects expression from *Pmga*

To determine the effect of alternative sugars on P*mga* transcriptional activation, the clinical M6 strain containing the P*mga-luc* plasmid was grown in either 0.25% or 1% (w/v) of the following: glucose, sucrose, or a glucose/sucrose mix. As before with the P*mga-gusA* reporter strain, cells grown in 0.25% sucrose alone had 2-fold reduced expression from P*mga* at all time points (Fig 15A). However, growth in the glucose/sucrose mixture restored higher expression levels, although the transcriptional profile was altered in that there was only a peak present at the transition to stationary phase instead of the characteristic mid-log phase peak followed by a peak in late stationary phase. Interestingly, when the cells are grown in 1% glucose or sucrose, the transcriptional activation of P*mga* is reduced compared to the 0.25% levels, further supporting the inverse correlation between amount of sugar and expression from P*mga* (Fig. 14 and 15B). The transcriptional pattern is also altered with a single peak at the transition to stationary phase and matches that seen with the 0.25% glucose/sucrose mixture. While the 1% mixture of glucose and sucrose exhibits the single-peak transcriptional activation profile, the expression from P*mga* is almost 2-fold reduced compared to growth in 1% of either sugar alone. This data shows that *mga* expression is influenced by sugar source, further supporting the link between sugar metabolism and virulence regulation in the GAS.

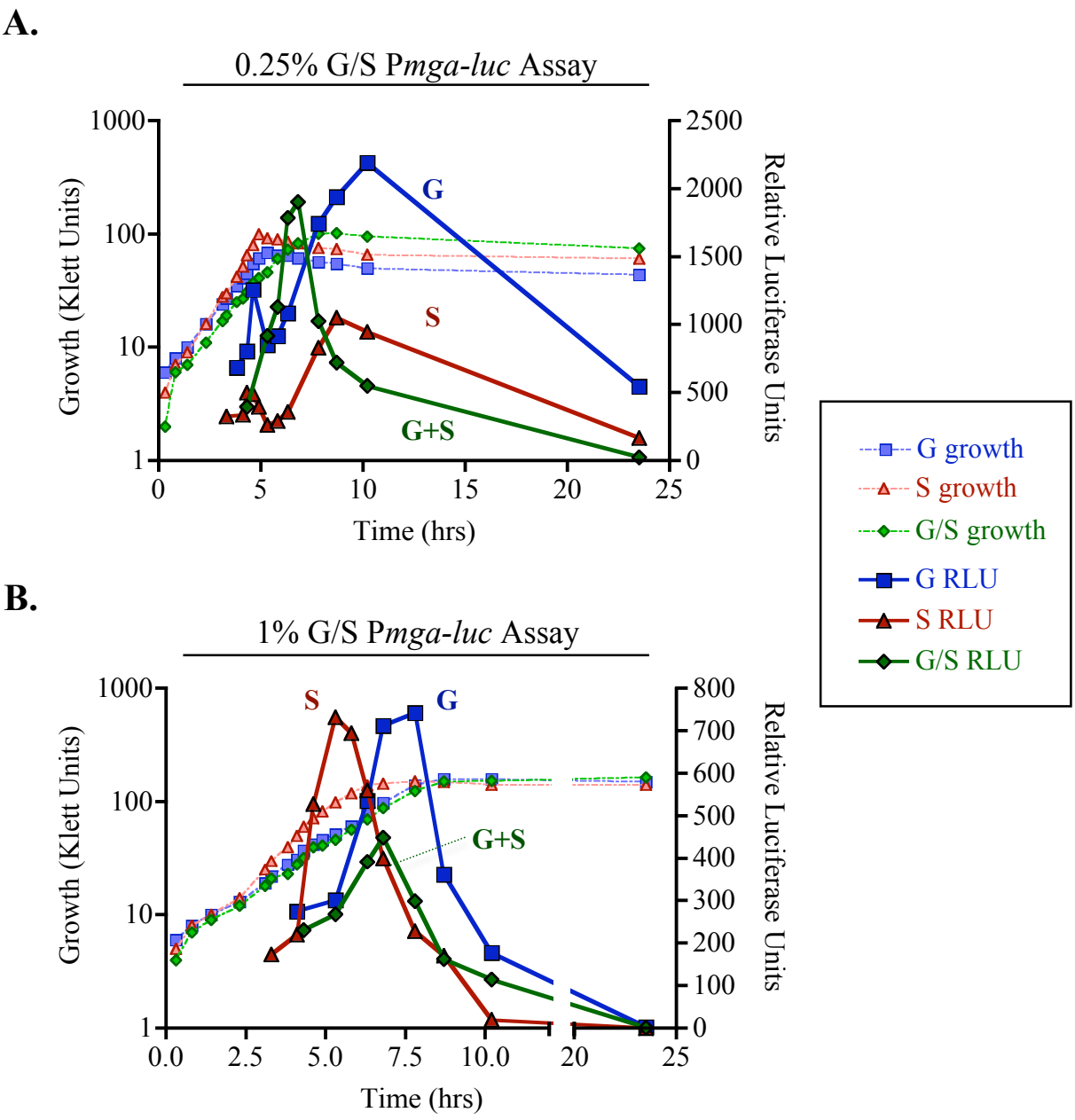

Fig. 15: Luciferase transcriptional reporter assay for P*mga* grown in various sugars
(A) P*mga-luc* assay for cells grown in CDM containing either 0.25% or **(B)** 1% (w/v) of the following sugars: glucose, sucrose, or a mixture of both sugars. Growth in each sugar is shown in dashed lines, while the relative luciferase profile is shown in solid bold lines. Samples for the luciferase assay were taken every 15 Klett unit beginning at Klett 30 and continued through late stationary phase with an overnight time point. Data is representative of 2 independent experiments.

Deletion of AmrA reduces *mga* expression across growth

To further assess the role of AmrA, a putative sugar transporter in *mga* regulation, the P*mga-luc* plasmid was transformed into the M6 Mga^+ strain, JRS4, the isogenic Mga^- strain, and the $AmrA^-$ mutant (Adel, Table 1). A previous study within the lab found that deletion of AmrA resulted in an almost 6-fold reduction in expression from both P*mga* and *Pemm* (176). The luciferase assay was performed to analyze the affects of a deletion of AmrA on *mga* expression across growth because the previous studies were limited to a single time point assessment. The AmrA deletion strain ($AmrA^-$) showed a 2-fold reduction in P*mga* transcriptional activation at all time points, compared to the WT strain (Mga^+) (Fig. 16). The negative control strain (Mga^-) did not exhibit any detectable expression from P*mga*. The influence of AmrA on *mga* expression appears to be in a global manner.

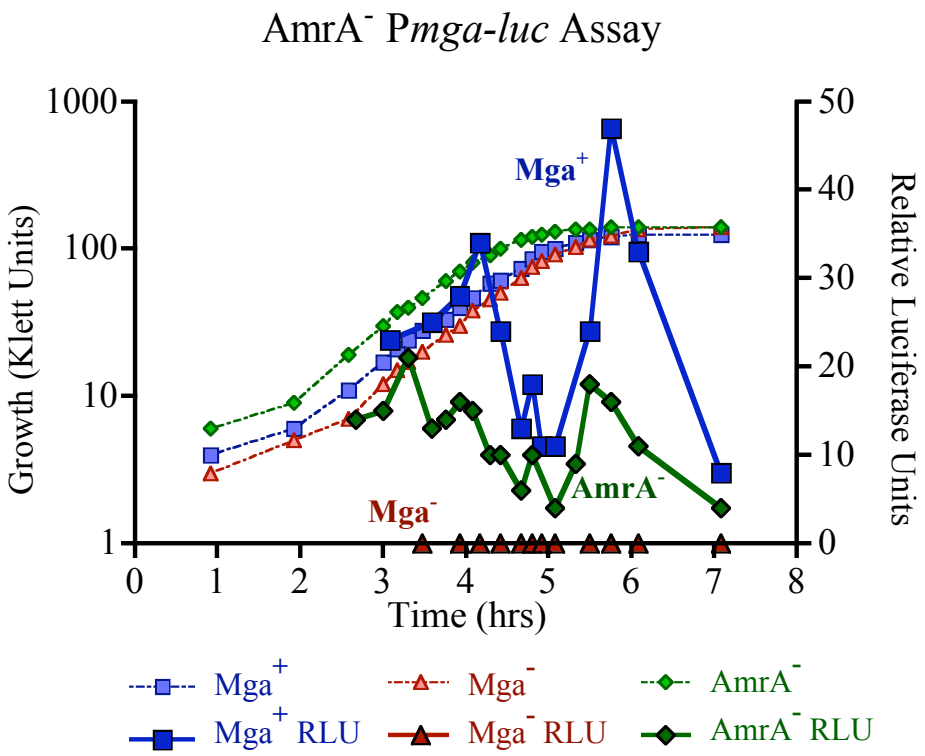

Fig. 16: P*mga* luciferase assay in AmrA$^-$ strain
The serotype M6 strain JRS4 (Mga$^+$, Mga$^-$, and AmrA$^-$) derived strains bearing the P*mga-luc* plasmid grown in THY broth. Growth for each strain is depicted with dashed lines and reported in Klett units. The relative luciferase units for each strain are shown in solid bold lines. Samples for the luciferase assay were taken every 15 Klett units, beginning at Klett 30. Data is representative of 2 independent experiments.

AmrA affects expression of *mga* and *emm* in a strain dependent fashion

To verify the effects of loss of AmrA on *mga* expression, a deletion of AmrA was constructed in the clinical M6 strain GA19681 (Table 1). Total RNA was extracted from the WT and isogenic AmrA$^-$ mutant from three different strain backgrounds, consisting of a serotype M3 (MGAS315) strain and 2 different M6 (JRS4 and GA19681) strains (Table 1). Quantitative real-time RT-PCR was performed using both the M6 *mga* and *emm*

primers to analyze the effects of AmrA inactivation on *mga* expression directly, and on Mga-regulated genes. The results demostrated that while the original AmrA$^-$ strain in the JRS4-derived background showed a reduction of *mga* transcripts beyond the 2-fold significance level, the AmrA mutant strains from the serotype M3 strain MGAS315 and the clinical M6 strain GA19681 were reduced but not within the 2-fold level for significance (Fig. 17). Furthermore, relative transcript levels of the Mga-regulated gene *emm* were also significantly down in the original AmrA mutant, but not in either of the other AmrA mutant strains. These results suggest that the influence of AmrA on *mga* expression is strain dependent.

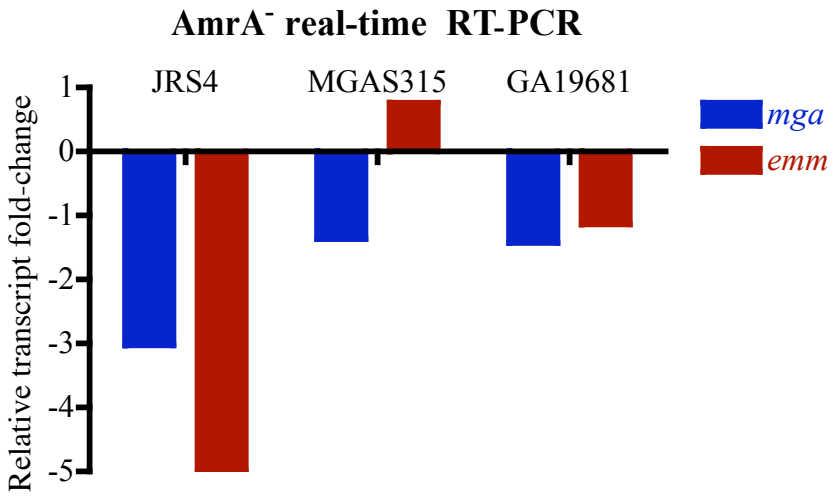

Fig. 17: Real-time RT-PCR analysis of *mga* and *emm* transcripts in AmrA$^-$ strains
Transcript levels from the AmrA$^-$ strains are shown as transcript fold-change relative to the corresponding wild type transcript levels normalized to the *gyrA* control.

DISCUSSION

While sugar metabolism has been widely known to influence the growth of bacteria, its influence on the regulation of virulence is just beginning to be appreciated. The evidence presented in this study shows direct binding of CcpA to the newly identified *cre* in P*mga*, which leads to activation of *mga* transcription and implicates CCR in the growth-phase control of the virulence regulator Mga. Furthermore, this work lays the groundwork for future experiments analyzing the influence of sugar metabolism on virulence regulation in the GAS.

The GAS *cre*

This study was the first to investigate the role of CcpA-mediated CCR in the GAS, and identified 98 unique putative *cre* sites (Appendix I). Many of the *cre* identified are located near metabolic operons, regulators of sugar metabolism, and other genes involved in energy metabolism for example *lctO, manL, celC, arcA*, *ackA,* and *licR* (Appendix I). Several of these genes, such as *ackA* (85), have been shown to be under CCR in other Gram-positive organisms, providing support for the identification of *cre* in the GAS. The in silico analysis was conducted using the *B. subtilis* consensus *cre* sequence with one mismatch allowed, given that only find 1 *cre* was identified without allowing a mismatch. This suggests that the GAS *cre* is divergent from the *B. subtilis* consensus *cre.* Direct binding of CcpA to the *cre* found in P*ccpA* and P*mga* (Fig. 7) helps to validate the in silico analysis, although more studies showing direct binding are needed to identify important residues and more fully develop a GAS consensus *cre*.

While a majority of *cre* sites detected in the GAS genome correlate to known CcpA-regulated genes in other Gram-positive organisms, several *cre* were identified in or near virulence factors. These include sites located in the promoters of *mga* and *sagA* and in the open reading frames of *speB* and *rivR* (Appendix I). The presence of the putative *cre* near *mga* and *speB* supports previous evidence for CCR of M protein expression and SpeB repression during growth in glucose (37). Furthermore, identification of these *cre* near virulence genes strengthens the link developing between sugar metabolism regulation and virulence expression in the GAS.

The role of CcpA and the *cre* in activation of *mga* expression

The direct binding of CcpA to the *cre* located in P*mga* (Fig. 7), and the requirement of this *cre* for activation of transcription from P1 (Fig. 8 and 9) indicates that CcpA directly regulates *mga* expression. However, the complex structure of P*mga* makes determining the level of CcpA influence on *mga* expression more difficult. The quantitative real-time RT-PCR analysis of *mga* transcripts from P1 alone versus P1 and P2 suggests that the absence of the *cre* reduces the expression of *mga* from both promoters equally. Furthermore, studies using a P*mga* GusA reporter strain, showed an almost complete reduction in expression from P*mga* in the *ccpA*-inactivated strain compared to the wild type parent strain (Fig. 10). These combined results provide strong evidence that binding of CcpA to the *cre* upstream of P1 directly activates expression from P*mga*.

The influence of CCR on Mga-regulated genes

Although the data presented in this study indicate direct activation of *mga* expression by CcpA, quantitative real-time RT-PCR analysis showed that inactivation of *ccpA* did not significantly affect the Mga-regulated genes *emm* and *scpA* (Fig. 11). This suggests that the limited expression of *mga* in the absence of CcpA is sufficient to activate expression of the Mga regulon. Since CcpA activates expression of *mga* from the P1 promoter, which does not involve autoregulation, it might suggest that CcpA initiates *mga* expression. Thus, in the absence of CcpA, *mga* expression is reduced at earlier time points in growth; however, once the level of Mga becomes sufficient, it can then amplify its own expression through the P2 promoter and further activate expression of downstream regulated genes.

Interestingly, studies using the P*emm* GusA reporter strain indicate that expression is reduced in a non-CCR inducing sugar such as sucrose compared to growth in glucose (Fig. 12). Although, results from this study show that *emm* expression is not altered in a *ccpA* inactivated strain, it still may be influenced by an alternative mechanism of CCR. Further experiments investigating the role of CCR on Mga-regulated genes are necessary to understand the influence of sugar metabolism on M protein expression.

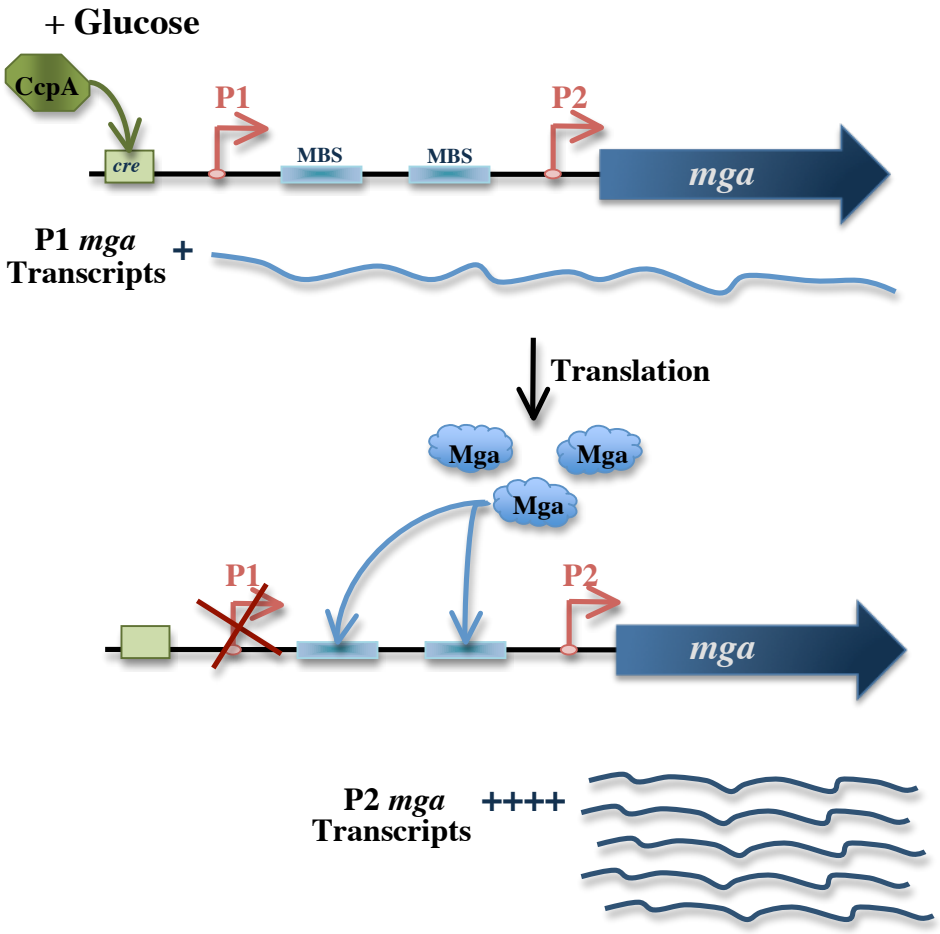

Fig. 18: Model of transcriptional activation from P*mga*
Early in exponential-phase, during growth in glucose, CcpA activates the transcription of *mga* from the P1 promoter via binding to the *cre* upstream. After translation of the P1 transcripts, Mga then binds to the Mga-binding sites upstream of P2 and auto-activates transcription from P2. The plus signs indicate the relative level of promoter specific transcripts from P1 and P2.

The influence of sugar metabolism on expression from P*mga*

The findings presented in this study provide support for both CcpA-mediated and CcpA-independent CCR on expression of P*mga*. Expression from P*mga* was reduced when the P*mga* reporter strains, both GusA and Luciferase, were grown in CDM containing sucrose as the sole carbon source compared to glucose (Fig. 12 and 15). Furthermore, this defect in transcriptional activation was not restored when strains were grown in a mixture of glucose and sucrose, suggesting that the presence of sucrose can directly inhibit *mga* expression. Additional studies are necessary to determine the specific mechanism for inhibition of *mga* expression by sucrose.

Interestingly, when the P*mga* luciferase reporter strain was grown in rich THY broth compared to CDM containing 1% glucose, the expression from P*mga* was much higher in the CDM (Fig. 14). Initially, the increased expression from P*mga* was hypothesized to be due to the higher amounts of glucose present; however, transcriptional activation of P*mga* was found to inversely correlate to the amount of glucose present in CDM by luciferase assay (Fig 14). This result suggests that increasing amounts of glucose can trigger inhibition of transcriptional activation at P*mga.* This may be directly affecting CcpA-mediated regulation at P*mga* by increased binding of CcpA, and therefore more expression from P1 P*mga* instead of the autoactivated P2 promoter (Fig. 18). Another possibility for the increased expression from P*mga* in lower amounts of glucose may be related to the pH of the growth media as the pH of the media decreases as lactic acid builds up. Testing the pH of the media after growth in the varied amounts of glucose did show a difference in pH ranging from pH 5 to 6.5 in the highest amount of glucose compared to the lowest amount of initial glucose present.

AmrA-mediated activation of P*mga* is strain dependent

The putative sugar transporter AmrA was previously shown to positively influence the expression of *mga* and the Mga regulon (176). Work presented in this study shows that AmrA only significantly activates *mga* and the Mga-regulated gene *emm* in the M6 serotype JRS4-derived strain where it was identified, but not in the clinical M6 strain GA19681 or the M3 serotype strain MGAS315 (Fig. 17). A recent transcriptome analysis across both classes of the GAS comprised of 3 different strains with or without Mga, determined that the M6 JRS4 strain differs significantly from the other strains tested (177). A majority of the deviations between JRS4 and the clinical M6 isolate were genes involved in metabolism, leading to the hypothesis that JRS4 has metabolic defects. Since the results presented here indicate that only JRS4 strains show that AmrA has an effect on *mga* expression, it could be related to the changes in metabolism seen in the transcriptome analysis. Further mutational analysis in other strains will help to elucidate the role of AmrA in regulation of *mga*.

CHAPTER FIVE:

CcpA-mediated repression of streptolysin S expression and virulence in the group A streptococcus

INTRODUCTION

Bacteria utilize carbon catabolite repression in order to both conserve and use energy in the most efficient way during metabolism. This global regulatory mechanism allows bacteria to coordinate their metabolic environment to gene expression. The mechanism for CCR in Gram-positive organisms involves HPr, a main protein of the PTS system and CcpA. During growth in glucose, the preferred sugar source, HPr becomes phosphorylated on a serine residue, and with CcpA, forms a complex that mediates regulation of gene expression by binding to specific sites present in or near the promoters of genes called *cre* for catabolite response elements. The binding of CcpA to *cre* can either lead to repression of genes involved in alternative sugar metabolism, or the activation gene expression of factors involved in glucose metabolism.

Experimental evidence in several important Gram-positive pathogens has begun to implicate CcpA in virulence gene regulation. For example, in *Listeria monocytogenes* the virulence regulator, PfrA, is under CCR (148). In *Clostridium perfringens*, expression of both the enterotoxin (*cpe*) and the Type IV pilus are controlled by CcpA-mediated regulation (147, 221). Importantly, in the human pathogen *Streptococcus pneumoniae,* a mutation in CcpA attenuates this organism for nasopharygeal colonization and virulence in the mouse pneumonia model of infection (100) and i.p. infection (79).

These results suggest a major role for CcpA in virulence gene regulation by Gram-positive pathogens

An *in silico* analysis of the M1 GAS SF370 genome using the *B. subtilis* consensus revealed *cre* associated with predicted sugar metabolism operons, as well as in the promoters (*mga*, *sagA*) or coding regions (*speB*) of known virulence regulators and genes (Appendix I and Chapter 4). CcpA was found to bind specifically to the P*mga* promoter, resulting in early activation of *mga* expression from the P1 start of transcription in an M6 GAS background (Fig. 7, 8, and 9). Furthermore, a *ccpA* mutant strain showed reduced transcriptional of P*mga*, supporting the role of CcpA in regulation of *mga* (Fig. 10). It was proposed that this might provide an avenue for direct interaction between carbon utilization and virulence gene regulation in GAS. However, further analysis of the parental M6 strain used for creation of the *ccpA* mutant was later shown to have metabolic defects associated with it. Further studies in other GAS strains will be necessary to uncover the effects of CcpA-mediated CCR, in addition to analyzing the influence of CcpA on pathogenesis in the GAS.

Interestingly, the putative *cre* found in P*sagA* overlaps the -35 binding site, indicating a strong likelihood for repression by CcpA. SLS is an oxygen stable hemolysin/cytolysin that has been shown to contribute to virulence in GAS, especially following the subcutaneous route of infection (59, 74). The 9-gene *sag* operon is required for production and secretion of SLS, with the first gene, *sagA*, encoding the structural gene. In addition, *sagA* has also been shown to contain the *pel* locus in some serotypes; a regulatory RNA, that positively influences the expression of many virulence factors (124, 136). Given the implication for CcpA-mediated CCR to influence virulence

regulation and SLS production in GAS, the role of CcpA in GAS pathogenesis was assessed. In this study, CcpA is shown to be a global regulator of carbon utilization that also represses virulence and expression of SLS in GAS.

RESULTS

A Δ*ccpA* mutant shows increased virulence in mice

To assess the role of CcpA in GAS pathogenesis, a Δ*ccpA* mutant was constructed in the mouse-virulent M1 strain MGAS5005. The organization of the *ccpA* genomic region is highly conserved in the GAS (Fig. 19A). Similar to other lactic acid bacteria, *ccpA* is divergently transcribed from the upstream *pepQ* XAA-Pro dipeptidase gene, with the predicted P*ccpA* promoter and *cre* present within the intergenic region as previously described (5). However, GAS specifically possess two genes directly downstream of *ccpA,* encoding a glycosyl transferase (5005_Spy0425) and a glucosyl transferase (5005_Spy0426), respectively, followed by a Rho-independent transcriptional terminator (Fig 19A). Although *ccpA* does not appear to be essential in GAS (127), attempts to inactivate *ccpA* using polar insertional strategies were unsuccessful. RT-PCR analysis found that *ccpA* and Spy0425 are transcriptionally linked (Fig. 19B), suggesting that *ccpA* may be in an operon together with a gene important for growth.

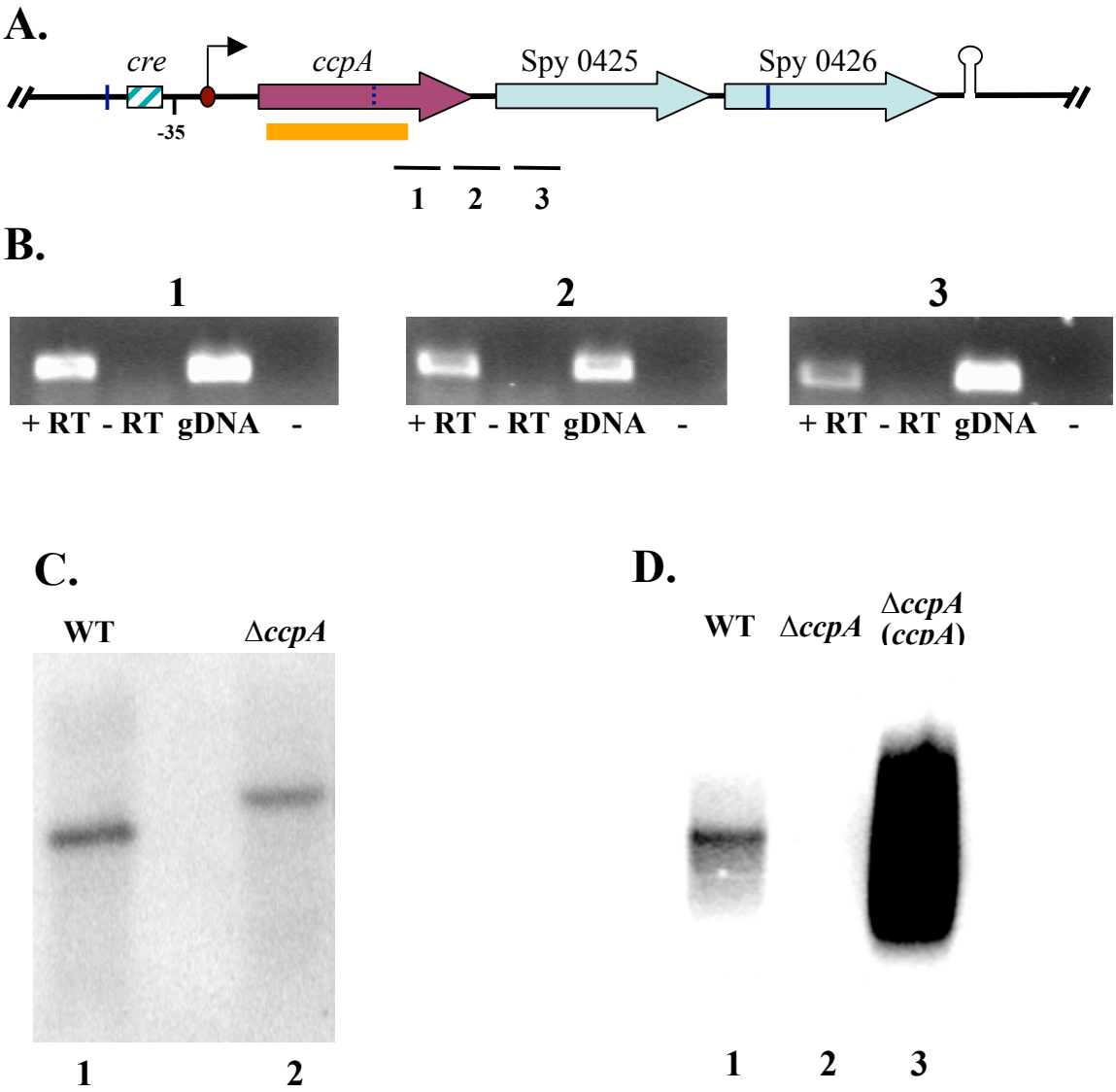

Fig. 19: MGAS5005 Δ*ccpA* mutant and complementation
(A) Schematic showing *ccpA* genomic region from MGAS5005 with downstream Spy0425 and Spy0426 open reading frames and putative Rho-independent terminator (lollipop). The predicted transcriptional start (P*ccpA*) is shown (arrow), including the identified *cre* at -63 from the start of transcription. Deleted *ccpA* region replaced with *aad9* (thick bar) is also indicated. Solid vertical lines represent *HindIII* sites and dashed line indicates loss of site. **(B)** Reverse transcriptase PCR reactions for regions numbered 1, 2, and 3 in panel A. Shown are reactions with RT (+RT), without RT (-RT), a genomic DNA positive control (gDNA), and a no DNA negative control PCR lane (-). **(C)** Southern blot of genomic DNA from WT MGAS5005 (lane 1) and Δ*ccpA* mutant (lane 2) using probe labeled (3) in panel A. **(D)** Northern blot on RNA isolated from WT MGAS5005 (lane 1), Δ*ccpA* mutant (lane 2), and complemented Δ*ccpA* (*ccpA*) mutant using the probe labeled (1) in panel A.

Therefore, an in-frame deletion of *ccpA* containing a non-polar *aad9* spectinomycin cassette (128) was introduced into the genome of MGAS5005 and the mutation verified by Southern blot (Fig. 19C). The resulting Δ*ccpA* mutant produced a small colony phenotype on THY agar plates, which has been observed for *ccpA* mutants in other bacteria (100, 236). Although the Δ*ccpA* strain produced a longer lag phase during growth in rich liquid media, the mutant had no noticeable growth defects upon entering logarithmic phase compared to the parent MGAS5005. A complementing plasmid pKSM719 containing *ccpA* under the control of its native promoter (P*ccpA*) resulted in elevated expression of *ccpA* transcript as demonstrated by northern blot (Fig. 19D).

To determine the role of CcpA in virulence, the Δ*ccpA* mutant was assayed in two mouse models of GAS infection. In the first model of systemic infection, CD-1 mice were infected i.p. with either the WT MGAS5005 containing empty vector, the Δ*ccpA* mutant with empty vector, or the Δ*ccpA* mutant strain complemented with *ccpA* in trans. Surprisingly, infection of mice with the Δ*ccpA* mutant led to a more rapid death than the parental MGAS5005, with 90 percent lethality by 17 hours post-infection (Fig. 20A). In addition, more than half of these mice exhibited severe hemorrhaging from several body sites such as the rectum and mouth. By comparison, only 50 percent of the MGAS5005 infected mice were dead at the end of 72 hours, which is statistically significant ($P<0.0001$). Overexpression of *ccpA* in the Δ*ccpA* mutant complemented the increased virulence to slightly less than WT level, linking CcpA to the observed hypervirulence phenotype. In a subcutaneous model of GAS skin infection, the Δ*ccpA* mutant showed significantly increased lesion size compared to both WT MGAS5005 and the complemented mutant (Fig 20B). Interestingly, increased lethality was not observed with

the Δ*ccpA* strain, suggesting no enhancement of dissemination from the skin leading to systemic disease. These data strongly suggest that CcpA acts to repress virulence in the GAS, leading to increased virulence in mouse models of both systemic and localized infection.

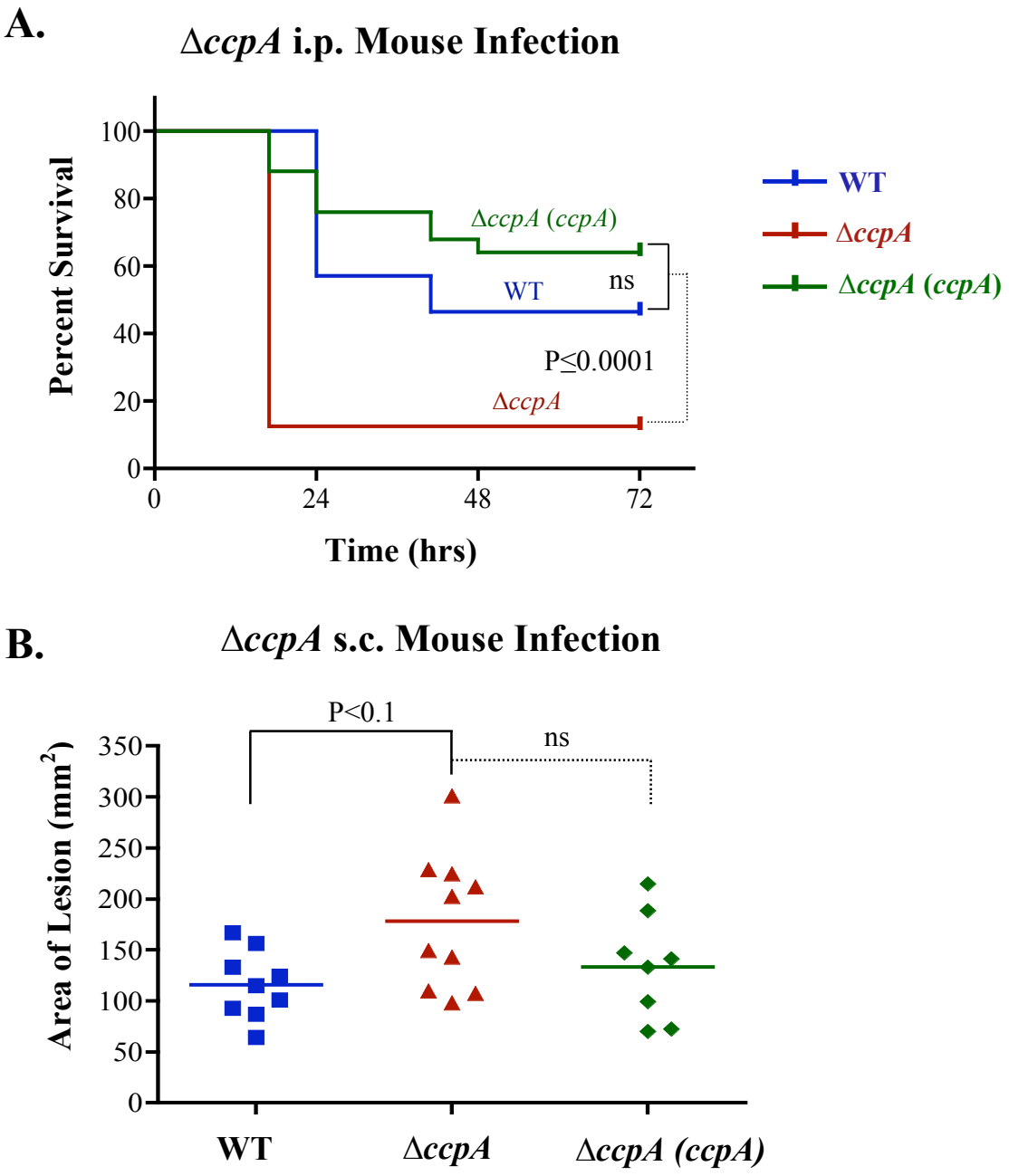

Fig. 20: A Δ*ccpA* mutant shows increased virulence in mice
(A) Survival curve for mice infected by the intraperitoneal route (i.p.) with WT MGAS5005 (empty vector) (n=30), Δ*ccpA* mutant (empty vector) (n=32), or complemented Δ*ccpA* (*ccpA*) (n=25) at a range of 1.1 to 2.4 x 10^7 CFU. Data shown represent 4 independent experiments. Significance was determined using Kaplan-Meier survival analysis and a logrank test. **(B)** Lesion sizes from mice infected by the subcutaneous route with WT MGAS5005 (n=9), mutant Δ*ccpA* (n=11), complemented Δ*ccpA* (*ccpA*) (n=8) using the a range of 2.0 to 2.4 x 10^8 CFU. Sizes of ulcerative lesions were measured (mm^2) at 72 hours post infection and every point represents a single animal with bars indicating statistical mean. P values were determined using an unpaired two-tailed t test.

Determining the CcpA regulon in GAS

To identify the CcpA-regulated genes that might be responsible for the increased virulence observed in mice, a transcriptome analysis of the Δ*ccpA* mutant was undertaken (see Chapter 3). Wild-type MGAS5005 was compared to the isogenic Δ*ccpA* mutant grown to mid-log phase in rich THY media with glucose, a point in growth at which CcpA-mediated regulation would be expected to be strongest. A decrease (CcpA activation) or increase (CcpA repression) in transcript levels in the mutant of greater than 2-fold over three biological replicates was considered significant. Under these conditions, CcpA was found to regulate about 6% of the M1 MGAS5005 genome (124 genes), with the vast majority (116 genes or 90%) showing repression by CcpA (Appendix II). The microarray analysis was validated by real-time RT-PCR on 15 differentially regulated genes (Table 7), resulting in a strong correlation with an r^2 value of 0.925 (Fig. 21).

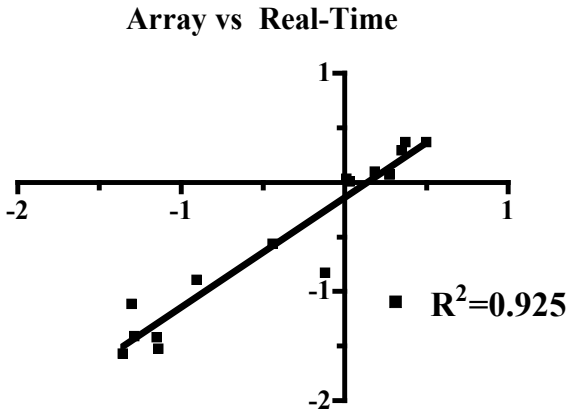

Fig. 21: Validation of microarray studies
The log of the mean value for both the WT vs. Δ*ccpA* microarray and the real-time RT-PCR data was plotted and a line of linear regression was calculated to determine the correlation efficient.

Table 7. Δ*ccpA* vs. MGAS5005 Microarray and Real-time RT-PCR validation

5005_ Spy#	Annotation (TIGR or NCBI)	Gene	Array Mean ± SE [a]	RT Mean ± SE	*cre*
Spy1275	arginine deiminase [b]	*arcA*	**0.027** ± 0.02	**0.044** ± 0.01	**Y**
Spy1065	α-cyclodextrin glycosyltransferase	*amyA*	**0.03** ± 0.01	**0.073** ± 0.01	**N**
SPy0475	PTS system, β-glucosides-specific IIABC	*bglP*	**0.038** ± 0.01	**0.071** ± 0.02	**N**
SPy0562	Streptolysin S (SLS) precursor; *pel* locus [b]	*sagA*	**0.039** ± 0.01	**0.052** ± 0.01	**Y**
Spy1067	maltose ABC transporter, periplasmic binding	*malX*	**0.077** ± 0.03	**0.05** ± 0.02	**N**
Spy0780	PTS system, mannose/fructose family IIA [b]	*ptsA*	**0.128** ± 0.08	**0.124** ± 0.04	**Y**
Spy1746	PTS system, cellobiose-specific IIA	*celC*	**0.148** ± 0.05	**0.759** ± 0.33	**Y**
Spy1381	glycerol kinase	*gplK*	**0.192** ± 0.11	**nt**	**Y**
Spy0127	ATP synthase, subunit K [b]	*ntpK*	**0.209** ± 0.17	**nt**	**Y**
Spy1305	2-component response regulator, TCS-10	*tcs10R*	**0.275** ± 0.28	**0.365** ± 0.18	**Y**[c]
Spy1479	PTS system mannose-specific IIAB [b]	*manL*	**0.361** ± 0.09	**nt**	**Y**
Spy0926	cardiolipin synthase, putative [b]		**0.408** ± 0.10	**nt**	**Y**
Spy1635	tagatose 1,6-diphosphate aldolase	*lacD.2*	**0.432** ± 0.31	**nt**	**N**
Spy0785	2-component response regulator, yesNM	*tcs5R*	**0.445** ± 0.08	**nt**	**Y**[c]
Spy1738	Secr. DNase; Streptodornase B; mitogenic factor	*spd*	**0.46** ± 0.10	**nt**	**N**
SPy0141	Streptolysin O (SLO) precursor	*slo*	**1.025** ± 0.13	**1.076** ± 0.21	**N**
Spy1720	Multigene regulator of virulence - Mga	*mga*	**1.087** ± 0.14	**1.024** ± 0.06	**Y**
Spy0283	2-component sensor kinase; virulence assoc.	*covS*	**1.187** ± 0.16	**1.881** ± 0.63	**N**
Spy1851	hyaluronate synthase; capsule synthesis	*hasA*	**1.189** ± 0.13	**1.889** ± 0.31	**N**
Spy0106	RofA; stand alone virulence regulator RofA	*rofA*	**1.26** ± 0.17	**1.536** ± 0.35	**N**
Spy0186	RofA-like protein, RALP-4; virulence regulator	*rivR*	**1.983** ± 0.32	**2.223** ± 0.29	**Y**
Spy0988	pyruvate kinase	*pyk*	**2.345** ± 0.22	**3.154** ± 0.64	**N**
Spy0576	ATP synthase subunit 6 [b]	*atpB*	**2.349** ± 0.30	**2.347** ± 0.27	**N**
Spy0424	catabolite control protein A; CcpA	*ccpA*	**4.615** ± 3.05	**1261** ± 105	**Y**

Shown above are the array mean values with standard error (SE) and quantitative real-time RT-PCR ± SE for CcpA-regulated genes of interest. Shading indicates CcpA regulation; repression (Top), activation (Bottom); unshaded indicates neutral (Middle).

[a] Data are sorted by Array mean value.

[b] Indicates first gene in CcpA-regulated operon.

[c] Associated with *cre* present at beginning of operon.

Similar to studies on the CcpA regulon in other Gram-positive bacteria (152, 236), CcpA repressed multiple operons important for non-glucose sugar utilization, including those encoding mannose, cellobiose, mannose/fructose, and ß-glucosidase PTS systems, as well as a maltose ABC transporter (Appendix II). It should be noted that not all alternative sugar utilization operons were regulated, suggesting that other mechanisms of CCR may exist in GAS (e.g., LacD.1). The arginine deiminase operon (*arcA-C*) was strongly repressed by CcpA, supporting previous studies showing that expression of the *arc* operon is inhibited by glucose, induced in stationary phase, and likely under CCR (38). A putative *cre* was previously identified upstream of *arcA* in an in silico search of the M1 GAS genome using the *B. subtilis* consensus *cre* (5). In fact, 76 of the 124 genes regulated by CcpA in the microarray study (61%) contained a predicted *cre* identified in that search or were associated with a *cre* present in the beginning of an operon. Ten percent of the CcpA-regulated genes found encode for transcriptional regulators, including several two-component system (TCS) response regulators. For example, TCS-5R (5005_Spy0785), which has been shown to regulate the adjacent mannose/fructose PTS operon (196), and the recently characterized virulence associated TCS TrxSR (TCS-10R; 5005_Spy1305) (Leday and Gold *et al*; submitted for publication). This might suggest a mechanism for further indirect regulation of those genes lacking an identifiable *cre*.

As predicted by the infection studies, CcpA also regulates several genes important for GAS pathogenesis. In particular, the most highly CcpA repressed locus in the array study represented the entire streptolysin S (SLS) operon (*sagA-I*, Table 7 and Appendix II). In addition to SLS being a well-characterized cytolysin and virulence factor (59,

151), the *sagA* locus also contains the *pel* regulatory RNA that has been shown to regulate expression of other virulence genes in GAS (136). However, effects were not observed on *emm*, *sic*, or *speB* expression that would be predicted by altering *pel* expression (136). CcpA was also able to repress expression of *spd* encoding a secreted DNase that contributes to the escape of GAS from the innate immune response (205).

Expression from P*mga* is reduced in the absence of CcpA

Previous results discussed in Chapter 4, indicate that CcpA activates the expression of *mga* by binding to the *cre* located upstream of the P1 transcriptional start site in P*mga*. However, *mga* expression was not significantly regulated in the microarray analysis. To further investigate the influence of CcpA on *mga* expression, the P*mga-luc* reporter plasmid was introduced into the M1 MGAS5005 Δ*ccpA* strain, and expression from P*mga* was monitored across growth. Transcriptional activation of P*mga* was consistently reduced at all time points in the Δ*ccpA* strain in comparison to the WT Mga^+ strain; however, it never exceeded a 2-fold difference for significance (Fig. 22). Although not evident in the array analysis, these results suggest that CcpA does influence *mga* expression.

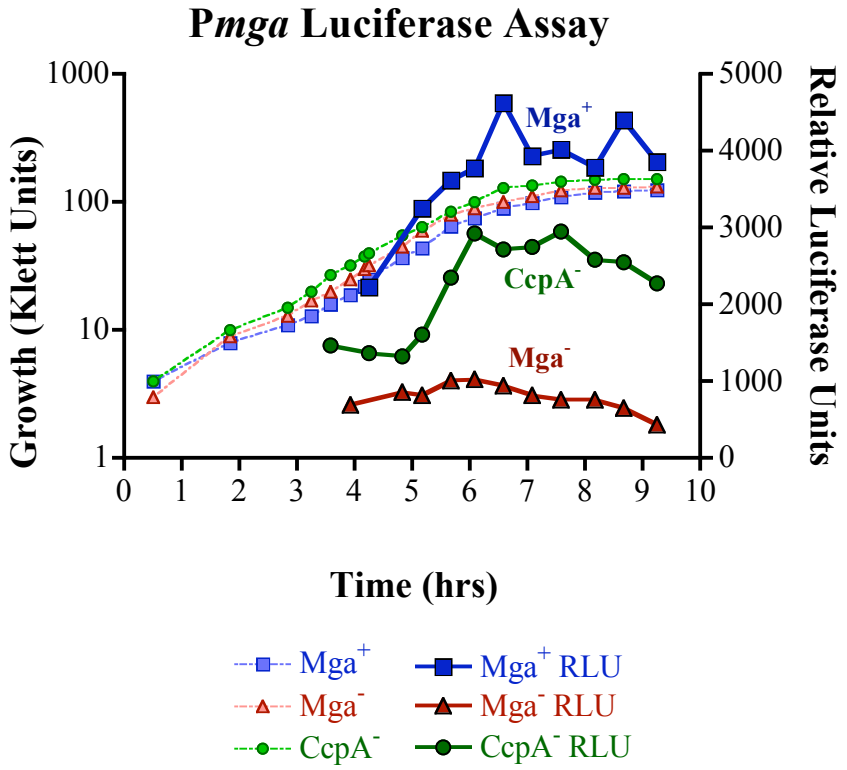

Fig. 22: P*mga* luciferase assay in Δ*ccpA* strain
Luciferase assay with WT MGAS5005 (Mga^+), the *mga* inactivated derivative KSM165-L.5005 (Mga^-), and the Δ*ccpA* strain MGAS5005.718 ($CcpA^-$) all containing either of the P*mga-luc* reporter plasmids pKSM721 or pKSM728 depending on antibiotic resistance required. Strains were grown in THY broth with appropriate antibiotic. Samples for luciferase assay were taken every 15 Klett units beginning at Klett 30. Growth for each strain is shown in the dashed lines, while relative luciferase units are shown for each strain in solid bold lines.

Expression of Streptolysin S (*sagA/pel*) is catabolite repressed by CcpA

The strong repression of *sagA/pel* by CcpA observed in the transcriptome analysis would predict a concomitant increase of SLS activity in the Δ*ccpA* mutant during exponential phase. To investigate this, SLS-specific hemolytic activity was assayed using 2.5% defibrinated sheep red blood cells incubated with culture supernatants taken at 1 hour time points during growth from WT MGAS5005 containing an empty vector, the Δ*ccpA* mutant containing an empty vector, and the complemented Δ*ccpA* mutant. SLS hemolytic activity indicated a dramatic increase early in logarithmic phase of the Δ*ccpA* mutant and remained elevated well into stationary phase (Fig. 23). In comparison, both WT MGAS5005 and the complemented Δ*ccpA* strain exhibited very little SLS hemolytic activity during logarithmic phase, followed by a rapid increase to maximum levels at the transition to stationary phase (Fig. 23). In experiments using the SLS inhibitor Trypan blue, no RBC lysis was seen from any of the samples, indicating all hemolytic activity is due to SLS and not Streptolysin O. These results correlate with the CcpA-mediated repression of the *sag* operon during exponential growth observed with the microarray study.

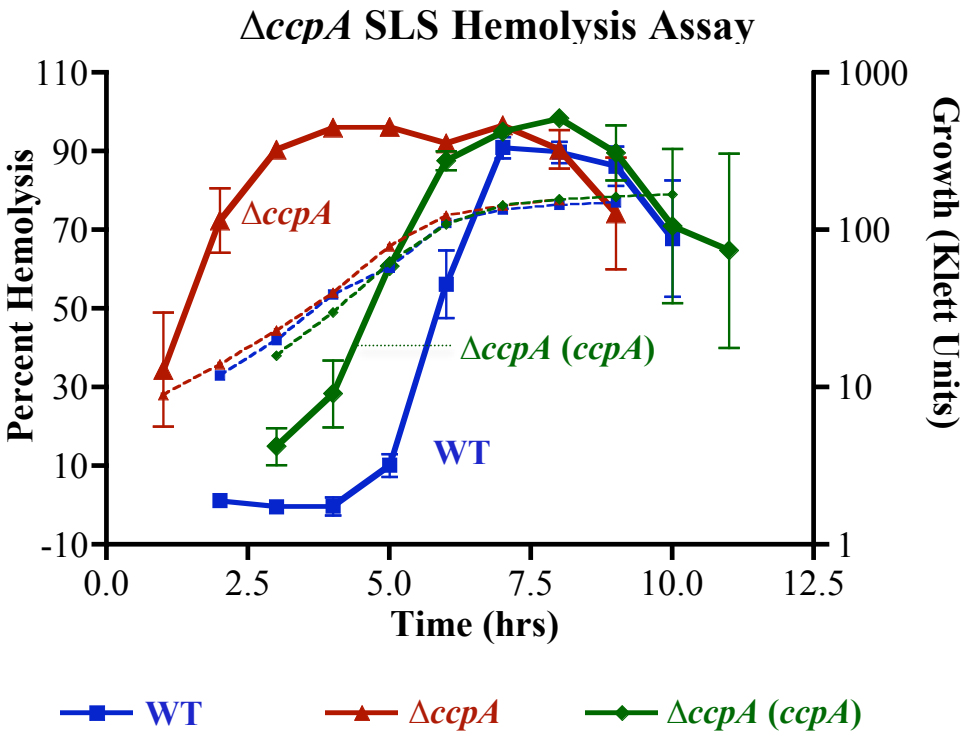

Fig. 23: Streptolysin-S hemolytic activity is repressed by CcpA
WT MGAS5005 (empty vector), Δ*ccpA* mutant (empty vector), and complemented Δ*ccpA* (*ccpA*) cells were grown in THY broth supplemented with 10% heat-inactivated horse-serum and supernatant samples were isolated at different time points for analysis of SLS activity. Data is presented as the average percent hemolysis (solid lines) from 3 independent experiments with standard error bars. The growth for each strain normalized to growth of WT MGAS5005 is shown in Klett Units from one representative experiment (dashed lines).

The CcpA-mediated repression of *sagA/pel* transcription and SLS activity strongly suggests that *sagA/pel* expression is under CCR and is regulated directly by CcpA. A P*sagA-luc* reporter plasmid was introduced into WT MGAS5005 and the resulting strain was grown in chemically defined media (CDM) supplemented either with 0.25% glucose, sucrose (non-repressing), or a mixture of glucose and fructose (non-repressing) to assay for CCR of *sagA/pel* expression. The P*sagA-luc* showed low levels of luciferase activity across logarithmic phase that increased at stationary phase when grown in glucose, indicating CCR is occurring (Fig. 24). When the same strain was grown in a non-CCR inducing sugar such as sucrose, transcriptional activation of P*sagA-luc* was elevated earlier in logarithmic phase compared to glucose and reached higher overall levels. Importantly, when the strain was grown in a complex sugar environment consisting of equal parts glucose and the non-CCR inducing fructose, expression from P*sagA* demonstrated CCR. Early in growth, P*sagA-luc* expression mirrored that of glucose alone; however, it rapidly transitioned to the higher expression level characteristic of a non-CCR inducing sugar when the glucose became depleted and fructose was utilized. These results indicate that expression of *sagA/pel* and SLS is under CcpA-mediated CCR.

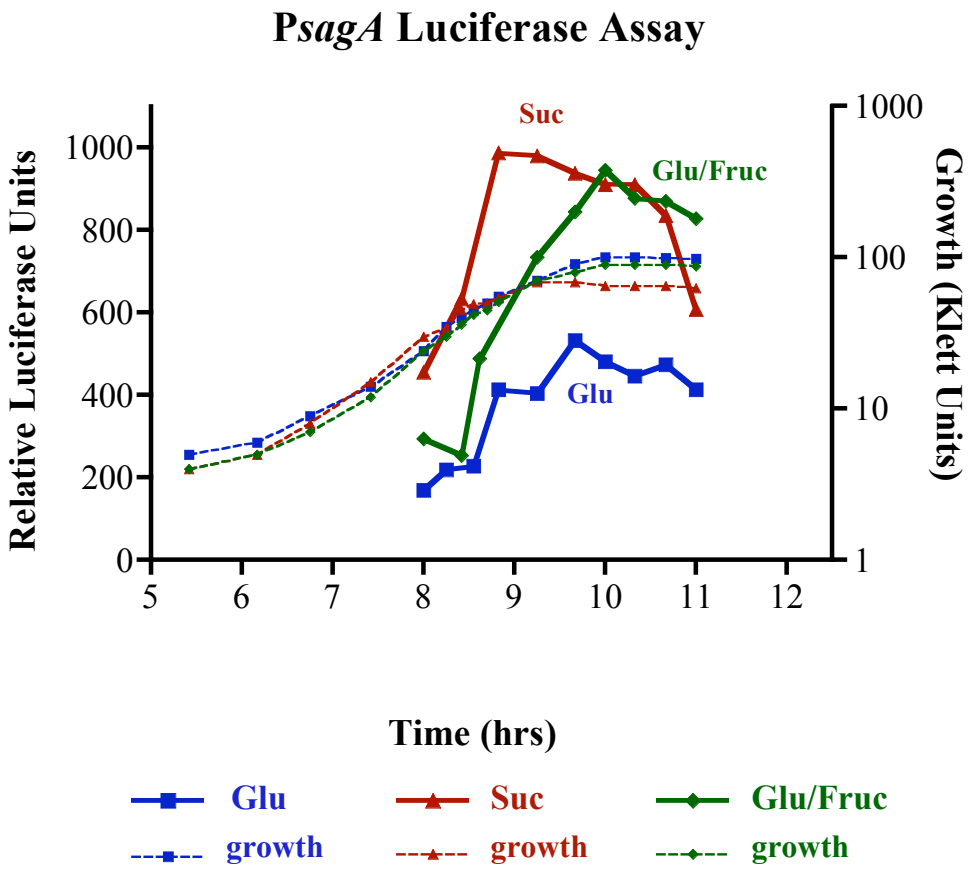

Fig. 24: P*sagA* luciferase assay with varied sugar source
WT MGAS5005 containing the P*sagA-luc* luciferase reporter plasmid was grown in chemically defined media containing either 0.25% (w/v) of glucose, sucrose or a mixture of glucose and fructose. Samples were taken every 15 Klett unit, beginning at Klett 30 shown in the dashed lines and assayed for luciferase production expressed as relative luciferase units displayed as solid bold lines. The graph shown is representative of 3 independent experiments.

CcpA binds directly to a *cre* in P*sagA*

During a previous in silico analysis, a putative *cre* was identified in the promoter region of *sagA/pel* (P*sagA*) overlapping the predicted -35 region (5). The results at this point strongly suggested that CcpA directly represses *sagA* production through binding to the P*sagA cre*. To investigate this possibility, an electrophoretic mobility shift assay (EMSA) was performed using a radiolabeled P*sagA* promoter probe (Middle) containing the putative *cre* (Fig. 25A). Mobility of the P*sagA* Middle probe was slowed in the presence of increasing amounts of purified GAS His-CcpA (1-3 μM) with 20 μM HPr-P-Ser in each. However, His-CcpA binding was comparable in the absence of HPr-P-Ser, suggesting that it was not required under these *in vitro* conditions (data not shown). The observed binding could be competed upon addition of cold P*sagA* Middle probe, but not with a P*sagA* probe that does not contain the *cre* (Right), indicating that CcpA binds specifically to the middle probe (Fig. 25AB). Interestingly, an upstream probe (Left) that also lacks the predicted *cre* appears to compete slightly, suggesting that CcpA may more weakly bind to other regions of P*sagA*.

To further demonstrate the specificity of CcpA for the predicted P*sagA cre*, a 30-mer double-stranded oligonucleotide (ds-Oligo) probe encompassing the established P*ccpA cre* was used. Radiolabeled P*ccpA* ds-Oligo *cre* showed decreased mobility with increasing amounts of between 5-12.5 μM His-CcpA (Fig. 25C, lanes 1-5). The addition of 20 μM Hpr-P-Ser does not appear to enhance binding to oligo probes and was not utilized further. Binding was competed upon addition of cold P*ccpA* ds-Oligo *cre*, but not a scrambled version of the same *cre* probe (Fig. 25C, lanes 6 and 7), showing specificity of His-CcpA binding. Importantly, cold ds-Oligo probes for the P*sagA cre* as

well as *cre* within P*mga* and *rivR* also compete for binding of His-CcpA to P*ccpA cre* to varying degrees (Fig. 25C, lanes 8-10). Thus, CcpA binds directly to the *cre* present in P*sagA* and provides a mechanism for the observed CcpA-mediated CCR of SLS expression.

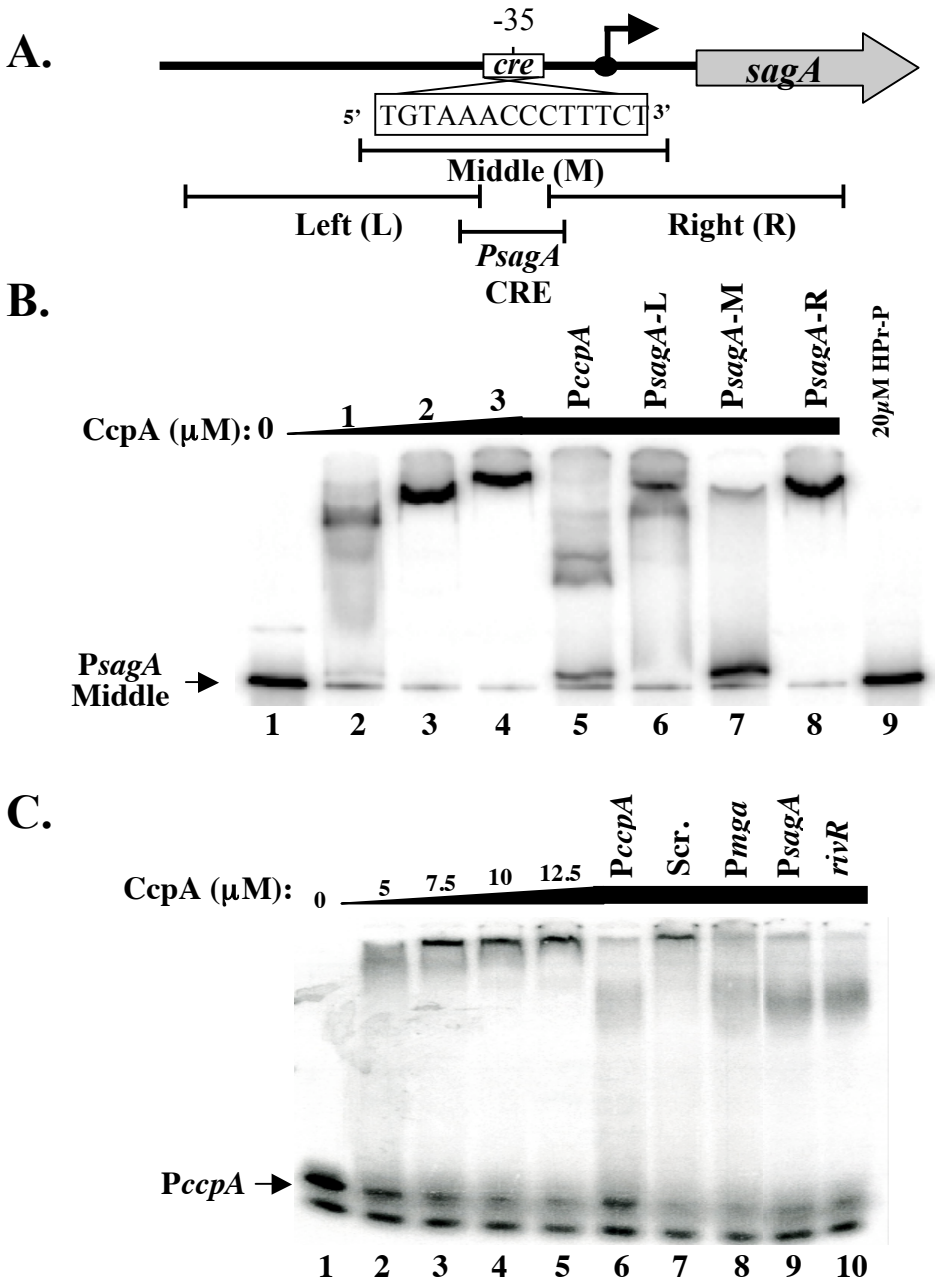

Fig. 25: EMSA with the P*sagA cre*

(A) Schematic showing P*sagA* region with putative *cre* on the antisense strand, overlapping the -35 consensus sequence. Promoter probes Left, Middle, Right and P*sagA cre* are shown below. **(B)** EMSA using P*sagA* Middle end-labeled probe. A constant amount of probe (10-25ng) was incubated with increasing amounts of GAS His-CcpA (1-3μM) and a constant amount of HPr-P-Ser (20μM) (Lanes 2-9). 500 ng of cold competitor probes are added to lanes 5-8, P*ccpA,* P*sagA*-Left, P*sagA*-Middle, and P*sagA*-Right, respectively. **(C)** EMSA using a double-stranded P*ccpA* oligonucleotide (ds-oligo) end-labeled probe. A constant amount (1-2 ng) of labeled probe was incubated with increasing amounts (5 to 12.5 μM) of purified GAS His-CcpA (lanes 1-5). Unlabeled competitor ds-oligo probes corresponding to P*ccpA* (lane 6), scrambled (lane 7), P*mga* (lane 8), P*sagA* (lane 9), and *rivR/ralp4* (lane 10) were incubated with 12.5μM CcpA to assay specific binding.

Role of Streptolysin S in the CcpA-mediated repression of virulence

Mutation of most genes in the *sag* operon, including *sagB*, leads to loss of SLS activity in GAS (59). To determine if the increased expression of SLS in the Δ*ccpA* mutant contributes to the increased virulence seen in mice, the *sagB* gene was inactivated in both WT MGAS5005 and the Δ*ccpA* mutant. Since the mutation of *sagB* is downstream of *sagA/pel*, it would be expected to inhibit SLS production independent of the *pel* transcript. Both the *sagB* single mutant and the *sagB* Δ*ccpA* double mutant showed complete loss of hemolysis on sheep blood agar plates compared to the WT MGAS5005 (Fig. 26A). In addition, culture supernatants from the *sagB* Δ*ccpA* double mutant did not exhibit any hemolytic activity in the hemolysis assay (Fig. 26B). However, the *sagB* single mutant began to regain a small amount of hemolytic activity at the end of the time-course assay suggesting that the insertional-inactivation mutation without antibiotic selection may not be fully stable, allowing for reversion to wild-type in a small percentage of the population (Fig. 26B).

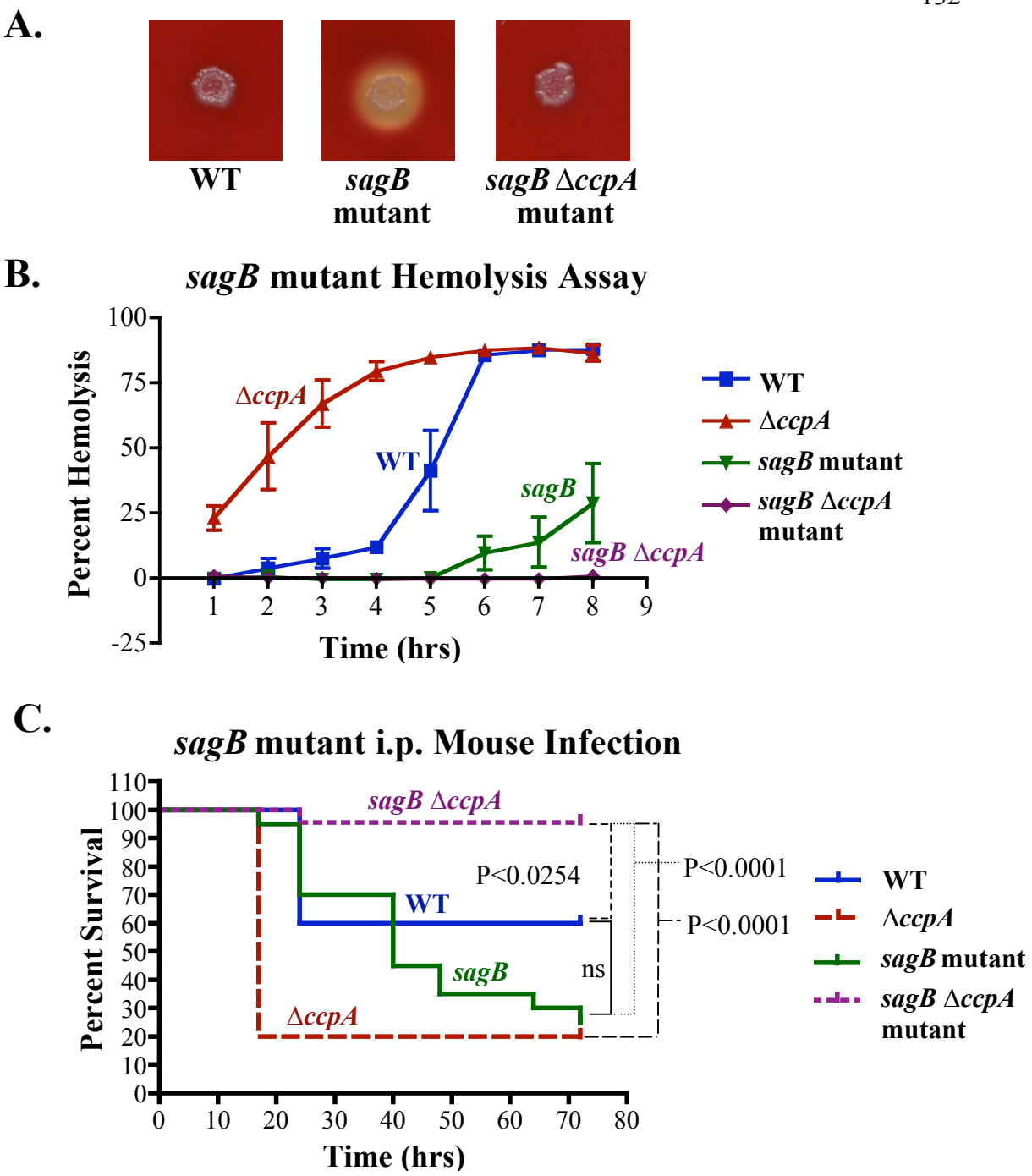

Fig. 26: Role of SLS in GAS systemic infection in mice
(A) Plate colonies of WT MGAS5005, *sagB* single mutant, and *sagB* Δ*ccpA* double mutant strains on 5% sheep blood agar plates after growth at 37°C. **(B)** SLS hemolysis assay with WT MGAS5005, Δ*ccpA*, *sagB* single mutant, and *sagB* Δ*ccpA* double mutant strains grown in THY broth supplemented with 10% heat-inactivated horse-serum and supernatant samples were isolated at different time points for analysis of SLS activity. Data is presented as the average percent hemolysis (solid lines) from 3 independent experiments with standard error bars. **(C)** Survival curve for WT MGAS5005 (n=5), MGAS5005 Δ*ccpA* (n=5), single *sagB* mutant (n=20) and double *sagB* Δ*ccpA* mutant (n=22) i.p. mouse infections. Data shown represent 2 independent experiments (n=52, total). Significance was determined using Kaplan-Meier survival analysis and a logrank test.

To assess the role of SLS *in vivo*, female CD-1 mice were infected i.p with either WT MGAS5005, the Δ*ccpA* mutant, the *sagB* single mutant, or the Δ*ccpA sagB* double mutant at an average dose of $2.73x10^7$cfu (Fig. 26C). The *sagB* single mutant had a small effect on virulence by the i.p. route of infection compared to WT MGAS5005, but this was not statistically significant (Fig. 26C). Published studies using the same route of infection also found a similar result (74). In contrast to the *sagB* single mutant, inactivation of *sagB* in the Δ*ccpA* mutant not only altered its hypervirulence phenotype, it resulted in significant attenuation ($p<0.0001$) compared to the *sagB* single mutant (Fig. 26C). In addition, the *sagB* Δ*ccpA* double mutant also showed significant attenuation ($P<0.0254$) as compared to the WT MGAS5005. Therefore, the CcpA-mediated repression of virulence observed following i.p. infection is dependent on SLS production. Furthermore, in the absence of SLS, loss of CcpA actually leads to attenuation of systemic virulence in GAS.

To address the stability of the *sagB* mutation *in vivo*, the spleen from a moribund mouse infected with the *sagB* mutant was extracted and homogenized. Upon serial dilution and plating on blood agar, only 4 out of 250 colonies, or approximately 98% of the colony forming units were non-hemolytic. This indicates that while the *sagB* mutation may fluctuate without antibiotic selection as seen in the hemolysis assay, the *sagB* mutation was mostly stable *in vivo*.

DISCUSSION

There is growing evidence that sugar metabolism influences disease progression in many Gram-positive pathogens, including GAS. Carbon catabolite repression (CCR)

mediated by CcpA represents a conserved pathway in Gram-positive bacteria that controls sugar utilization, providing an attractive mechanism whereby carbon metabolism could directly regulate virulence. The results from this study show that CcpA plays a significant role in GAS pathogenesis by repressing SLS expression and virulence during systemic infection, providing a regulatory link between sugar utilization and virulence.

Defining the CcpA regulon of GAS

In *Lactococcus lactis* and *Bacillus subtilis*, CcpA is a global regulator of gene expression, primarily affecting operons required for uptake and utilization of non-glucose sugar sources. However, in the oral pathogen *Streptococcus mutans*, CcpA was also able to regulate key virulence genes (1). To assess the CcpA regulon in the pathogenic GAS, a transcriptome analysis was completed comparing the wild type MGAS5005 with an isogenic Δ*ccpA* mutant during exponential growth in rich media, when glucose is present and CcpA activity would be expected to be highest. This study identified 124 regulated genes (6% of the GAS genome) either up or down-regulated at least 2-fold with an added cutoff that 4/6 biological replicates with dye swaps must also be significant (Appendix II). This is comparable to the number of regulated genes observed in *L. lactis* (118 in early-log, 86 in mid-log) and in *S. mutans* (170 in mid-log) (1, 236). However, given that 148 CcpA-regulated genes of *L. lactis* were also identified during the transition from exponential to stationary growth, the inclusion of later time points in our analysis would likely reveal even more of the GAS CcpA regulon.

The array analysis found that the majority of the GAS CcpA regulon (90%) is repressed during exponential growth phase, emphasizing that the primary function of

CcpA is to down regulate gene expression under high glucose conditions. As expected, over 60% of the genes regulated by CcpA are involved in metabolism and carbohydrate transport, which corresponds to studies in other Gram-positive bacteria (Fig. 27) (1, 236). As might be expected from these results, detectable growth phenotypes can be observed in a CcpA mutant, such as small colony size on plates and an increased lag phase in liquid media; although growth rate compared to wild type was not significantly altered. Thus, CcpA appears to regulate carbon uptake and metabolism in response to glucose in GAS and the inability to control this process does appear to have effects on GAS structure and growth.

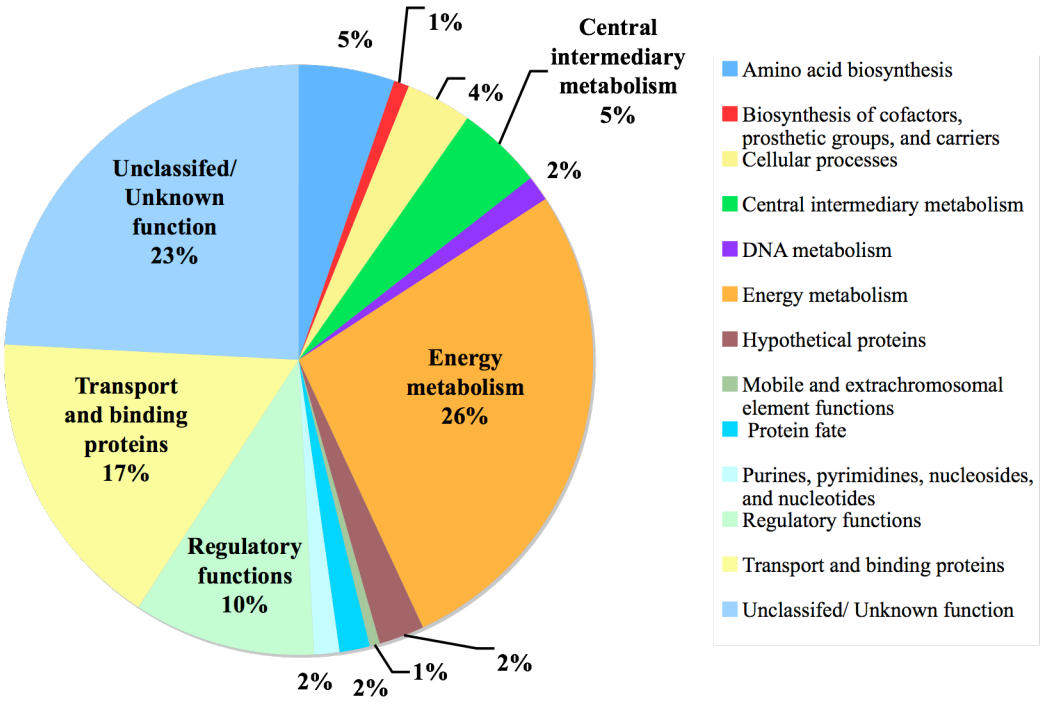

Fig. 27: Functions of CcpA-regulated genes
Pie chart shows percentages by category of predicted gene function for all CcpA-regulated genes.

Importantly, CcpA also regulates established virulence genes in GAS (Table 7), including the secreted DNase B (*spd*) and the entire *sag* operon necessary for SLS synthesis and secretion. Several studies have indicated that expression of *sagA/pel* was tightly growth-phase dependent, exhibiting low expression until transition into stationary phase (77, 136). Combined with the in silico analysis showing a putative *cre* within the *sagA/pel* promoter (Chapter 4, Appendix I), these data strongly suggested that the *sag* operon was under CCR. CCR of *sagA* was confirmed in this study based on the Δ*ccpA* transcriptome results, the P*sagA-luc* luciferase studies, and the SLS activity assays (Table 7, Fig. 23 and 24). Furthermore, EMSA demonstrated specific binding of His-CcpA to the *PsagA cre* (Fig. 25) indicating direct repression by CcpA. P*sagA* is also under direct repression by the CovRS two-component system both *in vitro* and *in vivo* (70, 77, 92, 207). In fact, the P*sagA cre* characterized here overlaps the -35 region and falls within the region protected by CovR in DNase I footprints (77). Whether these two systems interact to control *sag/pel* expression is not clear. Interestingly, the MGAS5005 parental strain used here is a *covS* mutant that exhibits increased *sagA* production compared to wild type strains and correlates with invasive potential in mice (207). Since both regulatory systems strongly repress SLS production in GAS, it suggests that this activity is tightly controlled during infection and only expressed under specific conditions.

CcpA represses the expression of the two-component systems TCS5 (5005_Spy1305/1306) and TrxSR (5005_Spy0784/0785), as well as activates expression of the RofA-like protein RivR (Table 7 and Appendix II). TCS5 has been shown to positively regulate an adjacent mannose/fructose PTS operon that also appears as repressed in our CcpA array data (Table 7) (196). RivR has been associated with

positively influencing expression of the Mga virulence regulon in GAS (179). Although results from Chapter 4 show that CcpA activates transcription of *mga* by binding to a *cre* upstream of P*mga* (Fig. 7), *mga* was not found to be significantly regulated by CcpA in the microarray analysis (Table 7). However, luciferase assays showed a consistent, although not significant reduction in expression from P*mga* in the Δ*ccpA* strain (Fig. 22), suggesting that CcpA still influences *mga* expression, just at varied levels in different strain backgrounds.

Determining a consensus GAS *cre*

Of the 124 CcpA-regulated genes identified in the Δ*ccpA* transcriptome analysis, 76 total genes contained 31 unique *cre* predicted in the previous in silico analysis either within their promoter regions, the gene itself, or associated with a 5' gene in their operon (5). Thus, 61% of the CcpA-regulated genes showed the potential for direct CcpA regulation through a *cre* identified using the *B. subtilis* consensus with one mismatch. The binding studies have now found four *cre* that are bound specifically by CcpA in GAS; P*ccpA*, P*mga*, P*sagA*, *rivR* (Fig. 6 and 23). Alignment of these sites along with the 28 other unique GAS *cre* associated with CcpA-regulated genes produces a GAS consensus *cre* that is more flexible at 5 positions (6, 7, 8, 9, and 13) and more specific at position 12 than the *B. subtilis* consensus (Fig. 26). This suggests that our initial screen was too strict and possibly missed potential sites. A new in silico search using the GAS consensus (Fig. 26) identified 6 new putative *cre* and 24 of 31 previously identified *cre* showing regulation on the microarray, with the remaining 7 being found with one mismatch. In addition, 11 more genes are associated with the newly described *cre* sites.

Thus, 93/124 CcpA-regulated genes (75%) found in the array were associated with a *cre* using the GAS consensus. Overall, it appears that a GAS *cre* exhibits more flexibility at several positions than a *B. subtilis cre*. However, this consensus will benefit from studying more CcpA/*cre* interactions in GAS.

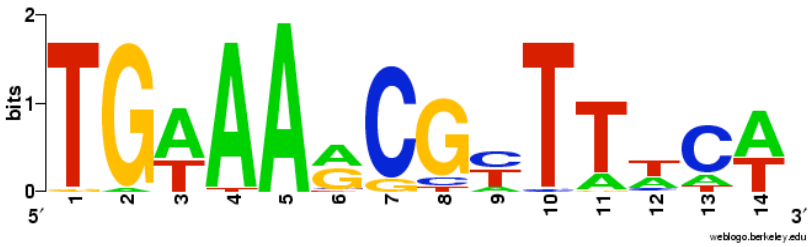

Bacillus sp.: T G W A A R C G Y T W N C W

GAS consensus: T G W A A N S B H T W H H W

Fig. 28: GAS *cre*.
Sequence logo representing GAS consensus *cre* of CcpA-regulated genes. The published *Bacillus sp.* consensus *cre* and a GAS consensus *cre* determined from the sequence logo are shown below. Underlined-shaded letters indicate difference from *Bacillus cre.* Degenerate nucleotide symbols: W= A or T; R= A or G; Y= C or T; N= A, C, G or T; S= C or G; B= C, G or T; H= A, C, or T.

CcpA represses virulence in mice

In this study, deletion of *ccpA* in the M1 MGAS5005 led to a surprisingly dramatic increase in virulence following both systemic (i.p.) and localized (s.c.) infections of mice (Fig. 20). This was most evident in the i.p. model of systemic infection, where the animals succumbed faster than wild type, and many exhibited evidence of severe hemorrhaging from various body sites. The hypervirulence phenotype in the GAS Δ*ccpA* mutant was complemented beyond WT levels with *ccpA* overexpressed in trans, suggesting that the release of CCR had a significant effect on virulence gene expression *in vivo*. These results contrast with published studies in the closely related organism *S. pneumoniae*, where Δ*ccpA* mutants were attenuated for virulence using three different mouse models of infection, including systemic (i.p.), pneumonia, and nasopharyngeal colonization (79, 100). The reason for the observed attenuation in the Δ*ccpA* mutant was suggested to be either reduced expression of cell wall proteins vital for metabolism *in vivo*, or regulation of polysaccharide synthesis. However, we did not see comparable changes in GAS for surface proteins or capsule at mid-logarithmic phase in our array analysis.

SLS is a CcpA-repressed virulence factor during GAS systemic infection

One of the most highly CcpA repressed genes in the array analysis was *sagA/pel* and the entire *sag* operon, leading to an increase in SLS hemolytic activity (Table 7, Fig. 22). This raised the question as to whether the increase in SLS production might be responsible for the hypervirulence seen in the mouse models of infection. Previous studies have shown that SLS contributes to the severity of localized necrotic lesions in

mice (59, 74), and would help to explain this phenotype observed in the subcutaneous infection model (Fig. 20B). However, SLS-deficient mutants in an M5 GAS background did not show a significant virulence defect compared to wild type following i.p. infection of mice (74). The same thing was observed here, where a *sagB* non-hemolytic mutant of MGAS5005 did not show a significant difference from the parental strain following i.p. infection (Fig. 26C). In contrast, inactivation of SLS production in the Δ*ccpA* mutant background (*sagB* Δ*ccpA*) showed a dramatic reduction in virulence ($P<0.0001$), abrogating the hypervirulence and resulting in an overall attenuation compared to either MGAS5005 or the *sagB* single mutant (Fig. 26C). This provides genetic evidence that the hypervirulent phenotype seen with the Δ*ccpA* mutant during systemic infection is attributable to the increased expression of SLS in this strain. Furthermore, in the absence of SLS production, a Δ*ccpA* mutation leads to attenuation.

The high level of CcpA-mediated repression of *sagA* might suggest that SLS has a role in secondary metabolism in the human host, where the function of the cytolysin *in vivo* may be to help release nutrients into the immediate environment surrounding the organism. This damage may have a cost of activating the host immune response, stimulating neutrophil migration to the site of infection and eliciting an inflammatory response. This would necessitate strict regulation of SLS expression, either through CcpA-mediated CCR or via CovRS repression. Thus, SLS expression is normally repressed *in vivo* potentially by the presence of high levels of glucose in the peritoneum. Additional experiments will be necessary to determine if this is also occurring during soft tissue infection at the skin.

During the preparation of this dissertation, a study from Shelburne *et al.* was published which also described the role of CcpA in the pathogenesis of the M1 GAS strain MGAS5005 (192). In fact, the parental MGAS5005 strain used in our work was obtained directly from the same group. Notably, the authors analyzed the transcriptome of their Δ*ccpA* mutant and found that CcpA strongly repressed expression of the *sag* operon and SLS activity in addition to other virulence and regulatory genes. In the majority of cases, the results described here closely mirror their data and help to strongly validate both studies, with one significant exception. Shelburne *et al.* found that their Δ*ccpA* mutant was attenuated following i.p. infection in female CD-1 mice, whereas the results described here showed an increase in virulence in the identical background. The authors did not investigate the mechanism of CcpA-mediated attenuation in their study. Although the difference could be attributed to a secondary mutation obtained during mutagenesis of *ccpA* for one of the groups, successful complementation analysis by both groups would appear to rule this out. Another possible explanation could be subtle difference in the execution of the i.p. infection model. Since we observed attenuation in a Δ*ccpA* mutant in the absence of SLS production, this provides a potential mechanism for the differences seen *in vivo*. Regardless, the two studies clearly demonstrate for the first time a direct link between carbon metabolism and virulence in GAS. In contrast, the work described in this section has revealed a significant role for CcpA-mediated repression of the cytolysin SLS in the severity of GAS systemic infection that was not previously appreciated.

CHAPTER SIX:

Conclusions and Recommendations

The GAS, a strict human pathogen, is capable of causing a variety of diseases in the diverse niches to which it has adapted. The ability of this organism to coordinate virulence gene regulation to growth in various environments is beginning to show a strong link to metabolism. These studies have shown that CcpA, the main regulator of CCR in the GAS, was not only able to activate expression of the major virulence regulator Mga, but was also able to repress a variety of virulence factors including the potent cytotoxin, SLS. Outside of direct CcpA-mediated regulation of specific virulence factors, the influence of sugar metabolism is emerging as major factor for global regulation of virulence expression in the GAS. Overall, this study aimed to investigate the role of sugar metabolism regulation on virulence and its contribution to the pathogenesis of the GAS.

Direct link between regulation of sugar metabolism and expression of the virulence regulator Mga

Prior to this study, only a few factors were known to influence *mga* expression, for example, autoregulation, levels of both CO_2 and iron, and the newly identified putative sugar transporter AmrA. Beyond the direct binding of Mga to the Mga-binding sites within P*mga*, none of the factors influencing *mga* expression were associated with a specific mechanism for regulation. This study determined that *mga* expression is under

CCR, and CcpA directly activates expression of *mga* through specific binding to the *cre* located upstream of the distal P1 promoter.

Two individual *ccpA* mutants were constructed, and while both showed a reduction in expression from P*mga* (Figs. 10 and 22), the levels of *mga* transcript were not significantly reduced in the transcriptome analysis using the M1 Δ*ccpA* strain. The current model for expression from *Pmga* suggests that CcpA activates *mga* expression through the P1 promoter, which was initially thought to be a low-level constititutive promoter (Fig. 18). Thus, the effect of CcpA-mediated regulation of *mga* may occur too early to detect using a genome-wide approach. Quantitative real-time RT-PCR on the serotype M6 background strains, with or without the *cre,* showed a reduction in both P1 and total P*mga* transcripts (Fig. 8). However, the levels of P1 *mga* transcript have not been tested in either of the *ccpA* mutant strains, the results of which might provide further support to the model for CcpA activation of early *mga* transcription from P1 (Fig. 18). In addition, transcriptional reporter assays with P1 P*mga* alone might be able to determine the contribution of CcpA to the activation of P*mga*. Preliminary results using a transcriptional fusion of P1 to luciferase did not show any expression whether the *cre* was present or not; however, these experiments may work if CDM is used as the growth media instead of THY broth. Expression from P*mga* was found to be much higher in CDM when glucose was the carbon source (Fig. 13).

Results presented in this work show that CcpA activates *mga* expression, while the same is not true for the Mga-regulated genes *emm* and *scpA* (Fig. 11). This suggests that Mga autoregulation can differ from activation of the Mga regulon. One possible reason for this might be that activation of *mga* transcription requires additional factors

that could be affected by CCR as well. Importantly, the Mga-binding sites within P*mga* vary greatly from the consensus binding sequence for both P*emm* and P*scpA* (140, 145). Thus, Mga autoactivation of *mga* transcription may require conditions distinct from activation of the Mga regulon. Furthermore, this suggests that additional factors may be cooperatively interacting with Mga during activation of *mga* transcription.

Interestingly, during growth in lower amounts of glucose (0.25%), the expression from P*mga* increased approximately 2-fold across exponential growth and 3-fold in stationary phase compared to growth in higher levels of glucose (1-2%) (Fig. 14). This indicates that there may be additional factors affecting the expression of P*mga* outside of CcpA-mediated CCR. The inverse correlation observed between P*mga* transcriptional activation and glucose levels leads to several questions about the cooperative nature of CcpA and Mga-mediated activation at P*mga.* First, do increased levels of glucose induce more CcpA-mediated activation of P*mga* expression, and if so, does it favor transcription from P1 over the autoregulation of P2? While the results presented in this study seem to indicate that higher levels of glucose trigger more transcriptional activation from P1, the role of autoregulation via the P2 promoter was not assessed. Secondly, what does the increased expression from P*mga* during stationary phase indicate? Is it a release of repression, and if so, what factors are involved? Or is there a more global environmental change leading to this increased expression, such as a change in pH? Further experimentation is necessary to completely understand the complex regulation of P*mga* by both CcpA and Mga.

Sugar source also appears to play a role in regulation of *mga*, through either direct CcpA-mediated CCR or other mechanisms. Both GusA and luciferase transcriptional

reporter assays showed a reduction in expression from P*mga* when sucrose was the sole carbon source (Fig. 12 and 15). Although expression was higher in glucose alone compared to sucrose alone, growth in a mixture of both glucose and sucrose did not seem to restore the levels of P*mga* expression to that seen in glucose alone. These results seem to contradict the mechanism for CcpA-mediated CCR, and suggest an alternative form of CCR is also affecting *mga* expression. Moreover, expression from P*emm* seems to show a pattern that follows CcpA-mediated CCR, where expression is reduced during growth in glucose, however, as discussed previously, *emm* transcription was not affected in the *ccpA* mutant strains. In addition, physiological studies by Pine and Reeves determined that levels of M protein expression were significantly reduced during growth in sucrose compared to growth in glucose, strongly suggesting catabolite repression of M protein expression (162). This work, along with the transcriptional data presented in this study implies that the Mga-regulated gene *emm* is under CCR, but it may not be through a CcpA-mediated mechanism. This leads to the questions of what other mechanisms are responsible for the CcpA-independent CCR seen at the level of transcription from P*mga* and P*emm*, and are they independent of each other as well? Furthermore, can sucrose directly inhibit expression of *mga* and the Mga-regulated genes, and if so how? Future experimentation utilizing both P*emm* and P*mga* reporter strains grown in varied conditions may help determine the CcpA-independent regulation of Mga and the Mga-regulated genes.

A potential mechanism for the CcpA-independent CCR seen in *mga* regulation may involve the putative sugar transporter AmrA. Data presented in this study shows that AmrA positively influences expression of *mga* in the M6 strains JRS4 and GA19681

(Fig. 16 and 17), as well as *emm* transcription only in the JRS4 strain. Preliminary experiments where the JRS4 Δ*amrA* strain, Adel, was grown in varied sugar sources indicate that expression from P*mga* is completely reduced when sucrose is the sole sugar source. While this could just be a cooperative reduction in transcriptional activation of *mga*, as both sucrose alone and deletion of *amrA* reduce expression from P*mga*, it could also be responsible for the inhibition of P*mga* activity seen during growth in sucrose. Furthermore, this might suggest that AmrA is somehow involved in sucrose transport in, and, or, out of the bacterium, and the absence of AmrA leads to either a build-up or the complete lack of sucrose within the cell causing the downstream effects on P*mga*. Future studies using additional AmrA mutant strains and various sugar sources will be necessary to determine the relationship between AmrA and sucrose-mediated repression of *mga*.

Although, CcpA-mediated activation was shown at P*mga*, expression of the Mga regulon was not altered. This leaves several questions unanswered about the complex regulation of P*mga* and the differences between Mga-mediated autoactivation versus activation of the Mga-regulated genes. Additional studies will be necessary to determine the role, if any, that AmrA plays in influencing expression of *mga*, and if it is involved in the CcpA-independent CCR seen in both regulation of P*mga* and P*emm.*

Identification of the CcpA regulon and its role in GAS pathogenesis

The influence of CcpA has been studied in great detail in the Gram-positive model organism *B. subtilis*; however, prior to this study, not much was known about CcpA-mediated CCR in the GAS. The results of the present study not only define the CcpA-regulon in the GAS, but also show that CcpA-mediated repression of SLS

influences pathogenesis of the GAS. Importantly in the GAS, like in other notable human pathogens such as *C. perfringens*, *S. aureus,* and *S. pneumoniae*, CcpA plays a significant role in modulating virulence gene expression.

The transcriptome analysis, completed in this work, has identified a subset of the CcpA regulon in the GAS. As expected, most of the genes identified as part of the CcpA regulon are involved in energy metabolism, such as PTS operons, other sugar transporters, and ATPase operons. While these findings helped to validate the array analysis, they also confirmed that the main function of CcpA is regulation of metabolism. The transcriptome analysis was completed at only one time point, during the mid-exponential growth phase when CcpA-mediated regulation would be expected to be at its peak. However, as shown in *L. lactis*, CcpA also influences gene expression at all other points during the growth phase, and therefore many additional CcpA-regulated genes remain to be identified in future studies (236).

In addition to the expected metabolic genes, it was also shown that CcpA regulates the expression of several notable virulence factors. This result, although intriguing, is not completely unique, as CcpA has been shown to regulate virulence factors in other Gram-positive organisms (1, 100, 147, 189, 221)}. The virulence factors regulated by CcpA in the GAS include: SLS, a hemolysin; Spd, a DNase; and several transcriptional regulators of virulence such as RivR and the TrxRS TCS. Beyond involvement in functions listed, CcpA-mediated regulation may suggest that these virulence factors have an unknown role in metabolism as well as being required for survival in the host.

Unlike in the closely related *S. pneumoniae*, deletion of *ccpA* in the GAS resulted in a hypervirulence in both the systemic (i.p) and localized skin (s.c) mouse models of infection (Fig. 20). While this result was initially unexpected, the subsequent transcriptome analysis identified that CcpA represses the transcription of several virulence genes, thus the expression of these factors are increased in the Δ*ccpA* strain, resulting in a hypervirulent phenotype. In contrast to the findings presented within this dissertation, a recent study also investigating the role of CcpA in GAS pathogenesis identified that the deletion of *ccpA* had the opposite effect, resulting in attenuation of the GAS strain (192). The results of the *in vivo* mouse infection were puzzling, as the authors of the contradictory study not only utilized the same strain of GAS, but also identified the same CcpA-regulated virulence factors in a similar transcriptome analysis. However, both studies were able to complement the opposing effects of *ccpA* and virulence was restored to wild type levels, suggesting the difference between the parallel studies may be a CcpA-mediated factor that is altered in one of the strains. To further verify the effects of the deletion of *ccpA*, experiments using an alternative animal model of infection such as the zebrafish model or non-human primates may provide more insight into the differences between the two CcpA mutant strains.

Notably, the genes encoding SLS (*sagA)* and the entire operon required for secretion, were identified as some of the most highly CcpA-repressed genes in the microarray study (Table 7 and Appendix II). This potent cytolysin plays a significant role in the pathogenesis of the GAS (59), and is under tight regulation by the virulence regulator, CovR (70, 93). The role of SLS in GAS infection was previously shown to only be involved in the subcutaneous mouse infection model (59); however, results

presented in this study indicate the SLS also plays a role in systemic GAS infection (Fig. 26). Uniquely, the strain used in these studies is a CovS mutant, and therefore lacks CovR mediated-repression of multiple factors including *sagA*. Thus, it may be possible that during the course of a wild type GAS systemic infection, where glucose levels are high, the expression of *sagA* remains repressed by both CcpA and CovR, and SLS exerts only minimal effects on GAS pathogenesis.

In addition to SLS, other factors regulated by CcpA may play a role in GAS pathogenesis. For example, the transcriptome analysis identified that the chromosomally encoded DNase, *sda* (Sda), was repressed 2-fold by CcpA (Table 7). Recent evidence suggests that the DNases found in the GAS play a role in escaping the innate immune response by breaking down NETs (28). A previous investigation into the role of the streptococcal DNases in pathogenesis identified that this function is redundant due to the presence of multiple DNases in most strains. In the strain used in this study, MGAS5005, there are two phage-encoded DNases, SdaD2 and Spd3, and one chromosomally encoded Sda (206). All 3 DNases seem to contribute to virulence, although, the phage-encoded DNase, SdaD2, appeared to play a more important role in GAS infection. However, this study also indicated that Spd was only expressed during stationary phase in a growth-phase dependent manner, which may be directly influenced by CcpA (205). Thus, the chromosomally encoded DNase, Spd, may play a significant role in virulence of the GAS in the absence of CcpA.

Another factor potentially regulated by CcpA that may play a significant role in GAS pathogenesis is the cysteine protease, SpeB. SpeB is a well-characterized virulence factor of the GAS, which has been implicated in multiple roles of GAS pathogenesis

including avoidance of complement recruitment by cleavage of surface-associated proteins and prevention of FcR-mediated phagocytosis by cleavage of IgG. Although not identified in this study as significantly regulated by CcpA, as it was only repressed 1.5-fold (Appendix II), several putative *cre* sites were identified in the 5' region of the open reading frame (Appendix I). Previous studies evaluating the expression of SpeB found higher levels of SpeB in the culture media only after the glucose had been depleted (37). Moreover, SpeB is only expressed in late stationary phase, and expression is strongly growth-phase regulated. Interestingly, not all strains of GAS produce the same amount of SpeB, and MGAS5005, the strain used in this study, is among the strains that produce lower amounts (Leday and McIver, unpublished results). These results suggest that SpeB expression is under CCR, which may be directly mediated by CcpA; however, future experiments using additional strains that produce SpeB and further biochemical assays are necessary to complete the connection between CcpA and SpeB.

While the majority of factors regulated by CcpA are involved in metabolism, several important virulence factors are also under CcpA-mediated CCR. These factors, such as SLS and possibly Sda and SpeB play a significant role in the pathogenesis of the GAS in the absence of CcpA. Interestingly, these factors may also have an unidentified function in metabolism, making CcpA-mediated regulation necessary. Alternatively, the GAS has adapted this metabolism regulatory mechanism to control virulence factors relative to the surrounding environment.

Global influence of metabolism on regulation in the GAS

The GAS is a well-adapted pathogen with the capacity to cause a variety of diseases in the human host. The ability of this organism to infect multiple sites within the body including the respiratory tract, the skin, and the bloodstream and to coordinate the regulation of factors necessary for survival in these various environments is a key area of research in the GAS. This study presents evidence suggesting that the GAS senses the availability of nutrients in the surrounding environment and coordinately regulates virulence factors necessary for survival.

Evidence presented in previous chapters of this dissertation show that the main mediator of CCR in the GAS, CcpA, influences the expression of numerous factors involved in virulence including activation of the virulence regulator Mga. Interestingly, a recent transcriptome analysis of the influence of Mga on the GAS identified that Mga also positively regulates *ccpA*, forming a positive-feedback loop (Fig. 29) (177). Mga also contains 2 putative PTS-regulatory domains (PRD), which are commonly found on regulators of sugar metabolism (97, 219). This provides an additional mechanism for Mga to be influenced by metabolism, and therefore regulate the expression of the Mga regulon in response to the surrounding environment. Future experiments investigating the role of these domains will be necessary to determine their role in Mga regulation.

In addition to regulation of Mga, CcpA also positively influences RivR, and negatively regulates the TCS regulator TrxR. Interestingly, both regulators positively influence the expression of Mga, and are under repression mediated by the stress response TCS regulator CovR (Fig. 29) (Leday and Gold, unpublished data) (5, 179, 180). The complex interaction between all of these virulence regulators along with CcpA

lays a solid foundation for metabolism to influence the expression of many virulence factors in the GAS.

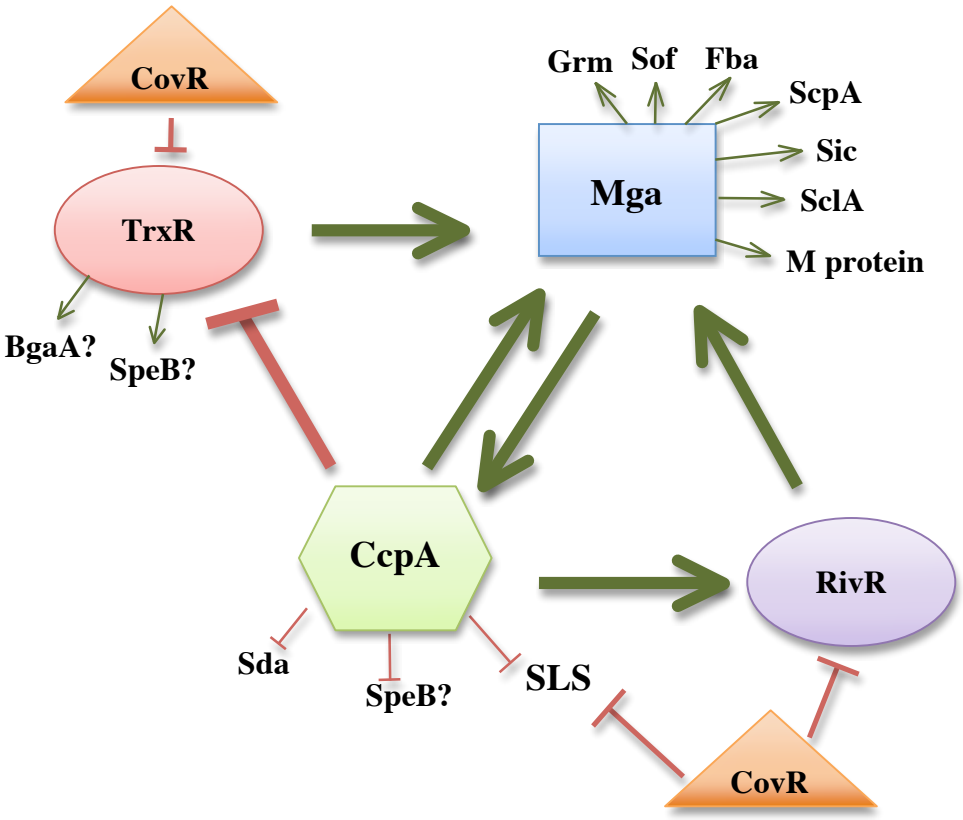

Fig. 29: Global regulatory interactions in the GAS
Diagram depicts the interactions between the global regulators CcpA, Mga, TrxR, RivR, CovR, and the regulated virulence factors. Green arrows indicate activation, while red lines with a bar indicate repression.

The interactions between these virulence regulators was determined using transcriptome analysis from cells grown in rich media, however, the question remains as to the importance of the connection between these factors in the context of human infection. Several recent studies have looked at the transcriptome of the GAS both during *in vivo* infection of a non-human primate model as well as ex vivo in human blood (83, 223). The data from these studies has provided a comparison relative to GAS disease at various locations within the human host, and has yielded information on the regulation of virulence factors during typical infection conditions. The Mga regulon, for example, was found to be the most highly expressed genes during the acute stage of a pharyngeal infection of cynomologus macaques (Fig. 30). In addition, expression of the Mga regulon was very high during the first 30 minutes of cultivation in human blood, where evasion of the immune response would be most critical. These studies also evaluated the link between metabolism and pathogenesis, in the non-human primate model as well as human blood. Glucose metabolism genes were upregulated during the early stages of both infection and growth, followed by a shift in expression to alternative carbohydrate metabolic genes (Fig. 30). Correspondingly, CcpA expression follows a similar pattern with higher expression early during pharyengeal infection and growth in human blood. SLS was found to be particularly important during growth in human blood as transcripts accumulated after the initial 30 minutes of growth, supporting a role for this cytolysin in acquiring nutrients (Fig. 30). Thus, the influence of metabolism on virulence regulation in the GAS does correlate to human infection, and merits future study to further elucidate this interesting connection.

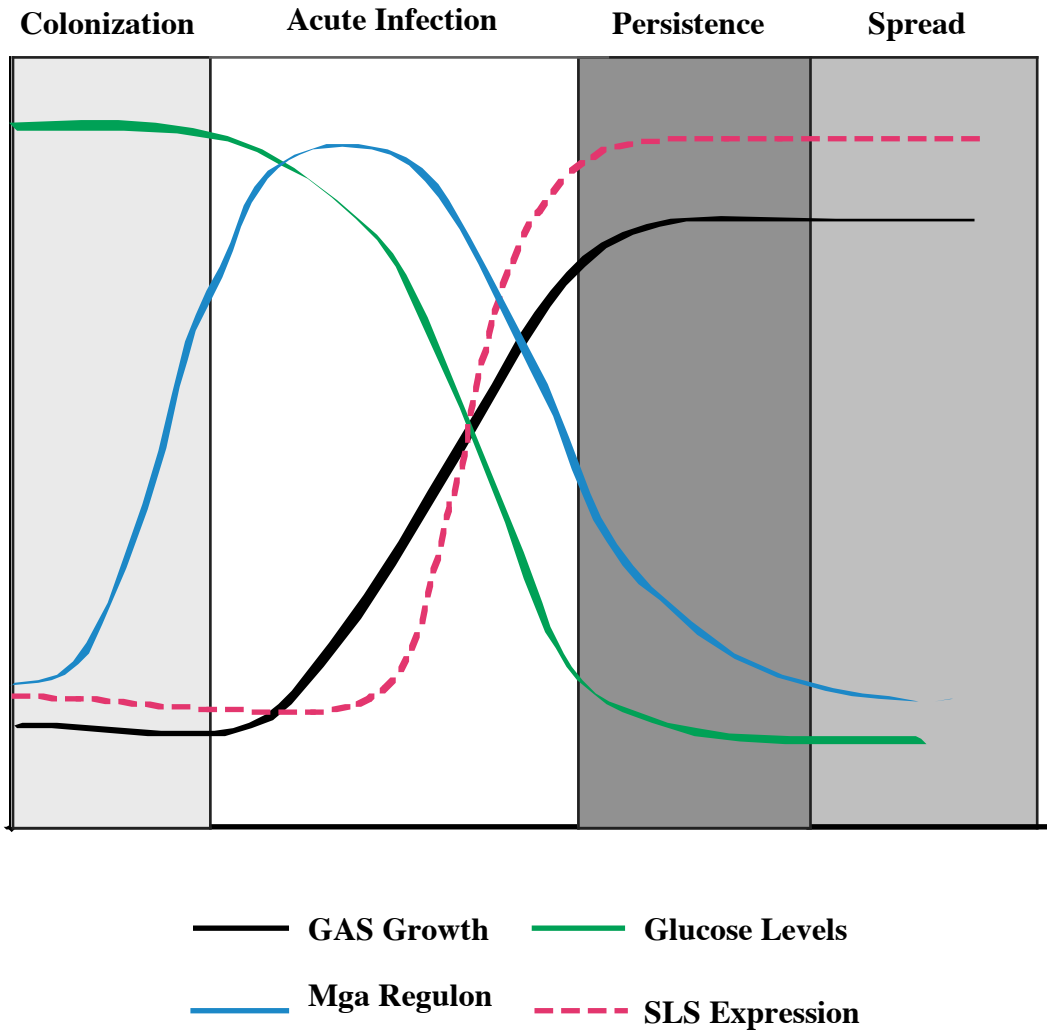

Fig. 30: Expression of the Mga regulon and SLS during the phases of GAS infection

Depicted in the diagram is the characteristic growth of the GAS, with the corresponding levels of glucose. Expression of the Mga regulon and SLS are shown relative to both growth phase and glucose levels.

Summary

In conclusion, the results of this work have identified the role of CcpA regulation of several virulence determinants including both activation of *mga* and repression of *sagA*. Beyond direct regulation of these factors, it was found that CcpA plays a significant role in the pathogenesis of the GAS, helping to adapt the GAS to the changing environment for better survival within the host. Overall, the results provided within this dissertation have established a strong link between virulence gene regulation and metabolism in the GAS.

APPENDIX I:

Putative GAS *cre* from M1 SF370

Direct Strand				
Sequence Start	**Sequence End**	**Spy Number**	**Gene Name**	**Intergenic**
4829	4842	Spy0007	*pth*	N
14497	14510	Spy0015	*ftsH*	N
14842	14855	Spy0016	-	Y
114510	114523	Spy0123	-	N
126272	126285	Spy0136/0137	*-/atoE*	Y
128900	128913	Spy0139/0140	*-/-*	Y
159861	159874	Spy0174	*(sgaT)*	Y
180206	180219	Spy0196	-	N
216908	216921	Spy0251	-	Y
312036	312049	Spy0359	-	Y
323925	323938	Spy0379	*pflC (pflA)*	Y
342637	342650	Spy0412/0414	*exoA(xth)/lctO*	Y
346423	346436	Spy0416	*prtS*	N
354025	354038	Spy0425	*nrdF.1*	N
365565	365578	Spy0442	-	Y
413360	413373	Spy0513/0514	*pepQ/ccpA*	Y
704617	704630	Spy0853	-	Y
854327	854340	Spy1046	-	Y
861325	861338	Spy1052	*(ndk)*	Y
866706	866719	Spy1057	-	Y
867168	867181	Spy1057	-	N
898807	898820	Spy1098	*folP*	N
923872	923885	Spy1127	*(rluD)*	N
946889	946902	Spy1151/1152	*ldh(lctE)/gyrA*	Y
971132	971145	Spy1180/1181	*(citMHS)/-*	Y
1005801	1005814	Spy1220/1221	*-/dpfB(dfp)*	Y
1007977	1007990	Spy1224	*pgmA*	Y
1101305	1101318	Spy1325	*(licR)*	Y
1103952	1103965	Spy1328/1329	*bglA.2/-*	Y
1108972	1108985	Spy1337/1339	*rsvA(rsuA)/-*	Y
1113492	1113505	Spy1345	-	Y
1157821	1157834	Spy1393	*pepB(pepF)*	N
1199331	1199344	Spy1447	-	N
1276058	1276071	Spy1549	*ahrC.2*	N
1285726	1285739	Spy1563	-	N
1320299	1320312	Spy1602/1603	*-/-*	Y
1382095	1382108	Spy1664	*pbpX*	N
1406497	1406510	Spy1693	-	Y
1439757	1439770	Spy1738	*manL*	Y
1455834	1455847	Spy1758	*phaB*	Y
1464244	1464257	Spy1770	*gatB*	N

1520729	1520742	Spy1833	*mutY*	N
1523066	1523079	Spy1836	-	N
1532713	1532726	Spy1846/1849	*dinP/pfl*	Y
1551880	1551893	Spy1869/1870	*vdp(deoD)/-(crgR)*	Y
1591144	1591157	-	-	Y
1602425	1602438	Spy1918	*lacF(celC)*	N
1605779	1605792	Spy1923/1924	*lacA.2/lacR.2*	Y
1647872	1647885	Spy1979	*ska*	N
1674900	1674913	Spy2007	*lmb*	N
1687459	1687472	Spy2019	*mga*	Y
1699359	1699372	Spy2039	*speB*	N
1699728	1699741	Spy2039	*speB*	N
1710150	1710163	Spy2052	*-(celC)*	Y
1719907	1719920	Spy2065/2066	*-/-*	Y
1728839	1728852	Spyt57/2079	*tRNA-Cys/ahpC*	Y
1734849	1734862	Spy2083	-	Y
1746157	1746170	Spy2091/2092	*-/rpsB*	Y
1786119	1786132	Spy2147	-	N
1824209	1824222	-	-	Y

Complementary Strand				
Sequence Start	**Sequence End**	**Spy Number**	**Gene Name**	**Intergenic**
57714	57727	-	*adhA (adhE)*	Y
106194	106207	SPy0109	*ackA*	Y
126272	126285	Spy0136/0137	*-/atoE*	Y
136525	136538	SPy0148	*ntpI*	N
159861	159874	Spy0174	*(sgaT)*	Y
193827	193840	SPy0216	*(ralp4)*	N
299937	299950	SPy0342	*snf*	N
323925	323938	Spy0379	*pflC (pflA)*	Y
342637	342650	Spy0412/0414	*exoA(xth)/lctO*	Y
344182	344195	SPy0416	*prtS*	N
365565	365578	Spy0442	-	Y
365932	365945	SPy0442	-	N
413360	413373	Spy0513/0514	*pepQ/ccpA*	Y
509836	509849	SPy0634/0636	*agaF/idnO(fabG)*	Y
598495	598508	SPy0738	*sagA*	Y
607207	607220	SPy0747	-	Y
635774	635787	SPy0777	*rexA*	N
666878	666891	SPy0809	*aroD*	N
704617	704630	Spy0853	-	Y
737183	737196	SPy0888/0889	*clpL/rpiA*	Y
770036	770049	SPy0926	*recJ*	N
799564	799577	SPy0976	-	Y
861325	861338	Spy1052	*(ndk)*	Y
866706	866719	Spy1057	-	Y
892043	892056	SPy1088	-	N
911262	911275	SPy1111/1113	*-/-*	Y
923872	923885	Spy1127	*(rluD)*	N

932269	932282	SPy1137	-	N
946889	946902	Spy1151/1152	*ldh(lctE)/gyrA*	Y
971132	971145	Spy1180/1181	*(citMHS)/-*	Y
1004677	1004690	SPy1219	-	N
1007977	1007990	Spy1224	*pgmA*	Y
1101305	1101318	Spy1325	*(licR)*	Y
1103952	1103965	Spy1328/1329	*bglA.2/-*	Y
1141322	1141335	SPy1373/1374	*ptsH/nrdI*	Y
1146123	1146136	SPy1379	-	N
1183361	1183374	SPy1424	-	Y
1251274	1251287	SPy1521	*ftsA*	Y
1274798	1274811	SPy1547	*sagP(arcA)*	Y
1292699	1292712	SPy1568	*valS*	N
1314366	1314379	SPy1595/1596	*-/-*	Y
1314433	1314446	SPy1595/1596	*-/-*	Y
1320299	1320312	Spy1602/1603	*-/-*	Y
1326808	1326821	SPy1606	-	N
1370837	1370850	SPy1651	*pepC*	N
1399987	1400000	SPy1684	*glpK*	Y
1439757	1439770	Spy1738	*manL*	Y
1455834	1455847	Spy1758	*phaB*	Y
1530771	1530784	SPy1844	*(recD)*	N
1560396	1560409	SPy1879	-	N
1605558	1605571	Spy1923/1924	*lacA.2/lacR.2*	Y
1625123	1625136	SPy1952	-	Y
1642625	1642638	SPy1972	*pulA*	N
1645826	1645839	SPy1976	*msmK(malK)*	Y
1710150	1710163	Spy2052	*-(celC)*	Y
1728839	1728852	Spyt57/2079	*tRNA-Cys/ahpC*	Y
1762139	1762152	SPy2110	*nrdD*	N
1847164	1847177	SPy2211	-	N

cre sites identified in the serotype M1 strain SF370 using the *B. subtilis* consensus sequence, with one mismatch allowed. Shading indicates that *cre* was identified on both strands. This table was constructed with the help of Dr. Audry Almengor.

APPENDIX II:

MGAS5005 vs. isogenic Δ*ccpA* mutant microarray results

5005 #	SF370 Spy#	Gene	Annotation (TIGR or NCBI)	Mean	Main Role	*cre*
0039	**SPy0042**	*adhE*	Alcohol/acetaldehyde dehydrogenase	**0.291**	Energy metabolism	Y
0040	**SPy0044**	*adhP*	alcohol dehydrogenase	**0.065**	Energy metabolism	Y+
0094	**SPy0109**	*ackA*	acetate kinase	**0.429**	Energy metabolism	Y
0117	**SPy0138**		transcriptional regulator, putative	**0.291**	Regulatory functions	^
0118	**SPy0139**		transcriptional regulator, LysR family	**0.065**	Regulatory functions	Y+
0125	**SPy0147**		hypothetical protein	**0.429**	Hypothetical proteins	^
0126	**SPy0148**	*ntpI*	v-type Na-ATPase	**0.291**	Energy metabolism	^
0127	**SPy0149**	*ntpK*	ATP synthase, subunit K	**0.065**	Energy metabolism	Y
0128	**SPy0150**	*ntpE*	v-type sodium ATP synthase subunit	**0.429**	Energy metabolism	^
0129	**SPy0151**	*ntpC*	ATP synthase (C/AC39) subunit	**0.291**	Energy metabolism	^
0130	**SPy0152**	*ntpF*	ATP synthase (F/14-kDa) subunit	**0.065**	Energy metabolism	^
0131	**SPy0154**	*ntpA*	ATP synthase archaeal, A subunit	**0.429**	Energy metabolism	^
0132	**SPy0155**	*ntpB*	ATP synthase archaeal, B subunit	**0.291**	Energy metabolism	^
0133	**SPy0157**	*ntpD*	V-type ATPase, subunit D	**0.065**	Transport and binding proteins	^
0157	**SPy0183**	*opuAA*	glycine betaine transport; ATP-binding	2.008	Transport and binding proteins	
0158	**SPy0184**	*opuABc*	glycine betaine transport system	1.834	Transport and binding proteins	
0186	**SPy0216**	*ralp4*	RofA-like, putative, RALP-4	**1.983**	Regulatory functions	Y
0212	**SPy0251**		N-acetylmannosamine-6-P epimerase	**0.294**	Central intermediary metabolism	Y
			hypothetical protein	**0.356**	Unknown function	^
0213	**SPy0252**		conserved hypothetical protein	**0.233**	Unknown function	^
0214	**SPy0254**		sugar ABC transporter, permease protein	**0.321**	Transport and binding proteins	^
0215	**SPy0255**		sugar ABC transporter, permease protein	**0.176**	Unknown function	^
0216	**SPy0256**		hypothetical protein	**0.223**	Unknown function	Y+
0217	**SPy0257**	*nanH*	N-acetylneuraminate lyase	**0.155**	Unclassified	^
0218	**SPy0258**		ROK family protein, putative	**0.212**	Energy metabolism	^
0340	**SPy0414**	*lctO*	L-lactate dehydrogenase, putative	**0.067**	Amino acid biosynthesis	Y
0342	**SPy0416**	*spyCEP*	cell envelope proteinase; IL-8 degrading enzyme	0.607	Cell Envelope	Y†
			hypothetical protein	**0.327**	Unknown function	
0361	**SPy0442**		glycerol-3-phosphate transporter, putative	**0.162**	Energy metabolism	Y*
0424	**SPy0514**	*ccpA*	catabolite control protein A	**4.615**	Regulatory functions	Y
0474	**SPy0571**	*licT*	beta-glucoside operon antiterminator	**0.045**	Regulatory functions	^
0475	**SPy0572**	*bglP*	PTS system, b-glucosides IIabc comp.	**0.038**	Energy metabolism	Y
0476	**SPy0574**	*bglA*	6-phospho-beta-glucosidase	**0.066**	Energy metabolism	^
0519	**SPy0629**	*agaD*	PTS permease for mannose subunit IIBMan	0.424	Energy metabolism	^
0520	**SPy0630**	*agaW*	PTS permease for mannose subunit IIPMan, putative	0.475	Energy metabolism	^

0521	**SPy0631**	*agaV*	mannose-specific phosphotransferase system component IIAB	0.337	Energy metabolism	^
0522	**SPy0632**		unsaturated glucuronyl hydrolase	0.374	Energy metabolism	^
0523	**SPy0634**	*agaF*	mannose-specific phosphotransferase system component IIAB	0.482	Energy metabolism	Y†
0524	**SPy0636**	*fabG*	3-oxoacyl-(acyl-carrier-protein) reductase	0.348	Energy metabolism	Y†
0525	**SPy0637**		Ribose/Galactose Isomerase family	0.636	Energy metabolism	^
0526	**SPy0638**		2-keto-3-deoxygluconate kinase, putative	0.599	Energy metabolism	^
0527	**SPy0639**	*eda*	2-deydro-3-deoxyphosphogluconate aldolase/4-hydroxy-2-oxoglutarate aldolase	0.501	Energy metabolism	^
0534	**SPy0647**		3-ketoacyl-acyl carrier protein reductase	**0.139**	Unclassified	^
0535	**SPy0648**		acetoacetyl-CoA reductase	**0.17**	Unclassified	^
0536	**SPy0649**	*dinG*	ATP-dependent helicase, putative	0.417	DNA metabolism	Y+
0562	**SPy0738**	*sagA*	Streptolysin S (SLS); pel locus	**0.039**	Virulence	Y
0563	**SPy0739**	*sagB*	SagB; SLS operon	**0.057**	Virulence	^
0564	**SPy0740**	*sagC*	SagC; SLS operon	**0.049**	Virulence	^
0565	**SPy0741**	*sagD*	SagD; SLS operon	**0.067**	Virulence	^
0566	**SPy0742**	*sagE*	SagE; SLS operon	**0.087**	Virulence	^
0567	**SPy0743**	*sagF*	SagF; SLS operon	**0.053**	Virulence	^
0568	**SPy0744**	*sagG*	ABC transporter; SLS operon	**0.09**	Virulence	^
0569	**SPy0745**	*sagH*	SagH; SLS operon	**0.083**	Virulence	^
0570	**SPy0746**	*sagI*	SagI; SLS operon	**0.099**	Virulence	^
0571	**SPy0747**		LPXTG cell wall anchor domain protein	**0.187**	Unclassified	Y+
			hypothetical protein	**0.157**	Unknown function	
0576	**SPy0755**	*atpB*	ATP synthase subunit 6	**2.349**	Energy metabolism	
0577	**SPy0756**	*atpF*	ATP synthase B chain, putative	1.91	Energy metabolism	
0578	**SPy0757**	*atpH*	ATP synthase delta (OSCP) subunit	**2.39**	Energy metabolism	
0579	**SPy0758**	*atpA*	ATP synthase F1, alpha subunit	1.96	Energy metabolism	
0580	**SPy0759**	*atpG*	ATP synthase	2.176	Energy metabolism	
0581	**SPy0760**	*atpD*	ATP synthase F1, beta subunit	**2.004**	Energy metabolism	
0582	**SPy0761**	*atpC*	ATP synthase, Delta/Epsilon chain	1.863	Energy metabolism	
0660	**SPy0853**	*fruR*	glycerol-3-phosphate regulon repressor	**0.45**	Regulatory functions	Y
0661	**SPy0854**	*fruB*	1-phosphofructokinase	0.513	Energy metabolism	^
0662	**SPy0854**	*fruA*	PTS system, fructose-specific IIABC component	0.436	Transport and binding proteins	^
0663	**SPy0856**	*mur1.1*	N-acetylmuramidase, putative	0.6	Energy metabolism	^
0780	**SPy1057**	*ptsA*	PTS system, mannose/fructose family IIA	**0.12**	Transport and binding proteins	Y
0781	**SPy1058**	*ptsB*	PTS system, mannose/fructose family IIB	**0.106**	Transport and binding proteins	^
0782	**SPy1059**	*ptsC*	PTS system, mannose/fructose family IIC	**0.091**	Transport and binding proteins	^
0783	**SPy1060**	*ptsD*	PTS system, mannose/fructose family IID	**0.081**	Transport and binding proteins	^
0784	**SPy1061**	*yesN*	sensor histidine kinase, yesN, *S.pneumo* hk09	**0.35**	Regulatory functions	^
0785	**SPy1062**	*yesM*	response regulator, yesM, *S.pneumo* rr09	**0.445**	Regulatory functions	Y+
0786	**SPy1063**		iron(III) ABC transporter, periplasmic	**0.365**	Transport and binding proteins	^
0790	**SPy1067**	*gabD*	succinate-semialdehyde dehydrogenase	**0.182**	Energy metabolism	Y+
0834	**SPy1111**		zinc-binding dehydrogenase, putative	**0.46**	Central intermediary metabolism	Y
0835	**SPy1113**		acid phosphatase	**0.174**	Central intermediary metabolism	^

0850	**SPy1128**	*pta*	phosphotransacetylase	**0.248**	Central intermediary metabolism	Y*
0852	**SPy1129**		3-oxoacyl-(acyl-carrier-protein) reductase,	**0.198**	Unclassified	^
0853	**SPy1130**		short chain dehydrogenase/reductase	**0.269**	Unclassified	^
0855	**SPy1133**	*proV*	amino acid ABC transporter, ATP-binding protein	**0.462**	Transport and binding proteins	^
0926	**SPy1212**		cardiolipin synthase, putative	**0.408**	Cellular processes	^
0927	**SPy1213**	*fhs*	formate--tetrahydrofolate ligase	**0.371**	Amino acid biosynthesis	^
0928	**SPy1214**	*lplA*	lipoate-protein ligase A, putative	**0.233**	Biosynthesis of cofactors, prosthetic groups, and carriers	^
0929	**SPy1215**		hypothetical protein	**0.227**	Hypothetical proteins	^
0930	**SPy1216**		Domain of unknown function, putative	**0.305**	Unclassified	^
0931	**SPy1217**		glycine cleavage system H protein	**0.254**	Unclassified	^
0932	**SPy1218**		unknown conserved protein	**0.28**	Unclassified	^
0933	**SPy1219**		NADH-dependent flavin oxidoreductase	**0.274**	Central intermediary metabolism	Y
0934	**SPy1220**		unknown conserved protein in B. subtilis	**0.356**	Unclassified	Y
0938	**SPy1224**	*pgmA*	phosphoglucomutase/phosphomannomutase	**0.397**	Energy metabolism	Y
0944	**SPy1232**		unknown conserved protein	**0.351**	Amino acid biosynthesis	Y
0988	**SPy1282**	*pyk*	pyruvate kinase	**2.345**	Energy metabolism	
0989	**SPy1283**	*pfk*	Phosphofructokinase	2.093	Energy metabolism	
1056	**SPy1292**	*malM*	4-alpha-glucanotransferase/amylomaltase	0.396	Energy metabolism	Y+
1057	**SPy1293**	*malR*	transcriptional regulator, LacI family, putative	0.341	Regulatory functions	
1062	**SPy1298**	*malA*	MalA protein	**0.045**	Energy metabolism	
1063	**SPy1299**	*malD*	maltose ABC transporter, permease	**0.039**	Energy metabolism	
1064	**SPy1301**	*malC*	maltose ABC transporter, permease	**0.039**	Energy metabolism	
1065	**SPy1302**	*amyA*	alpha-cyclodextrin glycosyltransferase	**0.03**	Energy metabolism	
1066	**SPy1304**	*amyB*	glycosyl hydrolase, family 13	**0.035**	Energy metabolism	
1067	**SPy1306**	*malX*	Maltose, ABC transporter, periplasmic-binding	**0.077**	Transport and binding proteins	
1079	**SPy1320**		PTS system, cellobiose-specific IIC component, putative	0.394	Transport and binding proteins	^
1080	**SPy1321**		PTS system, cellobiose-specific IIC component, putative	0.487	Transport and binding proteins	^
1081	**SPy1323**	*celC*	PTS system, cellobiose-specific IIA component	0.535	Transport and binding proteins	^
1082	**SPy1324**	*celA*	PTS system, cellobiose-specific IIB component	0.564	Transport and binding proteins	^
1083	**SPy1325**	*licR*	putative cel operon regulator	0.639	Regulatory functions	Y†
1085	**SPy1328**	*bglA.2*	6-phospho-beta-galactosidase	0.656	Energy metabolism	Y†
1093	**SPy1339**		hypothetical protein	**0.147**	Energy metabolism	Y
			conserved hypothetical protein	**2.249**	Unclassified	
1161	**SPy1424**		formate transporter 1, putative	**0.331**	Transport and binding proteins	Y*
1257	**SPy1529**	*glcK*	glucose kinase	**0.422**	Energy metabolism	
1269	**SPy1539**	*asnA*	aspartate-ammonia ligase	**0.278**	Amino acid biosynthesis	^
1270	**SPy1541**	*arcC*	carbamate kinase	**0.029**	Energy metabolism	^
1271	**SPy1542**		Peptidase family M20/M25/M40 superfamily	**0.02**	Unclassified	^
1272	**SPy1543**		conserved hypoth. transmembrane protein	**0.021**	Transport and binding proteins	^

1273	**SPy1544**	*arcB*	ornithine carbamoyltransferase	**0.025**	Amino acid biosynthesis	^
1274	**SPy1546**		acetyltransferase (GNAT) family	**0.023**	Unknown function	^
1275	**SPy1547**	*arcA*	arginine deiminase	**0.027**	Energy metabolism	Y
1276	**SPy1548**		Bacterial regulatory proteins, crp family	**0.217**	Regulatory functions	^
1277	**SPy1549**	*ahrC2*	arginine repressor, putative	**0.276**	Regulatory functions	Y*
1286	**SPy1562**		conserved hypoth. protein TIGR00287	**0.425**	Extrachromosomal element functions	^
1287	**SPy1563**		conserved hypothetical protein	0.419	Extrachromosomal element functions	Y†
1288	**SPy1564**		unknown conserved protein in others	0.503	Extrachromosomal element functions	^
1289	**SPy1565**		conserved hypothetical protein	0.592	Extrachromosomal element functions	^
1290	**SPy1566**		conserved hypothetical protein	0.525	Extrachromosomal element functions	^
1291	**SPy1567**		unknown conserved protein in others, putative	0.491	Extrachromosomal element functions	^
1300	**SPy1582**		methyltransferase	0.454	Central intermediary metabolism	^
1302	**SPy1584**		shikimate 5-dehydrogenase	0.461	Amino acid biosynthesis	^
1304	**SPy1586**		beta-galactosidase	0.342	Energy metabolism	^
1305	**SPy1587**	*tcs10R*	response regulator, spt10R	**0.275**	Regulatory functions	^
1306	**SPy1588**	*tcs10S*	histidine kinase; spt10S	0.351	Regulatory functions	^
1307	**SPy1589**		conserved hypothetical protein	**0.243**	Unknown function	^
	SPy1591		conserved hypothetical protein	0.319	Transport and binding proteins	^
1308	**SPy1592**		conserved hypothetical protein	**0.269**	Transport and binding proteins	^
1309	**SPy1593**		integral membrane protein	**0.266**	Transport and binding proteins	^
1310	**SPy1595**		starch degradation transport system permease	0.361	Transport and binding proteins	Y
1313	**SPy1599**		6-phospho-beta-galactosidas, putative	0.358	Energy metabolism	^
1314	**SPy1600**	*hyl*	hyaluronoglucosaminidase	0.266	Cellular processes	^
1315	**SPy1602**		transcriptional regulator (LacI family), putative	0.317	Regulatory functions	Y†
1316	**SPy1603**		unknown conserved protein in others	0.383	Hypothetical proteins	Y†
1317	**SPy1604**		unknown conserved protein in others	0.414	Hypothetical proteins	^
1329	**SPy1618**	*cysM*	cysteine synthase A	**2.264**	Amino acid biosynthesis	
1376	**SPy1678**		transaldolase, putative	**0.051**	Energy metabolism	^
1377	**SPy1680**		Mga-like HTH domain regulator	**0.045**	Regulatory functions	^
1378	**SPy1681**		NADH oxidase, putative	**0.057**	Cellular processes	^
1379	**SPy1682**	*glpF*	glycerol uptake facilitator protein	**0.15**	Transport and binding proteins	^
1380	**SPy1683**	*glpO1*	glycerol-3-phosphate dehydrogenase	0.569	Energy metabolism	^
1381	**SPy1684**	*gplK*	glycerol kinase	**0.192**	Energy metabolism	Y*
1387	**SPy1693**		probable aldehyde reductase (EC 1.1.1.-) -	**0.393**	Central intermediary metabolism	Y
1395	**SPy1704**	*lacD.1*	tagatose 1,6-diphosphate aldolase	0.578	Energy metabolism	
1396	**SPy1705**	*lacC.1*	tagatose-6-phosphate kinase	0.641	Energy metabolism	
1397	**SPy1707**	*lacB.1*	galactose-6-phosphate isomerase, LacB subunit	0.718	Energy metabolism	
1398	**SPy1708**	*lacA.1*	galactose-6-phosphate isomerase, LacA subunit	0.699	Energy metabolism	
1399	**SPy1709**		PTS, galactitol-specific component IIC	**0.288**	Transport and binding proteins	

1400	**SPy1710**		PTS, galactitol-specific component IIB	**0.26**	Transport and binding proteins	
1401	**SPy1711**		GatA, putative	0.381	Transport and binding proteins	
1479	**SPy1738**	*manL*	mannose-specific component IIAB	**0.361**	Cellular processes	Y
1480	**SPy1739**	*manM*	PTS, mannose-specific component IIC	**0.29**	Transport and binding proteins	Y
1481	**SPy1740**	*manN*	PTS, mannose-specific component IID	**0.345**	Transport and binding proteins	^
1585	**SPy1867**	*deoC*	deoxyribose-phosphate aldolase	**0.236**	Purines, pyrimidines, nucleosides, and nucleotides	^
1586	**SPy1868**	*nupC*	NupC family protein	**0.221**	Transport and binding proteins	^
1587	**SPy1869**	*deoD*	purine nucleoside phosphorylase	**0.188**	Purines, pyrimidines, nucleosides, and nucleotides	Y
1607	**SPy1889**	*fba*	fructose-bisphosphate aldolase (ec 4.1.2.13)	2.186	Energy metabolism	
1608	**SPy1892**		hypothetical 2-acetyl-1-alkylglycerophosphocholine esterase, putative	1.824	Unclassified	
1609	**SPy1894**	*pyrG*	CTP synthase	2.217	Purines, pyrimidines, nucleosides, and nucleotides	
1631	**SPy1915**	*salA*	lantibiotic salivaricin a precursor-related protein	0.609	Cell Envelope	^
1632	**SPy1916**	*lacG*	6-phospho-beta-galactosidas	0.633	Energy metabolism	^
1633	**SPy1917**	*lacE*	PTS system, cellobiose-specific IIC component, putative	0.595	Transport and binding proteins	^
1634	**SPy1918**	*lacF*	PTS system, cellobiose-specific IIA component	0.549	Transport and binding proteins	Y†
1635	**SPy1919**	*lacD.2*	tagatose 1,6-diphosphate aldolase	**0.432**	Energy metabolism	^
1636	**SPy1921**	*lacC.2*	1-phosphofructokinase, putative	**0.402**	Energy metabolism	^
1637	**SPy1922**	*lacB.2*	galactose-6-phosphate isomerase, LacB subunit	**0.419**	Energy metabolism	^
1638	**SPy1923**	*lacA.2*	galactose-6-phosphate isomerase, LacA subunit	0.546	Energy metabolism	^
1639	**SPy1924**	*lacR.2*	transcriptional regulator, DeoR family, putative	0.748	Regulatory functions	Y†
1661	**SPy1947**		transaldolase, putative, TalC family,	**0.429**	Energy metabolism	^
1662	**SPy1949**		SgaT protein, putative	0.439	Unclassified	^
1664	**SPy1952**		unknown conserved protein in bacilli, putative	0. 473	Cellular processes	Y†
1682	**SPy1976**	*msmK*	multiple sugar transport ATP-binding	**0.397**	Transport and binding proteins	Y
1720	**SPy2019**	*mga*	trans-acting positive regulator of M protein	1.087	Regulatory functions	Y†
1730	**SPy2034**		conserved hypothetical protein	**1.888**	Hypothetical proteins	
1735	**SPy2039**	*speB*	pyrogenic exotoxin B; streptopain precursor	0.649	Virulence	Y†
1738	**SPy2043**	*spd*	phage deoxyribonuclease; mitogenic factor	**0.46**	DNA metabolism	
1741	**SPy2047**	*gldA*	glycerol dehydrogenase	**0.437**	Unknown function	^
1742	**SPy2048**	*mipB*	transaldolase, putative	0.47	Energy metabolism	^
1743	**SPy2049**	*pflD*	formate acetyltransferase, putative	0.432	Energy metabolism	^
1744	**SPy2050**	*celB*	PTS system, cellobiose-specific IIC	**0.173**	Transport and binding proteins	^
1745	**SPy2051**	*celA*	PTS system, cellobiose-specific IIB	0.388	Transport and binding proteins	^
1746	**SPy2052**	*celC*	PTS system, cellobiose-specific IIA	**0.148**	Transport and binding proteins	Y
1757	**SPy2065**		hypothetical protein	2.516	Unclassified	
1758	**SPy2066**		dipeptidase, C-69 family	**0.299**	Protein fate	Y*
1770	**SPy2081**	*hutI*	imidazolonepropionase	**0.179**	Energy metabolism	

1779	**SPy2091**		hypothetical protein	**0.212**	Regulatory functions	Y*
1841	**SPy2189**	*sdhB*	L-serine dehydratase, beta subunit	**2.272**	Energy metabolism	

Results shown in the table include both the MGAS5005 Spy number and the SF370 number, the gene name, annotation, array mean, main function, and presence of *cre* (*cre?*). The shading indicates activation. Shown in bolded text are the array means within the 2-fold significance level. Shown in normal text is the array means that do not meet the 2-fold cutoff level. Sequential genes or operons are boxed.

Y: presence of putative *cre*, listed in Appendix I
Y+: *cre* identified with new GAS *cre*
Y*: previously identified GAS *cre*, found with one-mismatch to GAS *cre*
Y†: putative *cre* identified, gene not significantly regulated.
^: associated with *cre*

REFERENCES:

1. **Abranches, J., M. M. Nascimento, L. Zeng, C. M. Browngardt, Z. T. Wen, M. F. Rivera, and R. A. Burne.** 2008. CcpA regulates central metabolism and virulence gene expression in *Streptococcus mutans*. Journal of Bacteriology **190:**2340-9.
2. **Akesson, P., K. Schmidt, J. Cooney, and L. Bjorck.** 1994. M1 protein and protein H: IgGFc- and albumin-binding streptococcal surface proteins encoded by adjacent genes. Biochemistry Journal **300:**877-886.
3. **Akesson, P., A. G. Sjoholm, and L. Bjorck.** 1996. Protein SIC, a novel extracellular protein of *Streptococcus pyogenes* interfering with complement function. Journal of Biological Chemistry **271:**1081-1088.
4. **Akira, S., and K. Takeda.** 2004. Toll-Like Receptor Signalling. Nature Reviews Immunology **4:**499-511.
5. **Almengor, A. C., T. L. Kinkel, S. J. Day, and K. S. McIver.** 2007. The catabolite control protein CcpA binds to P*mga* and influences expression of the virulence regulator Mga in the group A streptococcus. Journal of Bacteriology **189:**8405-8416.
6. **Almengor, A. C., and K. S. McIver.** 2004. Transcriptional activation of *sclA* by Mga requires a distal binding site in *Streptococcus pyogenes*. Journal of Bacteriology **186:**7847-7857.
7. **Almengor, A. C., M. S. Walters, and K. S. McIver.** 2006. Mga is sufficient to activate transcription *in vitro* of *sof/sfbX* and other Mga-regulated virulence genes in the group A streptococcus. Journal of Bacteriology **188:**2038-2047.
8. **Anthony, B. F.** 2000. Streptococcal pyoderma, p. 144-151. *In* D. L. Stevens and E. L. Kaplan (ed.), Streptococcal Infections: Clinical Aspects, Microbiology, and Molecular Pathogenesis. Oxford University Press, New York.
9. **Ashbaugh, C., and M. Wessels.** 2001. Absence of a cysteine protease effect on bacterial virulence in two murine models of group A streptococcal infection. Infection and Immunity **69:**6683-6688.
10. **Ashbaugh, C. D., T. J. Moser, M. H. Shearer, G. L. White, R. C. Kennedy, and M. R. Wessels.** 2000. Bacterial determinants of persistent throat colonization and the associated immune response in a primate model of human group A streptococcal pharyngeal infection. Cellular Microbiology **2:**283-292.
11. **Aung-Hilbrich, L. M., G. Seidel, A. Wagner, and W. Hillen.** 2002. Quantification of the influence of HPrSer46P on CcpA-*cre* interaction. Journal of Molecular Biology **319:**77-85.
12. **Ausubel, F., R. Brent, R. Kingston, D. Moore, J. Seidman, J. Smith, and K. Struhl (ed.).** 1997. Short Protocols in Molecular Biology, 3rd ed. John Wiley & Sons, Inc., New York.
13. **Barrow, G.** 1955. Clinical and bacteriological aspects of impetigo contagiosa. Journal of Hygiene **53:**495-508.
14. **Beachey, E., G. Stollerman, R. Johnson, I. Ofek, and A. Bisno.** 1979. Human immune response to immunization with a structurally defined polypeptide

fragment of streptococcal M protein. Journal of Experimental Medicine **150:**862-877.

15. **Beall, B., R. Facklam, and T. Thompson.** 1996. Sequencing *emm*-specific PCR products for routine and accurate typing of group A streptococci. Journal of Clinical Microbiology **34:**953-958.
16. **Beckert, S., B. Kreikemeyer, and A. Podbielski.** 2001. Group A streptococcal *rofA* gene is involved in the control of several virulence genes and eukaryotic cell attachment and internalization. Infection and Immunity **69:**534-537.
17. **Behari, J., and P. Youngman.** 1998. A homolog of CcpA mediates catabolite control in *Listeria monocytogenes* but not carbon source regulation of virulence genes. Journal of Bacteriology **180:**6316-6324.
18. **Beres, S. B., G. L. Sylva, K. D. Barbian, B. Lei, J. S. Hoff, N. D. Mammarella, M. Y. Liu, J. C. Smoot, S. F. Porcella, L. D. Parkins, D. S. Campbell, T. M. Smith, J. K. McCormick, D. Y. Leung, P. M. Schlievert, and J. M. Musser.** 2002. Genome sequence of a serotype M3 strain of group A streptococcus: phage-encoded toxins, the high-virulence phenotype, and clone emergence. Proceedings of the National Academy of Sciences of the United States of America **99:**10078-10083.
19. **Bessen, D., K. F. Jones, and V. A. Fischetti.** 1989. Evidence for two distinct classes of streptococcal M protein and their relationship to rheumatic fever. Journal of Experimental Medicine **169:**269-283.
20. **Bessen, D. E., and A. Kalia.** 2002. Genomic localization of a T serotype locus to a recombinatorial zone encoding extracellular matrix-binding proteins in *Streptococcus pyogenes*. Infection and Immunity **70:**1159-1167.
21. **Bessen, D. E., C. M. Sotir, T. L. Readdy, and S. K. Hollingshead.** 1996. Genetic correlates of throat and skin isolates of group A streptococci. Journal of Infectious Diseases **173:**896-900.
22. **Betschel, S. D., S. M. Borgia, N. L. Barg, D. E. Low, and J. C. De Azavedo.** 1998. Reduced virulence of group A streptococcal Tn916 mutants that do not produce streptolysin S. Infection and Immunity **66:**1671-1679.
23. **Bisno, A. L.** 1996. Acute pharyngitis: etiology and diagnosis. Pediatrics **97:**949-954.
24. **Bisno, A. L., M. O. Brito, and C. M. Collins.** 2003. Molecular basis of group A streptococcal virulence. Lancet Infectious Diseases **3:**191-200.
25. **Biswas, I., P. Germon, K. McDade, and J. Scott.** 2001. Generation and Surface Localization of Intact M Protein in *Streptococcus pyogenes* are Dependent on *sagA*. Infection and Immunity **69:**7029-7038.
26. **Boyle, M. D., R. Raeder, A. Flosdorff, and A. Podbielski.** 1998. Role of emm and mrp genes in the virulence of group A streptococcal isolate 64/14 in a mouse model of skin infection. Journal of Infectious Disease **177:**991-997.
27. **Bricker, A.** 2002. NAD+ glycohydrolase acts as an intracellular toxin to enhance the extracellular survival of group A streptococci. Molecular Microbiology **44:**257-269.
28. **Buchanan, J., A. Simpson, R. Aziz, G. Liu, S. Kristian, M. Kotb, J. Feramisco, and V. Nizet.** 2006. DNase expression allows the pathogen group A

streptococcus to escape killing in neutrophil extracellular traps. Current Biology **16:**396-400.

29. **Cameron, A., and R. Redfield.** 2006. Non-canonical CRP sites control competence regulons in Escherichia coli and many other gamma-proteobacteria. Nucleic Acids Research **34:**6001-6014.
30. **Caparon, M. G., and J. R. Scott.** 1991. Genetic manipulation of pathogenic streptococci. Methods in Enzymology **204:**556-586.
31. **Carlsson, F., C. Sandin, and G. Lindahl.** 2005. Human fibrinogen bound to Streptococcus pyogenes M protein inhibits complement deposition via the classical pathway. Molecular Microbiology **56:**28-39.
32. **Carr, A., D. D. Sledjeski, A. Podbielski, M. D. Boyle, and B. Kreikemeyer.** 2001. Similarities between complement-mediated and streptolysin S-mediated hemolysis. Journal of Biological Chemistry **276:**41790-41796.
33. **Caswell, C., R. Han, K. Hovis, P. Ciborowski, D. Keene, R. Marconi, and S. Lukomski.** 2008. The Scl1 protein of M6-type group A streptococcus binds the human complement regulatory protein, factor H, and inhibits the alternative pathway of complement. Molecular Microbiology **67:**584-596.
34. **Caswell, C. C., E. Lukomska, N. S. Seo, M. Hook, and S. Lukomski.** 2007. Scl1-dependent internalization of group A Streptococcus via direct interactions with the alpha2beta(1) integrin enhances pathogen survival and re-emergence. Mol Microbiol **64:**1319-1331.
35. **Chassy, B. M.** 1976. A gentle method for the lysis of oral streptococci. Biochemical and Biophysical Research Communication **68:**603-608.
36. **Chaussee, M. A., E. A. Callegari, and M. S. Chaussee.** 2004. Rgg regulates growth phase-dependent expression of proteins associated with secondary metabolism and stress in *Streptococcus pyogenes*. Journal of Bacteriology **186:**7091-7099.
37. **Chaussee, M. S., E. R. Phillips, and J. J. Ferretti.** 1997. Temporal production of streptococcal erythrogenic toxin B (streptococcal cysteine proteinase) in response to nutrient depletion. Infection and Immunity **65:**1956-1959.
38. **Chaussee, M. S., G. A. Somerville, L. Reitzer, and J. M. Musser.** 2003. Rgg coordinates virulence factor synthesis and metabolism in *Streptococcus pyogenes*. Journal of Bacteriology **185:**6016-6024.
39. **Chaussee, M. S., G. L. Sylva, D. E. Sturdevant, L. M. Smoot, M. R. Graham, R. O. Watson, and J. M. Musser.** 2002. Rgg influences the expression of multiple regulatory loci to coregulate virulence factor expression in *Streptococcus pyogenes*. Infection and Immunity **70:**762-770.
40. **Chaussee, M. S., R. O. Watson, J. C. Smoot, and J. M. Musser.** 2001. Identification of Rgg-regulated exoproteins of *Streptococcus pyogenes*. Infection and Immunity **69:**822-831.
41. **Chin, J.** 2000. Streptococcal diseases caused by group A (beta-hemolytic) streptococci, p. 470-476. *In* J. Chin (ed.), Control of Communicable Diseases Manual, 17 ed.
42. **Cleary, P. P., U. Prahbu, J. B. Dale, D. E. Wexler, and J. Handley.** 1992. Streptococcal C5a peptidase is a highly specific endopeptidase. Infection and Immunity **60:**5219-5223.

43. **Cohen, J.** 1969. Effect of culture medium composition and pH on the production of M protein and proteinase by the group A streptococci. Journal of Bacteriology **99:**737-744.
44. **Collin, M., and A. Olsen.** 2001. EndoS, novel secreted enzyme from Streptococcus pyogenes with endoglycosidase activity on human IgG. EMBO J **20:**3046-3055.
45. **Courtney, H., Y. Zhang, M. Frank, and C. Rock.** 2006. Serum opacity factor, a streptococcal virulence factor that binds to apolipoproteins A-I and A-II disrupts high density lipoprotein structure. The Journal of Biological Chemistry **281:**5515-5521.
46. **Courtney, H. S., M. S. Bronze, J. B. Dale, and D. L. Hasty.** 1994. Analysis of the role of M24 protein in group A streptococcal adhesion and colonization by use of omega-interposon mutagenesis. Infection and Immunity **62:**4868-4873.
47. **Courtney, H. S., J. B. Dale, and D. I. Hasty.** 1996. Differential effects of the streptococcal fibronectin-binding protein, FBP54, on adhesion of group A streptococci to human buccal cells and HEp-2 tissue culture cells. Infection and Immunity **64:**2415-2419.
48. **Courtney, H. S., J. B. Dale, and D. L. Hasty.** 2002. Mapping the fibrinogen-binding domain of serum opacity factor of group A streptococci. Current Microbiology **44:**236-240.
49. **Courtney, H. S., D. L. Hasty, Y. Li, H. C. Chiang, J. L. Thacker, and J. B. Dale.** 1999. Serum opacity factor is a major fibronectin-binding protein and a virulence determinant of M type 2 *Streptococcus pyogenes*. Molecular Microbiology **32:**89-98.
50. **Cunningham, M., M. McCormack, P. Fenderson, M. Ho, E. Beachey, and J. Dale.** 1989. Human and murine antibodies cross-reactive with streptococcal M protein and myosin recognized the sequence Gln-Lys-Ser-Lys-Gln in M protein. Journal of Immunology **143:**2677-2683.
51. **Cunningham, M. W.** 2000. Pathogenesis of group A streptococcal infections. Clinical Microbiology Reviews **13:**470-511.
52. **Dajani, A., K. Taubert, P. Ferrieri, G. Peter, and S. Shulman.** 1995. Treatment of acute streptococcal pharyngitis and prevention of rheumatic fever. Pediatrics **96:**758-765.
53. **Dajani, A. S., E. Ayoub, and F. Z. Bierman.** 1993. Guidelines for the diagnosis of rheumatic fever: Jones Criteria, updated 1993. Circulation **87:**302-307.
54. **Dale, J.** 2000. Multivalent Group A Streptococcal Vaccines, p. 390-401. *In* D. Stevens and E. Kaplan (ed.), Streptococcal Infections.
55. **Dale, J., T. Penfound, E. Chiang, V. Long, S. Shulman, and B. Beall.** 2005. Multivalent Group A Streptococcal Vaccine Elicits Bactericidal Antibodies against Variant M Subtypes. Clinical and Diagnostic Laboratory Immunology **12**.
56. **Dale, J. B., and E. H. Beachey.** 1985. Epitopes of streptococcal M proteins shared with cardiac myosin. Journal of Experimental Medicine **162:**583-591.
57. **Dale, J. B., M. Simmons, E. C. Chiang, and E. Y. Chiang.** 1996. Recombinant, octavalent group A streptococcal M protein vaccine. Vaccine **14:**944-948.

58. **Dalton, T. L., and J. R. Scott.** 2004. CovS inactivates CovR and is required for growth under conditions of general stress in *Streptococcus pyogenes*. Journal of Bacteriology **186:**3928-3937.
59. **Datta, V., S. M. Myskowski, L. A. Kwinn, D. N. Chiem, N. Varki, R. G. Kansal, M. Kotb, and V. Nizet.** 2005. Mutational analysis of the group A streptococcal operon encoding streptolysin S and its virulence role in invasive infection. Molecular Microbiology **56:**681-695.
60. **Denny, F. W., Jr.** 2000. History of hemolytic streptococci and associated diseases, p. 1-18. *In* D. L. Stevens and E. L. Kaplan (ed.), Streptococcal Infections: Clinical Aspects, Microbiology, and Molecular Pathogenesis. Oxford University Press, New York.
61. **Deutscher, J., C. Francke, and P. W. Postma.** 2006. How phosphotransferase system-related protein phosphorylation regulates carbohydrate metabolism in bacteria. Microbiology and Molecular Biology Reviews **70:**939-1031.
62. **Deutscher, J., and M. H. Saier, Jr.** 1983. ATP-dependent protein kinase-catalyzed phosphorylation of a seryl residue in HPr, a phosphate carrier protein of the phosphotransferase system in *Streptococcus pyogenes*. Proceedings of the National Academy of Sciences of the United States of America **80:**6790-6794.
63. **Dmitriev, A. V., E. J. McDowell, K. V. Kappeler, M. A. Chaussee, L. D. Rieck, and M. S. Chaussee.** 2006. The Rgg regulator of *Streptococcus pyogenes* influences utilization of nonglucose carbohydrates, prophage induction, and expression of the NAD-glycohydrolase virulence operon. Journal of Bacteriology **188:**7230-7241.
64. **Dong, Y., Y. Y. Chen, and R. A. Burne.** 2004. Control of expression of the arginine deiminase operon of *Streptococcus gordonii* by CcpA and Flp. Journal of Bacteriology **186:**2511-2514.
65. **Edwards, R., G. Taylor, M. Ferguson, S. Murray, N. Rendell, A. Wrigley, Z. Bai, J. Boyle, S. Finney, A. Jones, H. Russell, C. Turner, J. Cohen, L. Faulkner, and S. Sriskandan.** 2005. Specific C-terminal cleavage and inactivation of interleukin-8 by invasive disease isolates of *Streptococcus pyogenes*. Journal of Infectious Diseases **192:**783-790.
66. **Egeter, O., and R. Bruckner.** 1996. Catabolite repression mediated by the catabolite control protein CcpA in *Staphylococcus xylosus*. Molecular Microbiology **21:**739-749.
67. **Eichenbaum, Z., M. J. Federle, D. Marra, W. M. de Vos, O. P. Kuipers, M. Kleerebezem, and J. R. Scott.** 1998. Use of the lactococcal *nisA* promoter to regulate gene expression in Gram-positive bacteria: comparison of induction level and promoter strength. Applied and Environmental Microbiology **64:**2763-2769.
68. **Elliott, S. D.** 1945. A proteolytic enzyme produced by group A streptococci with special reference to its effect on the type-specific M antigen. Journal of Experimental Medicine **81:**573-592.
69. **Engleberg, N. C., A. Heath, K. Vardaman, and V. J. DiRita.** 2004. Contribution of CsrR-regulated virulence factors to the progress and outcome of murine skin infections by *Streptococcus pyogenes*. Infection and Immunity **72:**623-628.

70. **Federle, M. J., K. S. McIver, and J. R. Scott.** 1999. A response regulator that represses transcription of several virulence operons in the group A streptococcus. Journal of Bacteriology **181:**3649-3657.
71. **Fernie-King, B. A., D. J. Seilly, A. Davies, and P. J. Lachmann.** 2002. Streptococcal inhibitor of complement inhibits two additional components of the mucosal innate immune system: secretory leukocyte proteinase inhibitor and lysozyme. Infection and Immunity **70:**4908-4916.
72. **Ferretti, J. J., W. M. McShan, D. Ajdic, D. J. Savic, G. Savic, K. Lyon, C. Primeaux, S. Sezate, A. N. Suvorov, S. Kenton, H. S. Lai, S. P. Lin, Y. Qian, H. G. Jia, F. Z. Najar, Q. Ren, H. Zhu, L. Song, J. White, X. Yuan, S. W. Clifton, B. A. Roe, and R. McLaughlin.** 2001. Complete genome sequence of an M1 strain of *Streptococcus pyogenes*. Proceedings of the National Academy of Sciences of the United States of America **98:**4658-4663.
73. **Fogg, G. C., and M. G. Caparon.** 1997. Constitutive expression of fibronectin binding in *Streptococcus pyogenes* as a result of anaerobic activation of *rofA*. Journal of Bacteriology **179:**6172-6180.
74. **Fontaine, M. C., J. J. Lee, and M. A. Kehoe.** 2003. Combined contributions of streptolysin O and streptolysin S to virulence of serotype M5 *Streptococcus pyogenes* strain Manfredo. Infection and Immunity **71:**3857-3865.
75. **Fujita, Y., Y. Miwa, A. Galinier, and J. Deutscher.** 1995. Specific recognition of the *Bacillus subtilis gnt* cis-acting catabolite-responsive element by a protein complex formed between CcpA and seryl-phosphorylated HPr. Molecular Microbiology **17:**953-960.
76. **Galinier, A., M. Kravanja, R. Engelmann, W. Hengstenberg, M. Kilhoffer, J. Deutscher, and J. Haiech.** 1998. New protein kinase and protein phosphatase families mediate signal transduction in bacterial catabolite repression. Proceedings of the National Academy of Science **95:**1823-1828.
77. **Gao, J., A. A. Gusa, J. R. Scott, and G. Churchward.** 2005. Binding of the global response regulator protein CovR to the *sag* promoter of *Streptococcus pyogenes* reveals a new mode of CovR-DNA interaction. Journal of Biological Chemistry **280:**38948-38956.
78. **Geist, R. T., N. Okada, and M. G. Caparon.** 1993. Analysis of *Streptococcus pyogenes* promoters by using novel Tn916-based shuttle vectors for the construction of transcriptional fusions to chloramphenicol acetyltransferase. Journal of Bacteriology **175:**7561-7570.
79. **Giammarinaro, P., and J. C. Paton.** 2002. Role of RegM, a homologue of the catabolite repressor protein CcpA, in the virulence of *Streptococcus pneumoniae*. Infection and Immunity **70:**5454-5461.
80. **Ginsberg, I., T. Harris, and N. Grossowicz.** 1963. Oxygen-stable hemolysins of group A streptococci. Journal of Experimental Medicine **118:**905-917.
81. **Ginsburg, I.** 1999. Is streptolysin S of group A streptococci a virulence factor? Apmis **107:**1051-1059.
82. **Graham, M. R., L. M. Smoot, C. A. Migliaccio, K. Virtaneva, D. E. Sturdevant, S. F. Porcella, M. J. Federle, G. J. Adams, J. R. Scott, and J. M. Musser.** 2002. Virulence control in group A streptococcus by a two-component gene regulatory system: global expression profiling and in vivo infection

modeling. Proceedings of the National Academy of Sciences of the United States of America **99:**13855-13860.

83. **Graham, M. R., K. Virtaneva, S. F. Porcella, W. T. Barry, B. B. Gowen, C. R. Johnson, F. A. Wright, and J. M. Musser.** 2005. Group A Streptococcus transcriptome dynamics during growth in human blood reveals bacterial adaptive and survival strategies. American Journal of Pathology **166:**455-465.
84. **Griffith, F.** 1934. The serological classification of *Streptococcus pyogenes*. Journal of Hygiene **34:**542-584.
85. **Grundy, F. J., D. A. Waters, S. H. Allen, and T. M. Henkin.** 1993. Regulation of the *Bacillus subtilis* acetate kinase gene by CcpA. Journal of Bacteriology **175:**7348-7355.
86. **Grunfeld, C., M. Marshall, J. Shigenaga, A. Moser, P. Tobias, and K. Feingold.** 1999. Lipoproteins inhibit macrophage activation by lipoteichoic acid. The Journal of Lipid Research **20:**245-252.
87. **Guilherme, L., E. Cunha-Neto, V. Coelho, R. Snitcowsky, P. Pomerantzeff, R. Assis, F. Pedra, J. Newmann, A. Goldberg, M. Patarroyo, F. Pileggi, and J. Kalil.** 1995. Human heart-infiltrating T cell clones from rheumatic heart disease patients recognize both streptococcal and cardiac proteins. Circulation **92:**415-420.
88. **Hanahan, D., and M. Meselson.** 1983. Plasmid screening at high colony density. Methods in Enzymology **100:**333-342.
89. **Hanski, E., and M. Caparon.** 1992. Protein F, a fibronectin-binding protein, is an adhesin of the group A streptococcus *Streptococcus pyogenes*. Proceedings of the National Academy of Sciences of the United States of America **89:**6172-6176.
90. **Harbeck, R., J. Teague, G. Crossen, D. Maul, and P. Childers.** 1993. Novel rapid optical immunoassay technique for detection fo group A streptococci from pharyngeal specimens: comparison with standard culture methods. Journal of Clinical Microbiology **31:**839-844.
91. **Hasty, D. L., I. Ofek, H. S. Courtney, and R. J. Doyle.** 1992. Multiple adhesins of streptococci. Infection and Immunity **60:**2147-2152.
92. **Heath, A., V. J. DiRita, N. L. Barg, and N. C. Engleberg.** 1999. A two-component regulatory system, CsrR-CsrS, represses expression of three *Streptococcus pyogenes* virulence factors, hyaluronic acid capsule, streptolysin S, and pyrogenic exotoxin B. Infection and Immunity **67:**5298-5305.
93. **Heath, A., A. Miller, V. J. DiRita, and C. N. Engleberg.** 2001. Identification of a major, CsrRS-regulated secreted protein of Group A streptococcus. Microbial Pathogenesis **31:**81-89.
94. **Herro, R., S. Poncet, P. Cossart, C. Buchrieser, E. Gouin, P. Glaser, and J. Deutscher.** 2005. How seryl-phosphorylated HPr inhibits PrfA, a transcription activator of *Listeria monocytogenes* virulence genes. Journal of Molecular Microbiology and Biotechnology **9:**224-234.
95. **Holden, M., and C. I. Scott A, Chillingworth T, Churcher C, Cronin A, Dowd L, Feltwell T, Hamlin N, Holroyd S, Jagels K, Moule S, Mungall K, Quail MA, Price C, Rabbinowitsch E, Sharp S, Skelton J, Whitehead S, Barrell BG, Kehoe M, Parkhill J.** 2006. Complete genome of acute rheumatic

fever-associated serotype M5 *Streptococcus pyogenes* strain manfredo. Journal of Bacteriology **189:**1473-1477.

96. **Holm, S. E., A. Nordstrand, D. L. Stevens, and M. Norgreen.** 2000. Acute poststreptococcal glomerulonephritis, p. 152-162. *In* D. L. Stevens and E. L. Kaplan (ed.), Streptococcal Infections: Clinical Aspects, Microbiology, and Molecular Pathogenesis. Oxford University Press, New York.
97. **Hondorp, E. R., and K. S. McIver.** 2007. The Mga virulence regulon: infection where the grass is greener. Molecular Microbiology **66:**1056-1065.
98. **Horstmann, R. D., H. J. Sievertsen, M. Leippe, and V. A. Fischetti.** 1992. Role of fibrinogen in complement inhibition by streptococcal M protein. Infection and Immunity **60:**5036-5041.
99. **Hryniewicz, W., and J. Pryjma.** 1977. Effect of streptolysin S on human and mouse T and B lymphocytes. Infection and Immunity **16:**730-733.
100. **Iyer, R., N. S. Baliga, and A. Camilli.** 2005. Catabolite control protein A (CcpA) contributes to virulence and regulation of sugar metabolism in *Streptococcus pneumoniae*. Journal of Bacteriology **187:**8340-8349.
101. **Jaffe, J., S. Natanson-Yaron, M. G. Caparon, and E. Hanski.** 1996. Protein F2, a novel fibronectin-binding protein from *Streptococcus pyogenes*, possesses two binding domains. Molecular Microbiology **21:**373-384.
102. **Jaggi, P., and S. Shulman.** 2006. Group A Streptococcal Infections. Pediatrics in Review **27:**99-105.
103. **Jeng, A., V. Sakota, Z. Li, V. Datta, B. Beall, and V. Nizet.** 2003. Molecular genetic analysis of a group A streptococcus operon encoding serum opacity factor and a novel fibronectin-binding protein, SfbX. Journal of Bacteriology **185:**1208-1217.
104. **Ji, Y., B. Carlson, A. Kondagunta, and P. P. Cleary.** 1997. Intranasal immunization with C5a peptidase prevents nasopharyngeal colonization of mice by the group A streptococcus. Infection and Immunity **65:**2080-2087.
105. **Joh, D., E. R. Wann, B. Kreikemeyer, P. Speziale, and M. Hook.** 1999. Role of fibronectin-binding MSCRAMMs in bacterial adherence and entry into mammalian cells. Matrix Biology **18:**211-223.
106. **Johnsson, E., K. Berggard, H. Kotarsky, J. Hellwage, P. F. Zipfel, U. Sjobring, and G. Lindahl.** 1998. Role of the hypervariable region in streptococcal M proteins: binding of a human complement inhibitor. Journal of Immunology **161:**4894-4901.
107. **Jones, B., V. Dossonnet, E. Kuster, W. Hillen, J. Deutscher, and R. Klevit.** 1997. Binding of the catabolite repressor protein CcpA to its DNA target is regulated by phosphorylation of its corepressor HPr. Journal of Biological Chemistry **272:**26530-26535.
108. **Jones, T. D.** 1944. The diagnosis of rheumatic fever. Journal of the American Medical Association **126:**481-484.
109. **Kantor, F. S.** 1965. Fibrinogen precipitation by streptococcal M protein. I. Identity of the reactants, and stoichiometry of the reaction. Journal of Experimental Medicine **121:**849-859.
110. **Keiser, H., G. Weissmann, and A. W. Bernheimer.** 1964. Studies on Lysosomes. Iv. Solubilization of Enzymes During Mitochondrial Swelling and

Disruption of Lysosomes by Streptolysin S and Other Hemolytic Agents. Journal of Cell Biology **22:**101-113.

111. **Kimata, K., H. Takahashi, T. Inada, P. Postma, and H. Aiba.** 1997. cAMP receptor protein- cAMP plays a crucial role in glucose-lactose diauxie by activation the major glucose transporter gene in *Escherichia coli.* Proceedings of the National Academy of Science **94:**12914-12919.
112. **Klenk, M., D. Koczan, R. Guthke, M. Nakata, H. Theisen, A. Podbielski, and B. Kreikemeyer.** 2005. Global epithelial cell transcriptional responses reveal *Streptococcus pyogenes* Fas regulator activity association with bacterial aggressiveness. Cellular Microbiology **7:**1237-1250.
113. **Koneman, E. W., S. D. Allen, W. M. Janda, P. C. Schreckenberger, and W. C. Winn, Jr.** 1997. Color Atlas and Textbook of Diagnostic Microbiology, 5th ed. Lippincott-Raven Publishers, Philadelphia.
114. **Kreikemeyer, B., S. Beckert, A. Braun-Kiewnick, and A. Podbielski.** 2002. Group A streptococcal RofA-type global regulators exhibit a strain-specific genomic presence and regulation pattern. Microbiology **148:**1501-1511.
115. **Kreikemeyer, B., M. D. Boyle, B. A. Buttaro, M. Heinemann, and A. Podbielski.** 2001. Group A streptococcal growth phase-associated virulence factor regulation by a novel operon (Fas) with homologies to two-component-type regulators requires a small RNA molecule. Molecular Microbiology **39:**392-406.
116. **Kreikemeyer, B., K. S. McIver, and A. Podbielski.** 2003. Virulence factor regulation and regulatory networks in *Streptococcus pyogenes* and their impact on pathogen-host interactions. Trends in Microbiology **11:**224-232.
117. **Kreikemeyer, B., M. Nakata, T. Koller, H. Hildisch, V. Kourakos, K. Standar, S. Kawabata, M. O. Glocker, and A. Podbielski.** 2007. The *Streptococcus pyogenes* serotype M49 Nra-Ralp3 transcriptional regulatory network and its control of virulence factor expression from the novel *eno ralp3 epf sagA* pathogenicity region. Infection and Immunity **75:**5698-5710.
118. **Kwinn, L. A., A. Khosravi, R. K. Aziz, A. M. Timmer, K. S. Doran, M. Kotb, and V. Nizet.** 2007. Genetic characterization and virulence role of the RALP3/LSA locus upstream of the streptolysin s operon in invasive M1T1 Group A Streptococcus. Journal of Bacteriology **189:**1322-1329.
119. **Lancefield, R., and E. Todd.** 1928. Antigenic differences between matt hemolytic streptococci and their glossy variants. Journal of Experimental Medicine **48:**769-790.
120. **Lancefield, R. C.** 1928. The antigenic complex of *Streptococcus haemolyticus*: I. Demonstration of a type-specific substance in extracts of *Streptococcus haemolyticus*. Journal of Experimental Medicine **47:**91-103.
121. **Lancefield, R. C.** 1962. Current knowledge of type-specific M antigens of group A streptococci. Journal of Immunology **89:**307-313.
122. **Lancefield, R. C.** 1933. A serological differentiation of human and other groups of hemolytic streptococci. Journal of Experimental Medicine **57:**571-595.
123. **Lee, S., D. Mitchell, A. Markley, M. Hensler, D. Gonzalez, A. Wohlrab, P. Dorrestein, V. Nizet, and J. Dixon.** 2008. Discovery of a widely distributed toxin biosynthetic gene cluster. Proceedings of the National Academy of Sciences.

124. **Li, Z., D. D. Sledjeski, B. Kreikemeyer, A. Podbielski, and M. D. Boyle.** 1999. Identification of *pel*, a *Streptococcus pyogenes* locus that affects both surface and secreted proteins. Journal of Bacteriology **181:**6019-6027.
125. **Liu, T., and S. Elliott.** 1965. Streptococcal proteainase: the zymogen to enzyme transformation. The Journal of Biological Chemistry **240:**1138-1142.
126. **Loll, B., W. Saenger, and J. Biesiadka.** 2007. Structure of full-length transcription regulator CcpA in the apo form. Biochimica et biophysica **1774:**732-736.
127. **Loughman, J. A., and M. G. Caparon.** 2006. A novel adaptation of aldolase regulates virulence in *Streptococcus pyogenes*. Embo Journal **25:**5414-5422.
128. **Lukomski, S., N. P. Hoe, I. Abdi, J. Rurangirwa, P. Kordari, M. Liu, S. J. Dou, G. G. Adams, and J. M. Musser.** 2000. Nonpolar inactivation of the hypervariable streptococcal inhibitor of complement gene (*sic*) in serotype M1 *Streptococcus pyogenes* significantly decreases mouse mucosal colonization. Infection and Immunity **68:**535-542.
129. **Lukomski, S., C. A. Montgomery, J. Rurangirwa, R. S. Geske, J. P. Barrish, G. J. Adams, and J. M. Musser.** 1999. Extracellular cysteine protease produced by *Streptococcus pyogenes* participates in the pathogenesis of invasive skin infection and dissemination in mice. Infection and Immunity **67:**1779-1788.
130. **Lukomski, S., K. Nakashima, I. Abdi, V. J. Cipriano, R. M. Ireland, S. D. Reid, G. G. Adams, and J. M. Musser.** 2000. Identification and characterization of the *scl* gene encoding a group A streptococcus extracellular protein virulence factor with similarity to human collagen. Infection and Immunity **68:**6542-6553.
131. **Luo, F., S. Lizano, and D. E. Bessen.** 2008. Heterogeneity in the Polarity of Nra Regulatory Effects on Streptococcal Pilus Gene Transcription and Virulence. Infection and Immunity.
132. **Lyon, W. R., C. M. Gibson, and M. G. Caparon.** 1998. A role for trigger factor and an *rgg*-like regulator in the transcription, secretion and processing of the cysteine proteinase of *Streptococcus pyogenes*. EMBO Journal **17:**6263-6275.
133. **Madden, J. C., N. Ruiz, and M. Caparon.** 2001. Cytolysin-mediated translocation (CMT): a functional equivalent of type III secretion in Gram-positive bacteria. Cell **104:**143-152.
134. **Mahr, K., W. Hillen, and F. Titgemeyer.** 2000. Carbon catabolite repression in *Lactobacillus pentosus*: analysis of the ccpA region. Applied and Environmental Microbiology **66:**277-283.
135. **Malke, H., K. Steiner, W. M. McShan, and J. J. Ferretti.** 2006. Linking the nutritional status of *Streptococcus pyogenes* to alteration of transcriptional gene expression: the action of CodY and RelA. International Journal of Medical Microbiology **296:**259-275.
136. **Mangold, M., M. Siller, B. Roppenser, B. J. Vlaminckx, T. A. Penfound, R. Klein, R. Novak, R. P. Novick, and E. Charpentier.** 2004. Synthesis of group A streptococcal virulence factors is controlled by a regulatory RNA molecule. Molecular Microbiology **53:**1515-1527.
137. **Markowitz, M., and E. Kaplan.** 2000. Rheumatic Fever, p. 133-143. *In* D. Stevens and E. Kaplan (ed.), Streptococcal Infections.

138. **Marrack, P., and J. Kappler.** 1990. The Staphylococcal Enterotoxins and Their Relatives. Science **248:**705-711.
139. **Maxted, W. R., J. P. Widdowson, C. A. Fraser, L. C. Ball, and D. C. Bassett.** 1973. The use of the serum opacity reaction in the typing of group A streptococci. Journal of Medical Microbiology **6:**83-90.
140. **McIver, K. S., A. S. Heath, B. D. Green, and J. R. Scott.** 1995. Specific binding of the activator Mga to promoter sequences of the *emm* and *scpA* genes in the group A streptococcus. Journal of Bacteriology **177:**6619-6624.
141. **McIver, K. S., A. S. Heath, and J. R. Scott.** 1995. Regulation of virulence by environmental signals in group A streptococci: influence of osmolarity, temperature, gas exchange, and iron limitation on *emm* transcription. Infection and Immunity **63:**4540-4542.
142. **McIver, K. S., and R. L. Myles.** 2002. Two DNA-binding domains of Mga are required for virulence gene activation in the group A streptococcus. Molecular Microbiology **43:**1591-1602.
143. **McIver, K. S., and J. R. Scott.** 1997. Role of *mga* in growth phase regulation of virulence genes of the group A streptococcus. Journal of Bacteriology **179:**5178-5187.
144. **McIver, K. S., S. Subbarao, E. M. Kellner, A. S. Heath, and J. R. Scott.** 1996. Identification of *isp*, a locus encoding an immunogenic secreted protein conserved among group A streptococci. Infection and Immunity **64:**2548-2555.
145. **McIver, K. S., A. S. Thurman, and J. R. Scott.** 1999. Regulation of *mga* transcription in the group A streptococcus: specific binding of Mga within its own promoter and evidence for a negative regulator. Journal of Bacteriology **181:**5373-5383.
146. **Meleney, F.** 1924. Hemolytic streptococcus gangrene. Archives of Surgery **9:**317-364.
147. **Mendez, M., I. H. Huang, K. Ohtani, R. Grau, T. Shimizu, and M. R. Sarker.** 2008. Carbon catabolite repression of type IV pilus-dependent gliding motility in the anaerobic pathogen *Clostridium perfringens*. Journal of Bacteriology **190:**48-60.
148. **Milenbachs, A. A., D. P. Brown, M. Moors, and P. Youngman.** 1997. Carbon-source regulation of virulence gene expression in *Listeria monocytogenes*. Molecular Microbiology **23:**1075-1085.
149. **Miorner, H., G. Johansson, and G. Kronvall.** 1983. Lipoteichoic acid is the major cell wall compenent responsible for the surface hydrophobicity of the group A streptococcus. Infection and Immunity **39:**336-343.
150. **Miwa, Y., A. Nakata, A. Ogiwara, M. Yamamoto, and Y. Fujita.** 2000. Evaluation and characterization of catabolite-responsive elements (*cre*) of Bacillus subtilis. Nucleic Acids Research **28:**1206-1210.
151. **Miyoshi-Akiyama, T., D. Takamatsu, M. Koyanagi, J. Zhao, K. Imanishi, and T. Uchiyama.** 2005. Cytocidal effect of *Streptococcus pyogenes* on mouse neutrophils in vivo and the critical role of streptolysin S. Journal of Infectious Disease **192:**107-116.
152. **Moreno, M. S., B. L. Schneider, R. R. Maile, W. Weyler, and M. H. Saier, Jr.** 2001. Catabolite repression mediated by the CcpA protein in B*acillus subtilis*:

novel modes of regulation revealed by whole-genome analyses. Molecular Microbiology **39:**1366-1381.

153. **Musser, J. M., and F. R. DeLeo.** 2005. Toward a genome-wide systems biology analysis of host-pathogen interactions in group A Streptococcus. American Journal of Pathology **167:**1461-1472.
154. **Nakata, M., A. Podbielski, and B. Kreikemeyer.** 2005. MsmR, a specific positive regulator of the *Streptococcus pyogenes* FCT pathogenicity region and cytolysin-mediated translocation system genes. Molecular Microbiology **57:**786-803.
155. **Neeman, R., N. Keller, A. Barzilai, Z. Korenman, and S. Sela.** 1998. Prevalence of internalisation-associated gene, prtF1, among persisting group-A streptococcus strains isolated from asymptomatic carriers. Lancet **352:**1974-1977.
156. **O'Loughlin, R., A. Roberson, P. Cieslak, R. Lynfield, K. Gershman, A. Craig, B. Albanese, M. Farley, N. Barrett, N. Spina, B. Beall, L. Harrison, A. Reingold, and C. Van Beneden.** 2007. The epidemiology of invasive group A streptococcal infection and potential vaccine implications: United States, 2000-2004. Clinical Infectious Diseases **45:**853-862.
157. **Pahlman, L., P. Marx, M. Morgelin, S. Lukomski, J. Meijers, and H. Herwald.** 2007. Thrombin-activatable Fibrinolysis Inhibitor binds to *Streptococcus pyogenes* by interacting with collagen-like Proteins A and B. The Journal of Biological Chemistry **282:**24873-24881.
158. **Park, H., and P. Cleary.** 2005. Active and Passive Intranasal immunizations with Streptococcal Surface Protein C5a Peptidase Prevent Infection of Murine Nasal Mucosa-Associated Lymphoid Tissue, a Functional Homologue of Human Tonsils. Infection and Immunity **73:**7878-7886.
159. **Perez-Casal, J., M. G. Caparon, and J. R. Scott.** 1991. Mry, a trans-acting positive regulator of the M protein gene of *Streptococcus pyogenes* with similarity to the receptor proteins of two-component regulatory systems. Journal of Bacteriology **173:**2617-2624.
160. **Perez-Casal, J., J. A. Price, E. Maguin, and J. R. Scott.** 1993. An M protein with a single C repeat prevents phagocytosis of *Streptococcus pyogenes*: use of a temperature-sensitive shuttle vector to deliver homologous sequences to the chromosome of *S. pyogenes*. Molecular Microbiology **8:**809-819.
161. **Pine, L., and M. W. Reeves.** 1972. Correlation of M protein production with those factors found to influence growth and substrate utilization of *Streptococcus pyogenes*. Infection and Immunity **5:**668-680.
162. **Pine, L., and M. W. Reeves.** 1978. Regulation of the synthesis of M protein by sugars, Todd Hewitt broth, and horse serum, in growing cells of *Streptococcus pyogenes*. Microbios **21:**185-212.
163. **Podbielski, A., M. Woischnik, B. Kreikemeyer, K. Bettenbrock, and B. A. Buttaro.** 1999. Cysteine protease SpeB expression in group A streptococci is influenced by the nutritional environment but SpeB does not contribute to obtaining essential nutrients. Medical Microbiology and Immunology **188:**99-109.

164. **Podbielski, A., M. Woischnik, B. A. Leonard, and K. H. Schmidt.** 1999. Characterization of *nra*, a global negative regulator gene in group A streptococci. Molecular Microbiology **31:**1051-1064.
165. **Polly, S., R. Waldman, P. High, M. Wittner, A. Dorfman, and E. Fox.** 1975. Protective studies with a group A streptococcal M protein vaccine. Journal of Infectious Disease **131:**217-224.
166. **Postma, P., J. Lengeler, and G. Jacobsen.** 1993. Phosphoenolpyruvate: carbohydrate phosphotransferase systems of bacteria. Microbiology Review **57:**543-594.
167. **Pulliainen, A. T., J. Hytonen, S. Haataja, and J. Finne.** 2008. Deficiency of the Rgg regulator promotes H_2O_2 resistance, AhpCF-mediated H_2O_2 decomposition and virulence in *Streptococcus pyogenes*. Journal of Bacteriology.
168. **Ramachandran, V., J. D. McArthur, C. E. Behm, C. Gutzeit, M. Dowton, P. K. Fagan, R. Towers, B. Currie, K. S. Sriprakash, and M. J. Walker.** 2004. Two distinct genotypes of *prtF2*, encoding a fibronectin binding protein, and evolution of the gene family in *Streptococcus pyogenes*. Journal of Bacteriology **186:**7601-7609.
169. **Rasmussen, M., and L. Bjorck.** 2002. Proteolysis and its regulation at the surface of *Streptococcus pyogenes*. Molecular Microbiology **43:**537-544.
170. **Rasmussen, M., and L. Bjorck.** 2001. Unique regulation of SclB- a novel collagen-like surface protein of *Streptococcus pyogenes*. Molecular Microbiology **40:**1427-1438.
171. **Rasmussen, M., H. P. Muller, and L. Bjorck.** 1999. Protein GRAB of *Streptococcus pyogenes* regulates proteolysis at the bacterial surface by binding α2-macroglobulin. Journal of Biological Chemistry **274:**15336-15344.
172. **Rasmussen, R., A. Eden, and L. Bjorck.** 2000. SclA, a novel collagen-like surface protein of *Streptococcus pyogenes*. Infection and Immunity **68:**6370-6377.
173. **Ravins, M., J. Jaffe, E. Hanski, I. Shetzigovski, S. Natanson-Yaron, and A. E. Moses.** 2000. Characterization of a mouse-passaged, highly encapsulated variant of group A streptococcus in in vitro and in vivo studies. Journal of Infectious Disease **182:**1702-1711.
174. **Reizer, J., C. Hoischen, F. Titgemeyer, C. Rivolta, R. Rabus, J. Stulke, D. Karamata, M. H. Saier, Jr., and W. Hillen.** 1998. A novel protein kinase that controls carbon catabolite repression in bacteria. Molecular Microbiology **27:**1157-1169.
175. **Ribardo, D. A., T. J. Lambert, and K. S. McIver.** 2004. Role of *Streptococcus pyogenes* two-component response regulators in the temporal control of Mga and the Mga-regulated virulence gene *emm*. Infection and Immunity **72:**3668-3673.
176. **Ribardo, D. A., and K. S. McIver.** 2003. *amrA* encodes a putative membrane protein necessary for maximal exponential phase expression of the Mga virulence regulon in *Streptococcus pyogenes*. Molecular Microbiology **50:**673-685.
177. **Ribardo, D. A., and K. S. McIver.** 2006. Defining the Mga regulon: comparative transcriptome analysis reveals both direct and indirect regulation by Mga in the group A streptococcus. Molecular Microbiology **62:**491-508.

178. **Ringdahl, U., Svensson M, Wistedt AC, Renné T, Kellner R, Müller-Esterl W, and S. U.** 1998. Molecular co-operation between protein PAM and streptokinase for plasmin acquisition by *Streptococcus pyogenes*. Journal of Biological Chemistry **273:**6424-6430.
179. **Roberts, S. A., G. G. Churchward, and J. R. Scott.** 2007. Unraveling the regulatory network in *Streptococcus pyogenes*: the global response regulator CovR represses *rivR* directly. Journal of Bacteriology **189:**1459-1463.
180. **Roberts, S. A., and J. R. Scott.** 2007. RivR and the small RNA RivX: the missing links between the CovR regulatory cascade and the Mga regulon. Molecular Microbiology **66:**1506-1522.
181. **Rocha, C. L., and V. A. Fischetti.** 1999. Identification and characterization of a novel fibronectin-binding protein on the surface of group A streptococci. Infection and Immunity **67:**2720-2728.
182. **Ruiz, N., B. Wang, A. Pentland, and M. Caparon.** 1998. Streptolysin O and adherence synergistically modulate proinflammatory responses of keratinocytes to group A streptococci. Molecular Microbiology **27:**337-346.
183. **Ryan, P. A., V. Pancholi, and V. A. Fischetti.** 2001. Group A streptococci bind to mucin and human pharyngeal cells through sialic acid-containing receptors. Infection and Immunity **69:**7402-7412.
184. **Sabharwal, H., F. Michon, D. Nelson, W. Dong, K. Fuchs, R. Manjarrez, A. Sarkar, C. Uitz, A. Viteri-Jackson, R. Suarez, M. Blake, and J. Zabriskie.** 2006. Group A Streptococcus Carbohydrate as an Immunogen for Protection against GAS Infection. The Journal of Infectious Dieases **193:**129-135.
185. **Schrager, H. M., S. Alberti, C. Cywes, G. J. Dougherty, and M. R. Wessels.** 1998. Hyaluronic acid capsule modulates M protein-mediated adherence and acts as a ligand for attachment of group A streptococcus to CD44 on human keratinocytes. Journal of Clinical Investigation **101:**1708-1716.
186. **Schrager, H. M., J. G. Rheinwald, and M. R. Wessels.** 1996. Hyaluronic acid capsule and the role of streptococcal entry into keratinocytes in invasive skin infection. Journal of Clinical Investigation **98:**1954-1958.
187. **Schwartz, M.** 1996. Historical Streptococci, p. 1-2. *In* T. Horaud (ed.), Streptococci and the Host.
188. **Scott, J. R., P. C. Guenthner, L. M. Malone, and V. A. Fischetti.** 1986. Conversion of an M- group A streptococcus to M+ by transfer of a plasmid containing an M6 gene. Journal of Experimental Medicine **164:**1641-1651.
189. **Seidl, K., M. Strucki, M. Ruegg, C. Goerke, C. Wolz, L. Harris, B. Berger-Bachi, and M. Bischoff.** 2006. *Staphylococcus aureus* CcpA Affects Virulence Determinant Production and Antibiotic Resistance. Antimicrobial Agents and Chemotherapy **50:**1183-1193.
190. **Shatursky, O., A. P. Heuck, L. A. Shepard, J. Rossjohn, M. W. Parker, A. E. Johnson, and R. K. Tweten.** 1999. The mechanism of membrane insertion for a cholesterol-dependent cytolysin: a novel paradigm for pore-forming toxins. Cell **99:**293-299.
191. **Shelburne, S. A., 3rd, C. Granville, M. Tokuyama, I. Sitkiewicz, P. Patel, and J. M. Musser.** 2005. Growth characteristics of and virulence factor production by

group A Streptococcus during cultivation in human saliva. Infection and Immunity **73:**4723-4731.

192. **Shelburne, S. A., 3rd, D. Keith, N. Horstmann, P. Sumby, M. T. Davenport, E. A. Graviss, R. G. Brennan, and J. M. Musser.** 2008. A direct link between carbohydrate utilization and virulence in the major human pathogen group A Streptococcus. Proceedings of the National Academy of Sciences of the United States of America **105:**1698-1703.
193. **Shelburne, S. A., 3rd, P. Sumby, I. Sitkiewicz, C. Granville, F. R. DeLeo, and J. M. Musser.** 2005. Central role of a bacterial two-component gene regulatory system of previously unknown function in pathogen persistence in human saliva. Proceedings of the National Academy of Sciences of the United States of America **102:**16037-16042.
194. **Shulman, S., R. Tanz, and M. Gerber.** 2000. Streptococcal Pharyngitis, p. 76-101. *In* D. Stevens and E. Kaplan (ed.), Streptococcal Infections.
195. **Singh, R., G. Palm, S. Panjikar, and W. Hinrichs.** 2007. Structure of the apo form o fthe catabolite control protein A (CcpA) from *Bacillius megaterium* with a DNA-binding domain. Acta crystallographica. Section F, Structural biology and crystallization communications **63:**253-257.
196. **Sitkiewicz, I., and J. M. Musser.** 2006. Expression microarray and mouse virulence analysis of four conserved two-component gene regulatory systems in group a streptococcus. Infection and Immunity **74:**1339-1351.
197. **Spanier, J. G., S. J. Jones, and P. Cleary.** 1984. Small DNA deletions creating avirulence in *Streptococcus pyogenes*. Science **225:**935-938.
198. **Steiner, K., and H. Malke.** 2000. Life in protein-rich environments: the *relA*-independent response of *Streptococcus pyogenes* to amino acid starvation. Molecular Microbiology **38:**1004-1016.
199. **Steiner, K., and H. Malke.** 2001. *relA*-Independent amino acid starvation response network of *Streptococcus pyogenes*. Journal of Bacteriology **183:**7354-7364.
200. **Stevens, D.** 2001. Invasive Streptococcal Infections. Journal of Infection and Chemotherapy **7:**69-80.
201. **Stevens, D. L.** 2000. Group A beta-hemolytic streptococci: virulence factors, pathogenesis, and spectrum of clinical infections, p. 37-56. *In* D. L. Stevens and E. L. Kaplan (ed.), Streptococcal Infections: Clinical Aspects, Microbiology, and Molecular Pathogenesis. Oxford University Press, New York.
202. **Stevens, D. L.** 2000. Life-threatening streptococcal infections: scarlet fever, necrotizing fasciitis, myositis, bacteremia, and streptococcal toxic shock syndrome, p. 163-179. *In* D. L. Stevens and E. L. Kaplan (ed.), Streptococcal Infections: Clinical Aspects, Microbiology, and Molecular Pathogenesis. Oxford University Press, New York.
203. **Stulke, J., and W. Hillen.** 1999. Carbon catabolite repression in bacteria. Current Opinion in Microbiology **2:**195-201.
204. **Stulke, J., and W. Hillen.** 2000. Regulation of carbon catabolism in *Bacillus* species. Annual Review of Microbiology **54:**849-880.
205. **Sumby, P., K. D. Barbian, D. J. Gardner, A. R. Whitney, D. M. Welty, R. D. Long, J. R. Bailey, M. J. Parnell, N. P. Hoe, G. G. Adams, F. R. Deleo, and J.**

M. Musser. 2005. Extracellular deoxyribonuclease made by group A streptococcus assists pathogenesis by enhancing evasion of the innate immune response. Proceedings of the National Academy of Sciences of the United States of America **102:**1679-1684.

206. **Sumby, P., S. F. Porcella, A. G. Madrigal, K. D. Barbian, K. Virtaneva, S. M. Ricklefs, D. E. Sturdevant, M. R. Graham, J. Vuopio-Varkila, N. P. Hoe, and J. M. Musser.** 2005. Evolutionary origin and emergence of a highly successful clone of serotype M1 group A streptococcus involved multiple horizontal gene transfer events. Journal of Infectious Diseases **192:**771-782.
207. **Sumby, P., A. R. Whitney, E. A. Graviss, F. R. DeLeo, and J. M. Musser.** 2006. Genome-wide analysis of group a streptococci reveals a mutation that modulates global phenotype and disease specificity. PLoS Pathogens **2:**e5.
208. **Sumby, P., S. Zhang, A. Whitney, F. Falugi, G. Grandi, E. Graviss, F. DeLeo, and J. Musser.** 2008. A chemokine-degrading extracellular protease made by group A streptococcus alters pathogenesis by enhancing evasion of the innate immune response. Infection and Immunity **76:**978-985.
209. **Sun, H., U. Ringdahl, J. W. Homeister, W. P. Fay, N. C. Engleberg, A. Y. Yang, L. S. Rozek, X. Wang, U. Sjobring, and D. Ginsburg.** 2004. Plasminogen is a critical host pathogenicity factor for group A streptococcal infection. Science **305:**1283-1286.
210. **Sung, K., S. A. Khan, M. S. Nawaz, and A. A. Khan.** 2003. A simple and efficient Triton X-100 boiling and chloroform extraction method of RNA isolation from Gram-positive and Gram-negative bacteria. FEMS Microbiology Letters **229:**97-101.
211. **Swift, H. F., A. T. Wilson, and R. C. Lancefield.** 1943. Typing group A hemolytic streptococci by M precipitin reactions in capillary pipettes. Journal of Experimental Medicine **78:**127-133.
212. **Terao, Y., S. Kawabata, E. Kunitomo, J. Murakami, I. Nakagawa, and S. Hamada.** 2001. Fba, a novel fibronectin-binding protein from *Streptococcus pyogenes*, promotes bacterial entry into epithelial cells, and the *fba* gene is positively transcribed under the Mga regulator. Molecular Microbiology **42:**75-86.
213. **Terao, Y., S. Kawabata, M. Nakata, I. Nakagawa, and S. Hamada.** 2002. Molecular characterization of a novel fibronectin-binding protein of *Streptococcus pyogenes* strains isolated from toxic shock-like syndrome patients. Journal of Biological Chemistry **277:**47428-47435.
214. **Thern, A., L. Stenberg, B. Dahlback, and G. Lindahl.** 1995. Ig-binding surface proteins of *Streptococcus pyogenes* also bind human C4b-binding protein (C4BP), a regulatory component of the complement system. The Journal of Immunology **154:**375-386.
215. **Titgemeyer, F., and W. Hillen.** 2002. Global control of sugar metabolism: a gram-positive solution. Antonie Van Leeuwenhoek **82:**59-71.
216. **Todd, E. W., and L. F. Hewitt.** 1932. A new culture medium for the production of antigenic streptococcal haemolysin. Journal of Pathology and Bacteriology **35:**973.

217. **Toppel, A. W., M. Rasmussen, M. Rohde, E. Medina, and G. S. Chhatwal.** 2003. Contribution of protein G-related α2-macroglobulin-binding protein to bacterial virulence in a mouse skin model of group A streptococcal infection. Journal of Infectious Diseases **187:**1694-1703.
218. **Turinsky, A. J., F. J. Grundy, J. H. Kim, G. H. Chambliss, and T. M. Henkin.** 1998. Transcriptional activation of the *Bacillus subtilis ackA* gene requires sequences upstream of the promoter. Journal of Bacteriology **180:**5961–5967.
219. **Vahling, C. M., and K. S. McIver.** 2006. Domains required for transcriptional activation show conservation in the Mga family of virulence gene regulators. Journal of Bacteriology **188:**863-73.
220. **Vahling, C. M., and K. S. McIver.** 2005. Identification of residues responsible for the defective virulence gene regulator Mga produced by a natural mutant of *Streptococcus pyogenes*. Journal of Bacteriology **187:**5955-66.
221. **Varga, J., V. L. Stirewalt, and S. B. Melville.** 2004. The CcpA protein is necessary for efficient sporulation and enterotoxin gene (*cpe*) regulation in *Clostridium perfringens*. Journal of Bacteriology **186:**5221-5229.
222. **Vincent, W. F., and K. J. Lisiewski.** 1969. Improved growth medium for group A streptococci. Applied Microbiology **18:**954-955.
223. **Virtaneva, K., S. F. Porcella, M. R. Graham, R. M. Ireland, C. A. Johnson, S. M. Ricklefs, I. Babar, L. D. Parkins, R. A. Romero, G. J. Corn, D. J. Gardner, J. R. Bailey, M. J. Parnell, and J. M. Musser.** 2005. Longitudinal analysis of the group A streptococcus transcriptome in experimental pharyngitis in cynomolgus macaques. Proceedings of the National Academy of Sciences of the United States of America **102:**9014-9019.
224. **von Pawel-Rammingen, U., and L. Bjorck.** 2003. IdeS and SpeB: immunoglobulin-degrading cysteine proteases of *Streptococcus pyogenes*. Current Opinion in Microbiology **6:**50-55.
225. **von Pawel-Rammingen, U., B. P. Johansson, and L. Bjorck.** 2002. IdeS, a novel streptococcal cysteine proteinase with unique specificity for immunoglobulin G. The EMBO Journal **21:**1607-1615.
226. **Voyich, J. M., D. E. Sturdevant, K. R. Braughton, S. D. Kobayashi, B. Lei, K. Virtaneva, D. W. Dorward, J. M. Musser, and F. R. DeLeo.** 2003. Genome-wide protective response used by group A streptococcus to evade destruction by human polymorphonuclear leukocytes. Proceedings of the National Academy of Sciences of the United States of America **100:**1996-2001.
227. **Walker, M., A. Hollands, M. Sanderson-Smith, J. Cole, J. Kirk, A. Henningham, J. MCArthur, K. Dinkla, R. Aziz, R. Kansal, A. Simpson, J. Buchanan, G. Chhatwal, M. Kotb, and V. Nizet.** 2007. DNase Sda1 provides selection pressure for a switch to invasive group A streptococcal infection. Nature Medicine **13:**981-985.
228. **Wang, B., P. Schlievert, A. Gaber, and M. Kotb.** 1993. Localization of an immunologically functional region of the streptococcal superantigen pepsin extracted fragment of type 5 M protein. Journal of Immunology **151:**1419-1429.

229. **Wannamaker, L.** 1958. The differentiation of the three distinct desoxyribonucleases of the group A streptococci. Journal of Experimental Medicine **107:**797-812.
230. **Wannamaker, L. W.** 1970. Differences between streptococcal infections of the throat and of the skin. I. The New England Journal of Medicine **282:**23-31.
231. **Wei, L., V. Pandiripally, E. Gregory, N. Clymer, and D. Cue.** 2005. Impact of the SpeB protease on binding of the complement regulatory proteins by *Streptococcus pyogenes*. Infection and Immunity **73:**2040-2050.
232. **Wessels, M. R., and M. S. Bronze.** 1994. Critical role of the group A streptococcal capsule in pharyngeal colonization and infection in mice. Proceedings of the National Academy of Sciences of the United States of America **91:**12238-12242.
233. **Wessels, M. R., A. E. Moses, J. B. Goldberg, and T. J. DiCesare.** 1991. Hyaluronic acid capsule is a virulence factor for mucoid group A streptococci. Proceedings of the National Academy of Sciences of the United States of America **88:**8317-8321.
234. **Woodbury, R., K. Klammer, Y. Xiong, T. Bailiff, A. Glennen, J. Bartkus, R. Lynfield, C. Van Beneden, and B. Beall.** 2008. Plasmid-Borne *erm*(T) from Invasive, Macrolide-Resistant *Streptococcus pyogenes* Strains. Antimicrobial Agents and Chemotherapy **52:**1140-1143.
235. **Yung, D. L., K. S. McIver, J. R. Scott, and S. K. Hollingshead.** 1999. Attenuated expression of the *mga* virulence regulon in an M serotype 50 mouse-virulent group A streptococcal strain. Infection and Immunity **67:**6691-6694.
236. **Zomer, A. L., G. Buist, R. Larsen, J. Kok, and O. P. Kuipers.** 2007. Time-resolved determination of the CcpA regulon of *Lactococcus lactis* subsp. *cremoris* MG1363. Journal of Bacteriology **189:**1366-1381.